

THE IMPACT OF EPIDERMAL GROWTH FACTOR RECEPTOR INHIBITION ON  
ENERGY HOMEOSTASIS

Melanie Beth Weed

A dissertation submitted to the faculty of the University of North Carolina at Chapel Hill  
in partial fulfillment of the requirements for the degree of Doctor of Philosophy in the  
Curriculum of Toxicology

Chapel Hill  
2010

Approved by:

David Threadgill

Sheila Collins

Lee Graves

Kay Lund

Daniel Pomp

## **ABSTRACT**

Melanie Beth Weed: THE IMPACT OF EPIDERMAL GROWTH FACTOR RECEPTOR INHIBITION ON ENERGY HOMEOSTASIS

(Under the direction of David W. Threadgill)

As a result of the worldwide rise in obesity and obesity-related complications such as diabetes, stroke, and cardiovascular disease, understanding the mechanisms associated with this disease and determining treatment options is necessary. A balance between food intake and energy expenditure, through a highly integrated multi-organ system, determines body weight regulation. Signals relaying energy storage and satiety from the periphery are sent to the central nervous system (CNS) where they, along with other neuronal signals, are used to maintain this balance. Accumulating evidence suggests signaling through the epidermal growth factor receptor (EGFR) is required for normal adipocyte development; therefore understanding how this signaling contributes to excess body fat mass is necessary to unravel the mechanisms associated with obesity. Our lab has previously shown that EGFR inhibition retards adipose deposition in a diet-induced obesity (DIO) model. To further delineate the role of EGFR in DIO, we performed two studies using pharmacological and genetic mouse models with either suppressed or conditionally deleted EGFR. In the first study, wild-type male C57BL/6J mice were chronically exposed to a high-fat western diet (WD) with or without a small molecule inhibitor to the EGFR tyrosine kinase, AG1478. In a separate experiment,

mice homozygous for the *Egfr*<sup>wa2</sup> mutation, a constitutionally impaired EGFR tyrosine kinase, and their control littermates were also challenged with this WD. The second study aimed to understand the role of EGFR in energy homeostasis in DIO. Mice with *Egfr* specifically deleted in peripheral tissues (intestines and adipocytes) and in the CNS using the *Egfr*<sup>tm1Dwt</sup> conditional allele and the *Villin-Cre*, *aP2-Cre*, and *GFAP-Cre*, transgenic lines, respectively, were chronically exposed to the WD. Significantly less body weight and fat mass were observed in mice with EGFR inhibition, either pharmacologically with AG1478 or genetically in the *Egfr*<sup>wa2</sup> and *GFAP-Cre* genetic lines. Alterations in adipocyte size, adipocyte-specific factors, food intake, energy expenditure, and clinical parameters were also observed in these mice. We conclude that alterations in energy homeostasis account for this fat mass decrease. These studies should aid in our understanding of the role of EGFR in appetite and metabolism and provide potential avenues for the treatment of obesity.

## ACKNOWLEDGEMENTS

Deciding to attend graduate school after having worked for several years was a hard decision for me, although one that was right. I left a job with flexible hours, an office, a paycheck, and the comfort of understanding my job, and the comfort of my friendships to come to North Carolina to pursue a degree in a field much different than what I had previously worked in, knowing no one. But I wanted a challenge and to feel uncomfortable again. So with support from my friends, family, and my boss I headed to UNC and it is one of the best decisions I could have made.

Not coming from a lab environment, I was most challenged by my steep learning curve at the bench but from working in my first rotation and with everyone in the Threadgill lab, I learned the many techniques I would need to succeed in my PhD. I will be forever thankful for the guidance and support from many members of my lab. They became good friends and helped me through my graduate career both technically and emotionally. Thank you to my advisor who gave me the freedom to work on what I was interested in and supported my growth through the many conferences I attended. Thank you to all my fellow Toxicology graduate students, their spouses, and other UNC graduate students for out of school fun and in school ideas. Coming down here and meeting such great people has made this experience that much more enjoyable! I would also like to thank my family, friends, and fiancé in the northeast and Florida for your love, support, and advice when I missed home or when I was having a bad day. I couldn't have asked for a better support group!!

## TABLE OF CONTENTS

LIST OF TABLES..... viii

LIST OF ABBREVIATIONS..... xi

**Chapter** **Page**

**I. THE ROLE OF EGFR SIGNALING IN ADIPOSE DEPOSITION AND OBESITY ..... 1**

Abstract..... 1

ERBB family..... 2

Obesity prevalence and complications..... 3

Adipose tissue biology..... 7

Adipogenesis..... 9

Factors Modulating Adipogenesis ..... 10

*In vivo* models..... 13

Energy Homeostasis ..... 17

Obesity Treatment..... 20

Conclusions ..... 23

**II. EPIDERMAL GROWTH FACTOR RECEPTOR INHIBITION RESULTS IN DECREASED FAT MASS IN MICE ON A HIGH-FAT DIET DUE TO DECREASED FOOD INTAKE..... 29**

Abstract..... 29

Introduction ..... 30

Materials and Methods..... 31

Results ..... 36

Inhibition of EGFR results in reduced fat mass deposition.....	36
Reduced fat mass is due to decreased food intake and feeding efficiency.....	37
Inhibition of EGFR results in smaller adipocytes.....	38
EGFR inhibition leads to improved clinical parameters.....	38
Discussion.....	39
<b>III. EGFR SIGNALING IS IMPORTANT IN THE CENTRAL NERVOUS SYSTEM FOR MAINTAINING ENERGY HOMEOSTASIS .....</b>	<b>56</b>
Abstract.....	56
Introduction .....	57
Methods and Materials.....	59
Results .....	63
Egfr ablation within the CNS results in reduced fat mass deposition .....	63
Use of the GFAP-Cre transgene leads to reduced Egfr and anorexigenic neuropeptide in the hypothalamus .....	64
Ablation of EGFR results in smaller adipocytes.....	65
Egfr deletion in the CNS leads to improved clinical parameters .....	65
Discussion.....	66
<b>IV. THE EPIDERMAL GROWTH FACTOR RECEPTOR IS NOT REQUIRED IN ADIPOCYTES FOR ADIPOSE DEPOSITION BUT IS REQUIRED FOR NORMAL GROWTH IN MICE.....</b>	<b>86</b>
Abstract.....	86
Introduction .....	87
Materials and Methods.....	88
Results .....	91
aP2-Cre Egfr <sup>flox/flox</sup> mice grow faster than controls but do not have higher adiposity .	91
Increased serum IGF1 levels in aP2-Cre Egfr <sup>flox/flox</sup> mice .....	92

Deletion of Egfr in adipocytes causes a decrease in serum cholesterol levels .....	92
Discussion .....	93
<b>V. CONCLUSIONS AND FUTURE DIRECTIONS .....</b>	<b>106</b>
<b>REFERENCES.....</b>	<b>115</b>

## LIST OF TABLES

Table 1. Summary of EGFR mutant models and phenotypes.....	24
Table 2. Effects of EGFR inhibition on adipocyte number and size. ....	45
Table 3. Effects of pharmacological EGFR inhibition on clinical serum parameters. ....	46
Table 4. Effects of <i>Egfr</i> CNS deletion with <i>GFAP-Cre</i> on adipocyte number and size..	75
Table 5. Clinical serum and expression data from control and <i>GFAP-Cre Egfr<sup>fllox/fllox</sup></i> mice.....	76
Table 6. Serum and expression clinical data from control and <i>aP2-Cre Egfr<sup>fllox/fllox</sup></i> mice.	98

## LIST OF FIGURES

Figure 1. The epidermal growth factor receptor family, its ligands, and signaling pathways.....	25
Figure 2. Adipogenesis .....	26
Figure 3. EGFR signaling is necessary at specific stages in adipogenesis. ....	27
Figure 4. Adiposity negative feedback loop. ....	28
Figure 5. Effects of genetic or pharmacological inhibition of EGFR on body weight and fat mass. ....	47
Figure 6. Effect of pharmacological EGFR inhibition on feeding and metabolic parameters. ....	48
Figure 7. Effect of pharmacological EGFR inhibition on uncoupling protein-1 expression.....	49
Figure 8. Effect of pharmacological EGFR inhibition on hypothalamic <i>Egfr</i> and neuropeptide expression.....	50
Figure 9. Representative inguinal fat pad histology sections from control and EGFR inhibited mice.....	51
Figure 10. Effect of pharmacological EGFR inhibition on adipocyte-specific factors in epididymal fat. ....	52
Figure 11. Effect of pharmacological EGFR inhibition on adipokine transcript expression in epididymal fat. ....	53
Figure 12. Glucose tolerance test measurements from B6 control and EGFR inhibited mice.....	54
Figure 13. Effect of pharmacological EGFR inhibition on HOMA-IR measurements. ...	55
Figure 14. Effects of conditional deletion of <i>Egfr</i> on body masses and organ weights. ..	77
Figure 15. Effects of <i>Egfr</i> CNS deletion with <i>GFAP-Cre</i> on food and water intake and feeding efficiency.....	78
Figure 16. Effects of <i>Egfr</i> CNS deletion with <i>GFAP-Cre</i> on energy expenditure and activity.....	79
Figure 17. Effects of <i>Egfr</i> CNS deletion with <i>GFAP-Cre</i> on uncoupling proteins-1 and 3 expression.....	80

Figure 18. Effects of <i>Egfr</i> CNS deletion with <i>GFAP-Cre</i> on hypothalamic neuropeptide and <i>Egfr</i> expression levels. ....	81
Figure 19. Representative inguinal fat pad histology from control and <i>GFAP-Cre Egfr<sup>lox/lox</sup></i> mice. ....	82
Figure 20. Effects of <i>Egfr</i> CNS deletion on adipocyte-specific factors in epididymal fat pads. ....	83
Figure 21. Glucose tolerance test measurements from control and <i>GFAP-Cre Egfr<sup>lox/lox</sup></i> mice. ....	84
Figure 22. Average HOMA-IR measurements from control and <i>GFAP-Cre Egfr<sup>lox/lox</sup></i> mice. ....	85
Figure 23. PCR analysis of DNA and expression of EGFR in liver of control and <i>aP2-Cre Egfr<sup>lox/lox</sup></i> mice. ....	99
Figure 24. Effect of <i>Egfr</i> deletion with in adipocytes on organ weights fat mass. ....	100
Figure 25. Effect of adipocyte-specific <i>Egfr</i> deletion on growth and food intake. ....	101
Figure 26. IGF1 serum levels and <i>Igf1</i> mRNA expression levels in control and <i>aP2-Cre Egfr<sup>lox/lox</sup></i> mice. ....	102
Figure 27. Effects of <i>Egfr</i> deletion in adipocytes on growth hormone receptor mRNA levels in epididymal fat depot and the liver. ....	103
Figure 28. Glucose tolerance test measurements in control and <i>aP2-Cre Egfr<sup>lox/lox</sup></i> mice. ....	104
Figure 29. Average HOMA-IR measurements from control and <i>aP2-Cre Egfr<sup>lox/lox</sup></i> mice. ....	105

## LIST OF ABBREVIATIONS

129/S1	129S1/SvImJ
ADAM	a disintegrin-like and metalloproteinase
AGRP	agouti-related protein
AMPK	AMP-activated protein kinase
ANOVA	analysis of variance
ARB	$\beta$ .adrenergic receptor
ARC	arcuate nucleus
AREG	amphiregulin
ap2	fatty acid binding protein
B6	C57Bl/6J
BAT	brown adipose tissue
BMI	body mass index
BTC	betacellulin
BW	body weight
CART	cocaine- and amphetamine-regulated transcript
CCK	cholecystokinin
C/EBP	CAAT/enhancer binding protein
CNS	central nervous system
CO <sub>2</sub>	carbon dioxide
<i>Cre</i>	cre recombinase; enzyme
CT	threshold cycle

DIO	diet-induced obesity
EGF	epidermal growth factor
EGFR	epidermal growth factor receptor
EREG	epiregulin
ERK	extracellular regulatory kinase
GLUT	glucose transporter
GFAP	glial fibrillary acidic protein
GPCR	G -protein-coupled receptor
GTT	glucose tolerance test
H&E	hematoxylin and eosin
HB-EGF	heparin-binding epidermal growth factor
HFD	high-fat diet
HOMA-IR	homeostasis model assessment of insulin resistance
IGF	insulin-like growth factor
IL	interleukin
INH	AG1478; EGFR inhibitor
IRS	insulin receptor substrate
LDL	low density lipoprotein level
LFD	low-fat diet
MAPK	mitogen-activated protein kinase
MC	melanocortin receptor
MDI	methylisobutylxanthine, dexamethasone, and insulin
MMP	metalloproteinase

MRI	magnetic resonance imaging
MSH	melanocyte stimulating hormone
NEFA	non-esterified fatty acids
NHANES	National Health and Nutrition Examination Survey
NPY	neuropeptide Y
NRG	neuregulin
O <sub>2</sub>	oxygen
PAI	plasminogen activator inhibitor
PCR	polymerase chain reaction
PDGF	platelet-derived growth factor
PI3K	phosphatidylinositol 3-kinase
PKA	protein kinase A
POMC	pro-opiomelanocortin
PPAR	peroxisome proliferator-activated receptor
Pref	preadipocyte factor
PYY	peptide YY
qPCR	quantitative real-time polymerase chain reaction
RER	respiratory exchange rate
TGF	transforming growth factor
TKI	tyrosine kinase inhibitor
TNF	tumor necrosis factor
W	watt
wa2	waved-2

WAT	white adipose tissue
WD	western diet
WD/INH	western diet with AG1478

## CHAPTER 1

### THE ROLE OF EGFR SIGNALING IN ADIPOSE DEPOSITION AND OBESITY

#### Abstract

Since the mid-1970s, the prevalence of overweight (BMI  $\geq 25$ ) and obesity (BMI  $\geq 30$ ) has increased sharply for both adults and children. Being overweight or obese increases the risk of many diseases and health conditions, including type-2 diabetes, hypertension, hyperglycemia, atherosclerosis, cancer, and stroke. Obesity is caused by a higher energy intake than expenditure and results in increased fat mass due to an increase in preadipocyte proliferation and adipocyte differentiation. Accumulating evidence suggests signaling through the epidermal growth factor receptor (EGFR) is required for adipocyte development. The EGFR, a member of the ERBB family, is expressed in a wide range of tissues and cell types that regulate a number of cellular processes such as proliferation, differentiation, motility, apoptosis, and survival. We review here the current literature surrounding obesity prevalence, the makeup of adipose tissue, and the process of adipogenesis. We then discuss how factors such as EGFR and its ligands influence adipogenesis and how the use of *in vivo* models can help elucidate EGFR signaling relating to adipose deposition. We next review the current understanding of energy regulation in the body and how EGFR signaling may be involved. Finally we discuss current therapies directed towards obesity and how an alternative obesity treatment may be to target EGFR.

## **ERBB family**

The epidermal growth factor receptor (EGFR), the prototypical member of the ERBB family, is expressed in a wide range of tissues and cell types that regulate a number of cellular processes such as proliferation, differentiation, motility, apoptosis, and survival (1-4). This family consists of four members: EGFR (ERBB1), ERBB2, ERBB3, and ERBB4 that each contain an extracellular ligand binding domain, a transmembrane region, an intracellular tyrosine kinase domain, and a C terminus. Upon binding of ligands to the extracellular domain, these members form homo or heterodimers that initiate autophosphorylation of tyrosine residues and signaling cascades (Figure 1). Due to the absence of a recognized ligand to ERBB2 and the impaired tyrosine kinase domain of ERBB3, these ERBB receptors only function through heterodimerization with a second, ligand-binding or kinase-active ERBB receptor, respectively (3-7).

Regulating the duration and potency of activation of these signaling cascades is a complex process, and ligand binding is an important aspect in this regulation. The epidermal growth factor (EGF)-related ligands are produced as transmembrane precursors, activated by protease cleavage to form soluble growth factors. The zinc-dependent disintegrin-like and metalloproteinase-containing proteins (ADAMs) are the proteases that cleave EGF proligands (7, 8). Three groups of EGFR ligands exist, based upon an EGF-like domain that determines receptor specificity. The first group includes EGF, transforming growth factor- $\alpha$  (TGFA), and amphiregulin (AREG), which bind specifically to EGFR. The second group includes betacellulin (BTC), heparin-binding EGF (HBEGF), and epiregulin (EREG), which can bind and activate EGFR and ERBB4. The third group is composed of four neuregulins (NRG1-4), which form two subgroups

based upon their binding to ERBB3 and ERBB4 (NRG1 and NRG2) or only ERBB4 (NRG3 and NRG4) (7, 9, 10). Therefore, ligand binding aids in controlling the formation of defined ERBB dimers through selective binding to their target receptor that influences which receptor tyrosine phosphorylation patterns and signaling pathways are activated throughout the body. The mitogen-activated protein kinase (MAPK) pathway is a common target downstream of all receptors, as is the phosphatidylinositol-3-kinase (PI3K) pathway. Signal downregulation for EGFR and other ERBB family members is through internalization and targeting to the endosomal compartment for degradation (7, 11).

Also aiding in the complexity of these signaling cascades is the transactivation of EGFR by G-protein coupled receptors (GPCRs), cytokine receptors, receptor tyrosine kinases, and oxidants. GPCRs involved in transactivation include thrombin, angiotensin II, and  $\alpha$  and  $\beta$  adrenergic receptors. This transaction process occurs when stimuli increase the activity of metalloproteases (MMPs), which leads to ligand shedding and binding to ERBB receptors in either an autocrine or paracrine fashion and signaling cascades involved in proliferation, migration, or inhibition of apoptosis (12, 13). Since EGFR signaling cascades are involved in proliferation and differentiation, they may also be involved in adipogenesis and therefore contribute to the development of obesity.

### **Obesity prevalence and complications**

Since the mid-1970s, the prevalence of overweight (BMI  $\geq$  25) and obesity (BMI  $\geq$  30) has increased sharply for both adults and children. Results from the 2007-2008 National Health and Nutrition Examination Survey (NHANES) indicate that in adults aged 20–74 years the prevalence of obesity has increased from 15.0% in 1976 to 33.8%

in 2008. The NHANES study from 2003-2004 indicated that an estimated 17% of children and adolescents 2-19 years of age are overweight, with the prevalence of overweight increasing from 7.2 to 17% from 1976 through 2004 (14, 15). Being overweight or obese increases the risk of many diseases and health conditions, including type-2 diabetes, hypertension, hyperglycemia, atherosclerosis, cancer, and stroke. Also, childhood obesity is associated with a higher chance of premature death and disability in adulthood (16, 17). Obese women show increased risk for postmenopausal breast cancer and obese breast cancer patients have a higher risk for large tumors, lymph node metastases, and death, compared to non-obese patients (18). It has also been suggested that there is an increased risk of developing hepatocellular carcinoma due to increased lipid in the liver of the obese (19). Due to these many health conditions, medical costs attributed to both overweight and obesity accounted for \$114 billion dollars in 2008 (20).

Obesity is just one of the factors associated with metabolic syndrome, which includes such symptoms as hypertension, insulin resistance, and hyperlipidemia. This syndrome is associated with a state of low-grade systemic inflammation with levels of cytokines such as tumor necrosis factor- $\alpha$  (TNF $\alpha$ ) and interleukin-6 (IL6) elevated in serum and adipose tissue as well as increased free fatty acid release (21-27). Obesity is associated with disrupted signaling efficacy of adipokines such as leptin, adiponectin, resistin, plasminogen activator inhibitor-1 (PAI1), and insulin, and occurs when energy balance is disrupted. Restoration of adipokine balance and responsiveness occurs with reduction in obesity (22, 28, 29). Leptin is a 16 kD protein that is produced and secreted from white adipose tissue and signals the amount of adipose tissue mass to the central nervous system (CNS) for energy regulation (30). Peripheral or central administration of

leptin has been shown to reduce body weight, food intake, and blood glucose levels in lean and obese mice with leptin deficiency; however, no effects are noted in another mouse model with a leptin receptor mutation. To try and overcome this resistance, adipocytes secrete more leptin resulting in higher leptin levels (31). Insulin works similar to leptin in that it inhibits feeding and increases energy expenditure. As weight and body fat increases, so does insulin secretion to maintain normal glucose homeostasis. Insulin resistance occurs if the pancreatic  $\beta$ -cell does not produce enough insulin leading to hyperglycemia and potentially producing type 2 diabetes. Therefore in times of weight gain, leptin and insulin production are increased, and with weight loss production decreases (31-33). Adiponectin is a 30 kD protein expressed and secreted at high levels in adipocytes. Decreased levels are associated with a high BMI, insulin resistance, inflammation, increased levels of plasma lipids, and cardiovascular disease (34, 35).

The increase in fat mass associated with overweight and obesity is related to a combination of (1) strong genetic and metabolic maintenance of energy stores; (2) the food environment that is available, usually leading to the over-consumption of calorie-dense and nutrient-poor foods; and (3) increases in lack of physical activity due to technology. Factors contributing to this obesogenic environment and the consequential toxic effects of overweight and obesity also include large portion sizes and visibility and accessibility of foods. Diets high in fat are also known to quickly cause insulin resistance and signs of inflammation, which disrupts adipokine levels. In genetic (i.e. *ob/ob* and Zucker *fa/fa* rat) and diet-induced obesity mouse models and in obese humans, a high-fat diet (HFD) is also known to reduce sympathetic nervous system activity and to reduce glucose transporter (GLUT)-2 and glucose-stimulated glucose tolerance (22, 31, 33, 36-

38). Another factor contributing to this obesogenic environment includes lack of physical activity, which along with a HFD are the primary environmental factors leading to increases in obesity (38, 39).

Being overweight or obese may also lead to potential changes in susceptibility to environmental contaminants. Since adipose tissue is mostly composed of lipids, it represents a major reservoir for many different lipophilic contaminants such as persistent organic pollutants (i.e., polychlorinated biphenyls or dioxins) (40, 41). Consequently, individuals with a large amount of adipose tissue are likely exposed to elevated endocrine or physiological disruption. These pollutants may alter the secretory function and metabolism of adipocytes and transcription factor activation in adipogenesis. It has been further hypothesized that exposure to environmental contaminants prenatally may lead to obesity as adults (40-43). For example, dioxins are environmental anti-estrogens and endocrine disruptors, are lipophilic, and are stored in fat. Exposure of 3T3-L1 preadipocytes to dioxins results in an impairment of adipose function by decreasing the activity of lipoprotein lipase, glucose transport, and accumulation of triglycerides, due to decreases in adipogenic transcription factors (44, 45). The mechanism of dioxin's toxic action involves the modulation of growth factor receptors and components of their signal transduction pathways. This was observed *in vivo* in immature female rats exposed to dioxin at a dose of 2 µg of dioxin/kg. This dose decreased body weight gain and adipose tissue weight in the immature rats by decreasing the activities of signaling pathways downstream of a receptor tyrosine kinase (44, 46, 47).

Because of the toxic obesogenic environment (both internal and external) that we are exposed to, the adverse health conditions that occur, high health care costs, and

exposure to lipophilic environmental contaminants, a better understanding of the mechanisms associated with this disease and identifying potential therapeutics are necessary. In order to understand these mechanisms behind obesity, we first need to understand adipose biology and the steps in adipogenesis.

### **Adipose tissue biology**

Adipose tissue is composed of many different cell types at varying stages of differentiation. Adipocytes, stromal-vascular cells, blood vessels, nerves, and lymph nodes make up adipose tissue (48, 49). Preadipocytes contain no lipid in their cytoplasm but as they mature they accumulate more lipid until they are fully differentiated and their cytoplasm is full. In a population of mature adipocytes, there are various sizes. When these cells grow, as in obesity, the heterogeneity of the sizes decreases (48, 49). Blood supply to the adipose tissue provides for the delivery of metabolic products and removal of wastes. With obesity, the supply of blood to adipose tissue can be 15-30% of the total cardiac output, leading potentially to high blood pressure and heart failure (48). Adipose tissue surrounding lymph nodes demonstrates a connection with the immune system since this organ can secrete inflammatory factors. Also, adipose tissue is innervated by the sympathetic nervous system and by sensory neurons regulating such important processes as lipolysis (48). The different adipose depots in the body possess regional differences in growth and cellularity as well as metabolism. In looking at *in vitro* and *in vivo* models, it was found that different adipose regions develop at different rates, possibly due to the local expression of factors, the cell populations present, or innervation, and respond to stimuli such as insulin differently. For example, epididymal depots show a higher blood

flow, growth modality, and innervation than inguinal depots, however the inguinal depot shows a higher proliferative capacity (48, 50).

White adipose tissue (WAT) stores energy as triglycerides and excess storage leads to obesity, with increased fat volume as a marker. The normal values of percent body fat for humans range from 9 to 18% in males and 14 to 28% in females. In obesity, percentages of 22% and 32% (and higher) in males and females, respectively, can be observed (48). Mild obesity results in hypertrophy of the adipocytes while severe obesity leads to both hyperplasia and hypertrophy, with the latter showing the poorest prognosis for weight loss (48, 49). In humans and mice, WAT is mostly absent at birth, developing postnatally, while brown adipose tissue (BAT) is developed during fetal life and found largely in the interscapular region. Mature WAT adipocytes contain single fat droplets within the cells while mature BAT adipocytes show a multicellular distribution of the fat droplets (50). These two adipose stores show functional differences with WAT storing extra nutrients in times of excess and releasing these nutrients in times of scarcity, while BAT is involved in non-shivering thermogenesis through the uncoupling of the mitochondrial  $\beta$ -oxidation pathway and wasting energy as heat (51). Recent data has also shown that brown and white adipocytes are present together in the same depots and may interconvert depending on energy needs, genetic background, and degree of sympathetic stimulation (52-54). It has been shown that BAT plays an essential role in energy balance and that its activity influences body weight in rodents, while it has been thought that humans do not possess enough BAT to impact energy in the body. However, recent evidence has shown that adult humans clearly have depots of metabolically active BAT,

suggesting that it may play a significant role in the regulation of body weight (49, 51, 55).

### **Adipogenesis**

Obesity is a result of increased fat mass due to higher energy intake than expenditure and is associated with an increase in preadipocyte proliferation and adipocyte differentiation. Proliferation leads to an increase in preadipocytes while differentiation is the transition of these cells from undifferentiated fibroblast-like cells to mature lipid-filled fat cells (35, 48). Most of our understanding of adipogenesis is through *in vitro* cell culture systems. The 3T3-L1 cell line is one such system, which is already committed to the adipogenic pathway and is used to study adipogenesis. When these preadipocytes undergo growth arrest and are treated with a combination of isobutylmethylxanthine, dexamethasone, and insulin (MDI), they start to produce a rounded phenotype. Within two to three days of this treatment, they begin to differentiate and accumulate lipids intracellularly in the form of lipid droplets (35, 48, 56).

Once preadipocytes reach confluence and differentiation is induced, terminal differentiation occurs through the induction of transcription factors, expression of adipogenic genes, and lipid accumulation (57, 58) (Figure 2). Transcription factor CAAT/Enhancer Binding Protein (C/EBP) is found in preadipocytes as  $\beta$ ,  $\alpha$ , and  $\delta$  isoforms. C/EBPB is part of the basic leucine zipper family and is one of the first transcription factors induced after the induction of differentiation. It promotes the transcription of a number of other adipogenic genes such as peroxisome proliferator-activated receptor  $\gamma$  (PPARG) and C/EBPA (35, 56-59). PPARG is a nuclear hormone receptor existing as two isoforms, with PPARG2 being most abundant in adipocytes. It is expressed in small amounts in preadipocytes and its synthesis increases during

differentiation (49, 54, 60). C/EBPA is essential for the development of mature adipocytes *in vitro* and *in vivo* and activates several adipocyte-specific genes such as GLUT4, fatty acid synthetase, fatty acid binding protein, leptin, adiponectin, and uncoupling proteins (49, 56, 58, 59). Inhibition of C/EBPA in 3T3-L1 cells leads to decreased lipid accumulation and expression of fat-specific markers, supported by the fact that mice with a targeted disruption of C/EBPA show reduced brown and white adipose mass (49). It is thought that retention of the adipocyte phenotype is through the interaction between C/EBPA and PPARG and that PPARG is required for adipose development given that PPARG-null pups lack adipose tissue and do not survive (49, 54).

### **Factors Modulating Adipogenesis**

Hormones, growth factors, and cytokines regulate adipogenesis, with some of these signals stimulating and others inhibiting this process. For development, cells need to balance their growth as well as their differentiation. A reversible growth arrest must occur in the G<sub>1</sub> phase of the cell cycle before preadipocytes can commit to differentiation and respond to signals for terminal differentiation. Therefore, factors that initiate growth may prevent this arrest and inhibit adipogenesis (35). Terminal differentiation is characterized by an irreversible loss of proliferative capacity resulting in the decrease of growth regulating genes (35, 61). Peptides, such as growth factors EGF, HBEGF, insulin-like growth factor-1 (IGF1), and platelet-derived growth factor (PDGF), stimulate cell growth and block preadipocyte differentiation (60-63). This has been shown *in vitro* in 3T3-L1 and primary rat preadipocytes and *in vivo* where administration of EGF or HBEGF decreases the development of adipose tissue. The administration of MDI however blocks increases in EGF so differentiation can occur (46, 63, 64).

Since it is known that growth arrest is necessary for adipogenesis to proceed, it is assumed that the signaling cascades induced by cytokines and growth factors affect the activity of transcription factors needed for the adipocyte phenotype. It is thought that this activity is mediated through the activation of the MAPK signaling pathway, by phosphorylating PPAR $\gamma$  on its MAPK consensus sites (54, 62). This MAPK-mediated phosphorylation of PPAR $\gamma$  then leads to blocking of transcriptional activity necessary for differentiation, due to ligands having a lower affinity for the phosphorylated form of PPAR $\gamma$ . This was shown in transcription reporter assays using 3T3-L1 preadipocytes where activated MAPK, through growth factor signaling, led to a suppression of PPAR $\gamma$  transcriptional activity (54, 62). There is also evidence that EGFR signaling via the MAPK pathway may inhibit adipogenesis through expression of *Myc*. It has been shown that expression of *Myc* in 3T3-L1 preadipocytes inhibits differentiation as well as preventing normal C/EBP $\alpha$  induction (61). Cytokines such as TNF $\alpha$ , IL1 and IL6 also inhibit adipogenesis. Treatment of 3T3-L1 preadipocytes with TNF $\alpha$  or C3H10T1/2 cells with HBEGF downregulates genes associated with the mature adipocyte phenotype such as PPAR $\gamma$ , GLUT-4 and C/EBP $\alpha$ . TNF $\alpha$  can also activate the MAPK pathway and by blocking this pathway with an inhibitor *in vitro*, TNF $\alpha$ 's effects on adipocyte differentiation are abolished (54, 60, 62, 65).

It is also shown that EGF has lipogenic and lipolytic effects based on when and how much is available (Figure 3). In a serum-free 3T3-L1 system, IGF1 only in combination with EGF can stimulate differentiation after growth arrest similar to that with insulin alone, showing the EGF supports cellular growth (66, 67). As stated previously, since EGFR is mitogenic, it may prevent the growth arrest needed for

differentiation to proceed and therefore its signaling activity would be suppressed before differentiation can occur. Increased amounts of EGF have been shown to increase adiposity in mature female mice and in 3T3-L1 mature adipocytes suggesting a lipogenic effect of this ligand, due in part to an increase in triglyceride synthesis (68). This effect is inhibited following treatment of these animals with either anti-EGF or by removing the submandibular gland from the mouse, which produces large amounts of EGF. Also noted in these studies is a decrease in acyl-coA synthase and lipoprotein lipase mRNA, which are part of the triglyceride synthesis pathway (68-70). The effect of EGF inhibition is thought to be specific to adipocytes since fat pad weights were decreased in these mice while other organs weights were not changed. This lipogenic effect is only noted, however, in adult mice or in mature adipocytes, where differentiation has already occurred (71). When neonatal mice were injected with EGF for 10 days, their body weights decreased as well as their inguinal fat pad weights and triglyceride synthesis, with larger lipolytic effects seen upon increasing concentrations of EGF (71). In 3T3-L1 preadipocytes, very low concentrations of EGF have been shown to stimulate extracellular regulatory kinase (ERK) and p38 MAPK activity through dimer formation of EGFR and/or ERBB2, showing that ERK is involved in preadipocyte proliferation (72). This is also observed with ERK1<sup>-/-</sup> mice where low adiposity and adipocyte number was noted versus wild-type mice on a HFD (73). Also in a study in young mice carrying the dominant negative or antimorphic allele *Egfr*<sup>W<sup>a</sup>5</sup> fed a normal chow diet, a significant reduction in percent body fat compared to their control littermates was noted, suggesting that reduced EGFR signaling is growth inhibitory to mature adipocytes (74). This would

be expected given that MAPK signaling is thought to inhibit differentiation and therefore smaller cells or preadipocytes would be prevalent (71-74).

A possible explanation for these controversial effects of EGF in adipogenesis could be EGFR's interaction with ERBB2 in adipocytes. ERBB2 expression is also found in 3T3-L1 preadipocytes with EGFR. It can be recalled that ERBB2 does not have a ligand binding domain and therefore heterodimerizes with other ERBB members, with EGFR being the preferred partner (72, 75). ERBB2's expression is found to increase during the proliferation and growth arrest phases of adipogenesis; however, addition of MDI and progression through differentiation leads to a decrease in expression, similar to EGFR (72). Also, when serum-starved 3T3-L1 preadipocytes were given EGF, an increase in ERBB2 activation was noted showing that EGF could activate ERBB2, through this heterodimerization with EGFR (72, 75). However when these cells were given a ligand specific to ERBB3 and ERBB4, no increase in phosphorylation of either EGFR or ERBB2 was observed, showing dependency on EGFR (67).

### ***In vivo models***

Many mouse models of obesity exist to examine obesity and these models have been used successfully to study human obesity. Common mechanisms between these models and human obesity imply that similar biochemical changes exist between mammalian species in energy homeostasis (32). Obesity in experimental animals is associated with central obesity, insulin resistance, hypertriglyceridemia, hyperinsulinemia, hyperleptinemia, and impaired glucose tolerance, similar to humans eating high-fat diets (31, 38). C57BL/6J (B6) mice fed a HFD are one of the most commonly used mouse models for diet-induced obesity (DIO) (37, 76). B6 mice develop

hyperleptinemia, with peripheral leptin administration decreasing feeding until they become resistant after 16 days on a HFD (31). This apparent resistance phenomenon is also observed in obese humans who also have high plasma leptin levels. They do not decrease food intake with exogenous leptin administration, which also does not affect weight loss (31, 33, 37). However, when fed a normal or low-fat diet (LFD), B6 mice remain lean and physiologically normal. Although these mice also have a higher feeding efficiency than other strains when challenged by a HFD, they also show increased activity levels relative to other leaner strains (36). Despite the fact that there is variation in the degree of adiposity among B6 mice even when they are maintained under similar conditions, this mouse model recapitulates many characteristics of the obesity phenotype in humans who also show varied adiposity (77).

Genetic models of obesity also exist and include the Zucker *fa/fa* rat and the *db/db*, *ob/ob*, and M16 mice. The *fa/fa* rat has a missense mutation in the leptin receptor gene, becoming obese due to an inability to respond to high leptin levels. The *db/db* mouse is similar to the *fa/fa* rat in that it also has a leptin receptor mutation, which accounts for its obesity phenotype. This *db/db* mouse model helped to predict a receptor for a circulating factor, namely leptin (78, 79). The *ob/ob* mouse however is obese due to a mutation in the leptin gene, preventing production of a functional protein, and leptin was discovered because of this model (80). With this mouse model, injection of leptin prevents obesity by regulating feeding through the leptin receptor (79). Since obesity and diabetes are both effected by environmental and genetic factors, the M16 polygenic obese mouse model was produced as an outbred animal model of early onset polygenic obesity and diabetes. These mice were selected for a large weight gain over 27 generations to

produce mice that are larger and have increased body fat, adipocytes, and organ weights when compared to a non-selected control line. As with the B6 DIO model, these genetic models also show hyperleptinemia, hyperphagia, hyperglycemia, and hyperinsulinemia similar to human obesity (16, 78, 79).

In order to dissect the role of EGFR in obesity, *in vivo* models exist that alter gene activity constitutionally (Table 1). Null mutations of EGFR have also been studied and they result in varying phenotypes depending on genetic background. These mice show a number of organ and embryonic abnormalities and die at different stages of embryogenesis or postnatally, dependent on genetic background (81, 82). The waved-2 (*Egfr<sup>wa2</sup>*) hypomorphic allele has a single nucleotide alteration that results in the substitution of a glycine for a valine in the highly conserved tyrosine kinase domain of EGFR (1). This results in a reduced rate of internalization of EGFR and up to 90% reduction in EGFR activity in mice homozygous for the mutation. *Egfr<sup>wa2</sup>* homozygous mice are healthy and show a mild wavy coat phenotype, curly whiskers, and some endocrine and reproductive disorders including enlarged and thickened aortic valves and small mammary glands, while those heterozygous for the mutation show no abnormalities (1, 74). The wa-1 mutation (*Tgfa<sup>wa1</sup>*) is a mutation of the *Tgfa* locus. Mice homozygous for the *Tgfa<sup>wa1</sup>* mutation are slightly smaller than their control littermates and similar to the *Egfr<sup>wa2</sup>* phenotype, *Tgfa<sup>wa1</sup>* mice show a wavy coat and whiskers (83, 84). *Egfr<sup>Dsk5</sup>* is a hypermorphic allele of *Egfr* with a T to A transversion causing a missense mutation and a Leu863Gln substitution in the tyrosine kinase domain. This is a gain-of-function mutation that causes an increase in tyrosine kinase activity and a decrease in receptor levels *in vivo* (85). In mice homo or heterozygous for the *Egfr<sup>Dsk5</sup>* mutation, abnormal

skin pigmentation in the footpads and in the first digit are observed as is a wavy coat, a thicker epidermis, and increased nail length (85). The waved-5 (*Egfr<sup>Wa5</sup>*) dominant negative allele houses a single point mutation causing a missense mutation in exon 21. This mutation causing an aspartic acid to glycine change at amino acid residue 833 and altered tyrosine kinase function (74, 86). Phenotypes for the *Egfr<sup>Wa5</sup>* mutation include peri and prenatal lethality in fetal growth and development, with embryos living longer than embryonic day 12.5 dying before or shortly after birth. Wavy hair, curly whiskers, corneal scarring, and eyelids open at birth are other features of mice heterozygous for the *Egfr<sup>Wa5</sup>* mutant allele, similar to mice with the *Egfr<sup>wa2</sup>* and *Egfr<sup>Dsk5</sup>* mutations (74, 86).

Other model systems conditionally delete *Egfr* in specific cell types to study EGFR signaling, using *Cre* recombinase. *Cre* recombinase is an enzyme derived from the bacteriophage P1 that specifically recognizes loxP sites. *Cre* has been shown to effectively mediate the excision of DNA located between the loxP sites (87). After this excision, the DNA ends recombine leaving a single loxP site in place of the intervening sequence. *Cre* recombinase can be expressed under the control of different promoters such as the human glial fibrillary acidic protein (*Gfap*) promoter in the CNS, affecting astrocytes, oligodendroglia, and some neurons or under the fatty acid binding protein (*ap2*) promoter expressed highly in differentiated adipocytes as well as macrophages (88, 89). When the *Cre* system is combined with a loxP-flanked *Egfr* allele, EGFR should be excised in cells expressing the *Cre* recombinase, therefore producing mice where effects of EGFR deficiency can be investigated in specific cell types.

## Energy Homeostasis

Energy homeostasis within the body is based on a balance between energy intake and expenditure. Obesity results from taking in more calories than required for this homeostasis. Energy balance depends on the regulation of two principal systems. First is the peripheral system that senses satiety and energy balance throughout the body and sends that information to the CNS. Second is the CNS itself, which takes these signals along with other neuronal signals for food intake and energy and uses them to regulate homeostasis (90, 91). The peripheral signals come from the adipose tissue, gastrointestinal tract, and other organs via fibers that innervate the nucleus tractus solitarius which then send afferent fibers to the hypothalamus and other regions (30).

Body adiposity is regulated by an endocrine “adiposity” negative feedback loop involving insulin and leptin. Both hormones function in a negative feedback manner to reduce food intake while increasing energy expenditure via actions on target neurons found in the arcuate nucleus (ARC) of the hypothalamus (Figure 4). Such neurons express receptors for insulin and leptin, respond directly to these hormones, and project to key brain areas involved in energy homeostasis, including the paraventricular nucleus and the lateral hypothalamic area (32, 91).

Two key sets of neurons that are important for conveying appetite and energy signals are found in the ARC. One set synthesizes orexigenic neuropeptides agouti-related protein (AGRP) and neuropeptide Y (NPY), which stimulate food intake and decrease energy expenditure throughout the body (30). Ablation of these neurons results in severe anorexia, while over activity results in obesity. Insulin and leptin reduce the expression of these orexigenic neuropeptides (30, 32). The other set of neurons

synthesize  $\alpha$ -melanocyte-stimulation hormone (MSHA), derived from the pro-opiomelanocortin (POMC) precursor molecule, and cocaine- and amphetamine-regulated transcript (CART) anorexigenic neuropeptides and they reduce food intake and increase energy expenditure when stimulated (32). Mutations in the POMC gene lead to profound obesity and insulin and leptin induce the expression of these anorexigenic neuropeptides (30, 92). MSHA binds to its melanocortin receptors (MC3 and MC4) in the brain to elicit a response. In mice lacking the MC4 receptor, hyperphagia and obesity occurs, showing that these receptors are necessary to reduce food intake. Importantly, this has also been noted in humans with mutations in the MC4 receptor (31, 92, 93).

Other peptides that aid in the regulation of energy homeostasis include cholecystokinin (CCK), ghrelin, and peptide YY (PYY). CCK is released upon eating and can decrease food intake in rodents by decreasing NPY levels (78). Ghrelin is a gastric peptide, also produced in the hypothalamus, that possesses orexigenic properties through NPY and AGRP stimulation in the brain to stimulate food intake and appetite (78). PYY is released by cells in the intestines in proportion to food ingested to stimulate POMC neurons in the ARC and inhibit feeding (30).

It has been hypothesized that fatty acid metabolic pathways contribute to the regulation of energy balance and homeostasis within the hypothalamus and in the periphery. During times of energy excess, lipolysis of triglycerides is decreased and during times of energy need lipolysis is increased (92). The regulation of this process in the hypothalamus occurs in response to different stimuli such as diet, insulin, and glucose. It has been demonstrated that enzymes of fatty acid metabolic pathways are highly expressed in hypothalamic neurons involved in regulating feeding behavior (94).

Peripheral tissues such as WAT and BAT are also involved in this energy homeostasis. Both tissues are innervated by the sympathetic nervous system and possess adrenergic receptors, a large family of GPCRs that couple to members of the heterotrimeric G proteins to activate adenylyl cyclase and cAMP-dependent protein kinase A (PKA). PKA then phosphorylates hormone sensitive lipase, which acts upon proteins surrounding the lipid droplet for increased access and lipid breakdown (95, 96). Signaling through PKA has been shown to protect mice from diet-induced obesity, insulin resistance, and dyslipidemia when fed a high-fat diet by increasing lipolysis (97). This is shown in mice with an RIIbeta mutation. Since PKA is composed of two regulatory subunits and two catalytic subunits, this RIIbeta mutation is compensated by an increase in the RI $\alpha$  regulatory subunit, which is more sensitive to cAMP activation and results in a net increase in basal PKA activity (97, 98). In times of energy need, the sympathetic nervous system stimulates GPCRs, namely the  $\beta$ -adrenergic (ARB) receptors, for lipolysis in WAT and non-shivering thermogenesis in BAT (95). ARB3 can also activate the MAPK pathway to account for 15 to 25% of total lipolysis in WAT in rodents. ARA receptors on the other hand are antilipolytic through the inhibition of cAMP production (95, 96, 99). One study using 3T3-L1 preadipocytes showed that ARB3 works through EGFR and Src to activate the MAPK pathway and that inhibition of EGFR with tyrosine kinase inhibitor (TKI) AG1478 inhibits ERK activation and partially blocks lipolysis by an ARB3 agonist (100, 101).

All members of the ERBB family are expressed in the developing and adult human brains. TGFA and EGFR are expressed in a similar pattern in the brain, with both being found in neurons and astrocytes and EGFR also in oligodendrocytes (10, 102, 103).

TGFA is considered the major ligand for EGFR in the CNS and its mRNA is found throughout the brain, being especially high in the hypothalamus, while EGF expression is lower in the hypothalamus and cerebellum. TGFA, EGF, and HBEGF have important roles in the development of the nervous system, from the proliferation of neural progenitor cells to the differentiation of precursor neuronal and glial cells (10). EGF is found in body fluids such as saliva, blood, and cerebrospinal fluid and adult levels in the mice are achieved by four months (102). EGF can act via paracrine, autocrine, or endocrine mechanisms within the CNS and has been shown to work directly in the CNS to suppress food intake. In sheep, administration of mouse EGF for one day led to food intake suppression while intravenous infusion of EGF has been shown to suppress nighttime food intake in rats (102, 103).

### **Obesity Treatment**

Given the increase in overweight and obesity, treatment is a necessity and even a modest weight loss between 5% and 10% is associated with improvements in such risk factors as hypertension, hyperglycemia, and hypercholesterolemia levels, and this weight loss has been shown to increase survival (104). Conventional treatment of obesity includes weight loss through reduced caloric intake and increasing physical activity, however less than 10% of those who lose weight maintain weight loss (38, 48). It has been reported that an overall better clinical profile is noted with less weight, such as with weight loss in moderate and morbid obesity or in individuals of normal body mass index. In overweight or obese people, weight loss shows decreased serum levels of many pro-inflammatory cytokines such as IL6 and TNFA (21, 22, 28, 105, 106). It has also been shown in humans studies that even a modest weight loss brings serum adipokine levels

towards a better overall profile such as decreases in serum leptin, resistin, triglycerides, and cholesterol levels, improvements in insulin sensitivity, and an increase in serum adiponectin (21, 22, 107).

Another way to treat this disease is to look at signaling within the body related to energy homeostasis. The use of drugs that block lipid absorption or increase satiety signals can be used to treat obesity. Such drugs include orlistat, a lipase inhibitor; dexfenfluramine, a serotonin reuptake inhibitor; and sibutramine, which suppresses appetite by also inhibiting serotonin and norepinephrine reuptake (104, 108-110). These drugs can be useful as anti-obesity agents however their side effects may limit usage. Such side effects include cardiovascular complications with dexfenfluramine and sibutramine and gastrointestinal side effects by orlistat (104, 109). Other avenues for treatment include manipulation of neuropeptides that affect food intake. For example, since NPY is a stimulator of feeding, antagonizing this protein may aid in decreasing obesity (110).

New therapies are also being assessed which include pharmacological inhibition of PAI-1 which is synthesized by adipocytes and is increased in obesity (111, 112); inhibition of  $11\beta$ -hydroxysteroid dehydrogenase type 1 which lowers blood glucose and insulin in DIO models (113); and telmisartan inhibition of angiotensin II, which is increased in DIO models (114). These therapies show potential for anti-obesity treatment due to decreases or maintenance of body weight, decreases in percentage of body fat, decreases in cholesterol and triglyceride concentrations, or decreases in perirenal or epididymal fat weight in DIO mice (111, 113, 114). An alternative anti-obesity treatment may be to target EGFR.

EGFR is essential for the regulation of normal cell growth and differentiation. However, aberrant EGFR activation can also result in the initiation of intracellular signaling pathways that promote malignant behavior, including angiogenesis, invasion, metastasis, and inhibition of apoptosis (115-117). EGFR overexpression has been reported in many cancers including breast, head and neck, and colon with EGFR expression correlating with poor clinical outcome (116). Due to these factors, monoclonal antibodies and TKIs have been directed against this receptor. TKIs interact with the intracellular tyrosine kinase domain and inhibit the ligand-induced receptor phosphorylation of EGFR by binding to the receptor's kinase pocket to inhibit signaling cascades (115, 117, 118). AG1478 is a TKI that is highly selective for EGFR with a nanomolar range necessary to inhibit 50% of EGFR signaling, while a micromolar range is needed for other ERBB receptors (2, 5, 119). Others have shown that inhibition of EGF causes an adipocyte-specific weight decrease with no effect on other organ weights (68, 69, 120). Also, when male Swiss mice were fed a HFD for eight weeks and then administered the EGFR TKI PD153035 for two weeks, body weight and fat pad weight decreases were noted (121). Decreased EGFR signaling may decrease low density lipoprotein levels (LDLs), which deliver cholesterol to vascular smooth muscle cells subsequently leading to atherosclerosis through cell proliferation involving EGFR signaling. Therefore, a decrease in EGFR signaling could lead to a decrease in cholesterol levels by inhibiting LDLs and reducing lesion formation (122, 123). Given TKI's specificity to EGFR and adipose specific weight loss, an alternative obesity treatment may be to target EGFR.

## Conclusions

Obesity results from taking in more calories than required for energy homeostasis and can lead to prolonged exposure to lipophilic toxicants. A balance of food intake and energy expenditure, through a highly integrated multi-organ system, determines body weight regulation. Signals relaying energy storage and satiety from the periphery are sent to the CNS where they, along with other neuronal signals, are used to maintain this balance. As a result of the worldwide rise in obesity and obesity-related complications such as diabetes, stroke, and cardiovascular disease, understanding the mechanisms associated with this disease and determining treatment options are necessary. The EGFR is involved in adipogenesis and therefore may contribute to the regulation of energy homeostasis. To assess the role of EGFR in body weight regulation, we first investigated the effects of EGFR inhibition pharmacologically with a small molecule inhibitor against the EGFR tyrosine kinase (AG1478) or genetically with the *Egfr*<sup>wa2</sup> hypomorphic allele in DIO mouse models. We found that EGFR inhibition slows adipose mass deposition due to a decrease in food intake. Therefore, we deleted *Egfr* specifically in peripheral tissues (intestines and adipocytes) and in the CNS using the *Egfr*<sup>tm1Dwt</sup> conditional allele and the *Villin-Cre*, *aP2-Cre*, and *GFAP-Cre*, transgenic lines, respectively, to show the importance of EGFR activity in regulating adipose deposition in energy homeostasis. These studies will aid in our understanding of EGFR signaling within the body with respect to obesity and appetite and metabolism regulation.

Model	Mutation	Phenotype
<i>Egfr</i> <sup>-/-</sup>	Null	Dependent on genetic background; Organ and embryonic abnormalities; Die at different stages of embryogenesis or postnatally (81, 82)
<i>Egfr</i> <sup>wa2</sup>	Hypomorph; Glycine to valine substitution in tyrosine kinase domain	Homozygous mice - mild wavy coat; curly whiskers; endocrine and reproductive disorders (1)
<i>Tgfa</i> <sup>wa1</sup>	Spontaneous mutation in <i>Tgfa</i> locus	Homozygous mice – Wavy coat; curly whiskers; smaller size than controls (83, 84)
<i>Egfr</i> <sup>Dsk5</sup>	Hypermorph; Missense mutation (T to A transversion) and Leu863Gln substitution in tyrosine kinase domain	Abnormal skin pigmentation in footpads and first digit; wavy coat; thick epidermis; increased nail length (85)
<i>Egfr</i> <sup>Wa5</sup>	Dominant negative; Missense mutation (D to G change) in tyrosine kinase domain	Peri and prenatal lethality; Wavy coat; curly whiskers; corneal scarring (74, 86)

**Table 1.** Summary of EGFR mutant models and phenotypes.

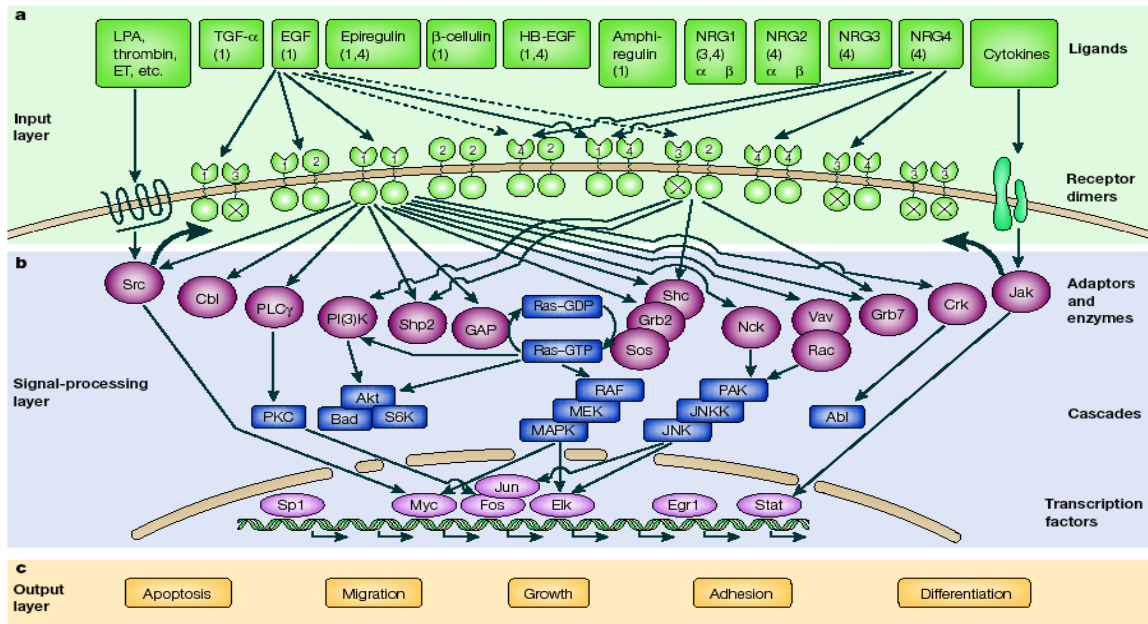


**Figure 1.** The epidermal growth factor receptor family, its ligands, and signaling pathways.

(9)

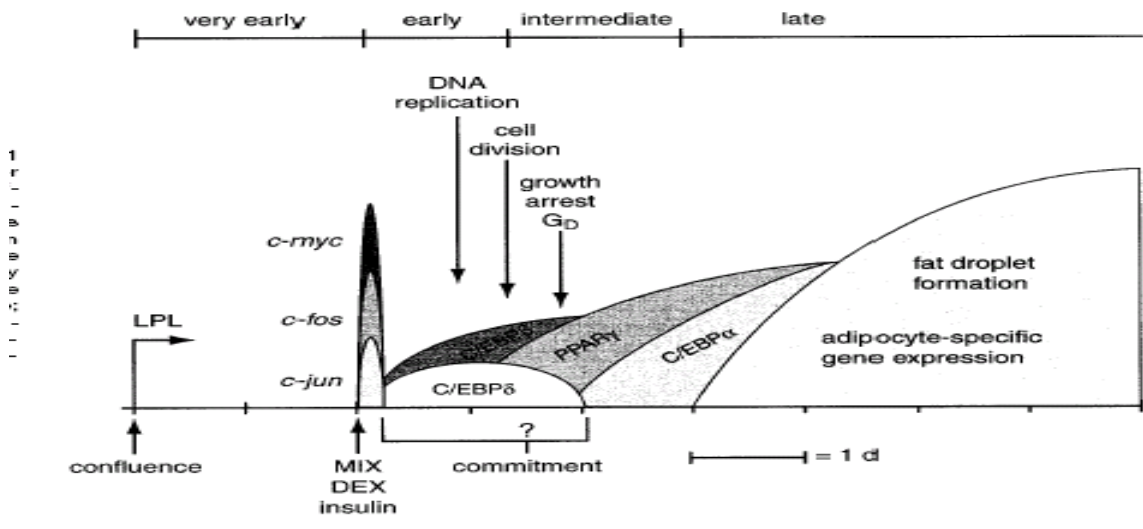


**Figure 2.** Adipogenesis  
(58)

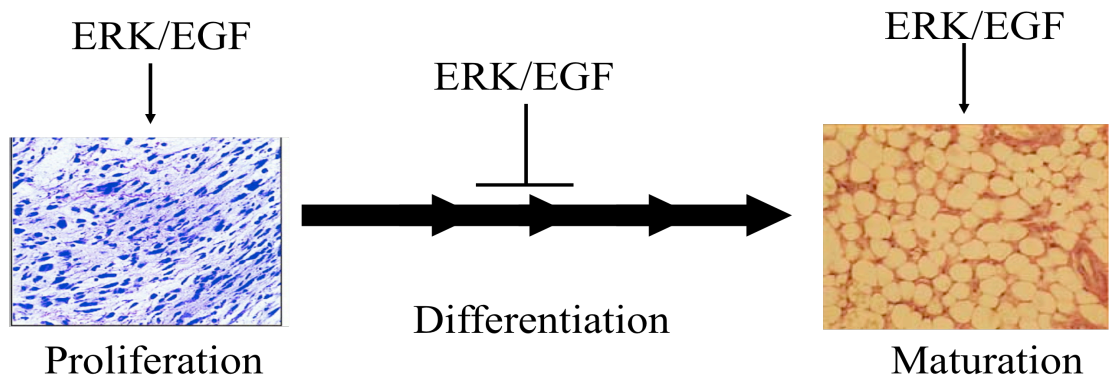


**Figure 3.** EGFR signaling is necessary at specific stages in adipogenesis.

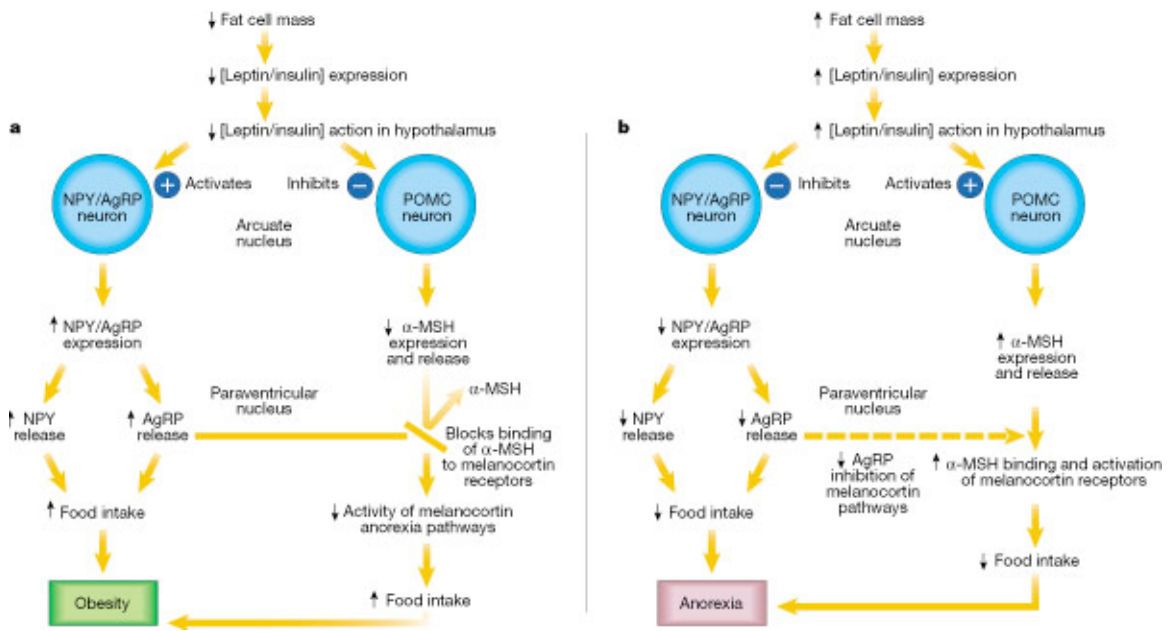


**Figure 4.** Adiposity negative feedback loop.  
 (32)

## CHAPTER 2

# EPIDERMAL GROWTH FACTOR RECEPTOR INHIBITION RESULTS IN DECREASED FAT MASS IN MICE ON A HIGH-FAT DIET DUE TO DECREASED FOOD INTAKE

**Melanie B. Weed,<sup>1</sup> Cordelia J. Barrick,<sup>1</sup> Daniel Pomp,<sup>2</sup> Troy Ghashghaei,<sup>3</sup> and  
David W. Threadgill<sup>1,2</sup>**

*<sup>1</sup>Curriculum in Toxicology, University of North Carolina, Chapel Hill, North Carolina;*

*<sup>2</sup>Department of Genetics, University of North Carolina, Chapel Hill, North Carolina;*

*<sup>3</sup>Department of Molecular and Biomedical Sciences, College of Veterinary Medicine,  
North Carolina State University, Raleigh, North Carolina*

### Abstract

Due to worldwide increases in both the prevalence and incidence of obesity, understanding the mechanisms behind adipose tissue development and energy homeostasis is important. Accumulating evidence suggests that signaling through the epidermal growth factor receptor (EGFR) is required for normal adipocyte development; therefore understanding how this signaling contributes to excess body fat mass is necessary to unravel the mechanisms associated with obesity. Our lab has previously shown that chronic EGFR inhibition decreases adipose mass deposition in a diet-induced obesity model. In this study, we used both pharmacological and genetic mouse models

with suppressed EGFR signaling to further delineate the role of EGFR in diet-induced obesity. Wild-type C57BL/6J mice were chronically exposed to a high-fat western diet with or without a small molecule inhibitor to the EGFR tyrosine kinase, AG1478. In a separate experiment, mice homozygous for the *Egfr*<sup>wa2</sup> mutation, a constitutionally impaired EGFR tyrosine kinase, and their control littermates were also challenged with this WD. Monthly MRI and metabolism endpoints and weekly body weight and food and water intake measurements were collected. Upon sacrifice, heart, liver, and fat depots were dissected, weighed, and stored. Brains were also collected for hypothalamic extraction. In both models, there was significantly less fat mass when EGFR was inhibited. Moreover, decreased food intake, feeding efficiency, and smaller adipocyte size, as well as improvements in overall clinical profile were observed in mice fed AG1478. These results imply that EGFR signaling may be important in regulating energy homeostasis.

### **Introduction**

Obesity is just one of the factors associated with metabolic syndrome, which includes such symptoms as hypertension, insulin resistance, and hyperlipidemia. Metabolic syndrome is also known to be associated with increased inflammatory responses such as cytokine and free fatty acid release (26, 27, 124, 125). Being overweight or obese increases the risk of many diseases and health conditions, including type 2 diabetes, atherosclerosis, cancer, and stroke. Also, childhood obesity is associated with a higher chance of premature death and disability in adulthood (16, 17). Mechanistically, obesity is the result of increased fat mass due to an increase in preadipocyte proliferation and adipocyte differentiation. Recent studies implicating a key

role of EGFR in adipogenesis suggest activation of this signaling pathway may contribute to obesity.

The EGFR family is expressed in a wide range of tissues and cell types that regulate proliferation, differentiation, motility, and apoptosis (1-4). This family consists of four members: ERBB1 (EGFR), ERBB2, ERBB3, and ERBB4 and upon binding of ligands to the extracellular domain of these receptors, homo or heterodimers form to initiate autophosphorylation of tyrosine residues. Signaling cascades, such as the mitogen-activated protein kinase (MAPK) family of extracellular regulated kinases (ERK)-1 and -2, are then initiated which are involved in adipocyte proliferation and differentiation (9, 72). Lipogenic and lipolytic effects are noted for a ligand to EGFR and thus studying EGFR signaling cascades may be an important step in understanding the underlying mechanisms of adipose deposition and obesity (68-70, 73).

We have previously shown that female wild-type C57BL/6J mice chronically exposed to small molecule EGFR inhibitors exhibit decreased weight gain over the course of exposure compared to controls (120). Although we have shown this decrease in weight due to fat mass with EGFR inhibition, the mechanisms have not been studied. Therefore, we sought to determine the mechanisms behind this phenotype by characterizing the metabolic and developmental consequences of EGFR inhibition in male wild-type B6 mice. We found a decrease in food intake and feeding efficiency and smaller adipocytes resulting in fat mass reduction.

## **Materials and Methods**

*Animals and treatment.* Mice were bred in house or obtained from The Jackson Laboratory (Bar Harbor, ME). Aged-matched wild-type C57BL/6J (B6) male mice and

male mice congenic for the *Egfr*<sup>wa2</sup> allele on B6 and 129S1/SvImJ (129/S1) backgrounds were used. Mice were placed on a high-fat western-style diet (WD, Research Diets, D12079B, New Brunswick, NJ, 40% calories from fat) or WD with an inhibitor to the epidermal growth factor receptor (EGFR), AG1478 (WD/INH, LC Labs, Billerica, MA, 0.144g/kg (120)) starting at eight weeks of age for three months. The WD is nutritionally matched with the STD AIN-93G diet (Research Diets, D10012G) except for increased fat and reduced fiber, calcium, and vitamin D, more consistent with the diets consumed by people in North America. In the M16 polygenic obesity mouse model, mice were fed a control low-fat diet (Research Diets, D12450B, 10% calories from fat) with or without AG1478 starting at three weeks of age for two months. Mice had free access to food and water throughout each study. Body weight and food and water intake measurements were collected at the start of the study and every week thereafter. All mice were sacrificed according to an approved University of North Carolina (UNC) Institutional Animal Care and Use Committee's protocol. Inguinal, epididymal, perirenal, and interscapular fat pads, heart, liver, and skeletal muscle were collected and stored at -80°C. Brains were also collected and stored in cold RNAlater for hypothalamic extraction.

*Histology.* At necropsy, inguinal, epididymal, perirenal, and interscapular fat pads were dissected from control and treated B6 mice, rinsed in PBS, and weighed. The fat pads were formalin-fixed and embedded in paraffin. Sections (7-10  $\mu$ m) were prepared at 100  $\mu$ m intervals and stained with hematoxylin and eosin (H&E) for examination of gross appearance and adipocyte size and number. Cell counts and area

measurements were obtained using ImageJ software from at least 200 cells per fat pad (NIH, version 1.41).

*Indirect Calorimetry.* 24-hour caloric expenditure and respiratory exchange rate (RER) were measured by indirect calorimetry from B6 mice fed either the WD or WD/INH once a month starting at eight weeks of age (126). Briefly, mice were housed individually with free access to food and water. Indirect calorimetry was performed using the LabMaster System (TSE Systems, Hamburg, Germany). Oxygen (O<sub>2</sub>) consumption and carbon dioxide (CO<sub>2</sub>) production (ml/kg · h) measures were used to calculate the RER (Volume CO<sub>2</sub> / Volume O<sub>2</sub>).

*Activity.* B6 mice fed either the WD or WD/INH were given access to a running wheel for one week after the calorimetry measurements. Mice were housed individually in a cage with a solid-surface running wheel attached (145-mm diameter, Ware Manufacturing, Phoenix, AZ). Total daily distance (m) and total daily exercise time (sec) were recorded every 24 h for each mouse, with average daily running speed (m/sec) being subsequently calculated by dividing distance by duration.

*MRI.* Body composition was collected by magnetic resonance imaging (MRI) (EchoMRI, Houston, TX) from B6 mice fed either the WD or WD/INH once a month starting at eight weeks of age.

*Blood Biochemical Analyses.* Blood samples were collected at the beginning of the study and monthly thereafter by tail clip or terminal cardiac puncture. Serum cholesterol and triglycerides were analyzed monthly at the UNC Clinical Chemistry Core. Blood glucose levels were measured using a Freestyle Glucose Monitoring System (Abbott Laboratories, Abbott Park, IL). Adipokine measurements including leptin,

adiponectin, insulin, interleukin-6 (IL6), tumor necrosis factor- $\alpha$  (TNFA), plasminogen activator inhibitor-1 (PAI1), and resistin were analyzed using a mouse serum adipokine kit (Linco Research, MADPK-71K, St. Charles, MI) and a BioRad Luminex Instrument (Austin, TX).

*Glucose Tolerance Test.* Mice were fasted overnight prior to administration of the GTT. d-glucose (Sigma, St. Louis, MO) was dissolved in phosphate buffered saline and administered to mice via i.p. injection (2 g/kg). Samples of whole-blood (2–3  $\mu$ l each) were collected from a tail clip bleed immediately before and 15, 30, 60, 90, and 120 minutes after glucose injection. Blood glucose levels were measured using a Freestyle Glucose Monitoring System (Abbott Laboratories, Abbott Park, IL).

*Homeostatic model assessment of insulin resistance.* HOMA-IR calculations were performed using the HOMA Calculator 2.2.2 (University of Oxford, United Kingdom).

*Acid Steatocrit.* In short, 0.05 g of powdered fecal specimen was mixed in 200  $\mu$ L of 1 N perchloric acid. One drop of 0.5% oil red O was added and mixed. Specimens were placed in nonheparinized capillary tubes and spun. Steatocrit was calculated as  $100 \times \text{length of fatty layer} / (\text{length of solid layer} + \text{length of fatty layer})$ .

*Brain processing.* Whole brains were collected in cold RNAlater and processed within 4 hours. 500  $\mu$ m whole brain sections from WD and WD/INH fed mice were obtained using a vibratome (Leica Instruments, Bannockburn, IL) and collected in RNAlater. The hypothalamus was then microdissected using microforceps and tissue isolated by mechanical removal was placed in TRIzol (Invitrogen, Carlsbad, CA) for later RNA extraction.

*Gene expression.* Total RNA was extracted from fat pads and brains of B6 mice fed WD or WD/INH using TRIzol (Invitrogen). 400 ng of total RNA was reverse transcribed using the AffinityScript™ QPCR cDNA synthesis kit (Stratagene, La Jolla, CA). The expression of pre-adipocyte factor (*Pref1*), CAAT/enhancer binding proteins- $\alpha$  and  $\beta$ , (*Cebpa*; *Cebpb*), adrenergic receptor  $\beta_3$  (*Arb3*), fatty acid-binding protein (*aP2*), uncoupling protein-1 (*Ucp1*), interleukin-6 (*Il6*), tumor necrosis factor- $\alpha$  (*Tnfa*), leptin (*lep*), *Egfr*, pro-opiomelanocortin (*Pomc*), and neuropeptide Y (*Npy*) were determined by real-time quantitative PCR (qPCR) using the Brilliant® II QPCR Master Mix (Stratagene) and Assays-on Demand primers and probes (Applied Biosystems, Foster City, CA). Results are represented as mean fold changes relative to controls. Reactions were run on a Stratagene MX3000P machine and threshold cycles (CT) were determined by an in-program algorithm assigning a fluorescence baseline based on readings prior to exponential amplification. Fold change in expression was calculated using the  $2^{-\Delta\Delta C_t}$  method (127), with ribosomal protein 36B4 and 18s rRNA as the endogenous controls for adipose tissue and hypothalamus, respectively.

*Statistics.* Results are expressed as mean  $\pm$  SEM. Unpaired t-tests were used to determine statistical significance of these measurements between treated and control groups using Prism 4.0 (GraphPad). Repeated measures ANOVAs were used to determine statistical significance between energy expenditure and food intake and for GTT (SPSS, Chicago, Illinois) and between control and treated groups with regards to adipokine measurements (SAS, Cary, North Carolina). Statistical significant was considered at  $p < 0.05$ .

## Results

### *Inhibition of EGFR results in reduced fat mass deposition*

Mice homozygous for the waved-2 ( $Egfr^{wa2}$ ) hypomorphic allele, which reduces EGFR activity as much as 90% (1, 128), have significantly lower body weights compared to  $Egfr^{wa2/+}$  littermates with normal EGFR activity (Figure 5A). The reduced body weight observed with  $Egfr^{wa2/wa2}$  mice is a consequence of a reduction in total fat mass with lean mass weights indistinguishable between  $Egfr^{wa2/wa2}$  and their control littermates. This effect of reduced EGFR activity is independent of sex or genetic background as both males and females from B6-  $Egfr^{wa2/wa2}$  or 129/S1-  $Egfr^{wa2/wa2}$  congenic lines display this reduced fat mass compared to their respective control littermates. Furthermore, this effect is independent of diet as mice on a standard chow also have smaller fat masses, albeit not as dramatic as mice on a WD (data not shown). Although only inguinal and interscapular fat pads reached significance, all fat depots trended smaller in  $Egfr^{wa2/wa2}$  mice compared to their control littermates (Figure 5B).

To determine if pharmacological inhibition of EGFR in adult animals could achieve a similar effect as genetic reduction of EGFR that occurs throughout development, wild-type male B6 mice were fed a WD with or without the selective EGFR inhibitor AG1478 (WD/INH). Chronic pharmacological inhibition of EGFR resulted in a lower body weight due to reduced fat mass, which was observed in all fat depots (Figure 5C and Figure 5D, respectively). Other organ weights were unchanged, demonstrating specificity for adipose deposition. Steatocrit was also measured in the feces of these animals and no differences were noted between groups (data not shown). A similar decrease in fat mass deposition with AG1478 administration was also observed

in the M16 polygenic model of obesity, suggesting the effect of reduced EGFR activity on fat deposition is not specific to a diet-induced model (data not shown).

*Reduced fat mass is due to decreased food intake and feeding efficiency*

In order to identify the physiological mechanism responsible for this fat mass phenotype observed with decreased EGFR signaling, wild-type male B6 mice on the WD or WD/INH were placed in individual calorimeter cages to measure RER and energy expenditure. AG1478 administration resulted in a significant reduction in food intake as compared to WD alone (Figure 6A) with no difference in water intake between groups (data not shown). Mice on the WD/INH also showed a lower feeding efficiency as compared to mice on the WD alone throughout the study (Figure 6B). A lower energy expenditure was observed throughout the study in mice on the WD/INH compared to WD alone. However, when normalized to food intake, the differences were not significant (Figure 6C). There were also no significant differences in RER (Figure 6D) or in voluntary wheel running (data not shown) between groups.

In addition to measuring energy expenditure indirectly with calorimetry, energy usage by thermogenesis was also measured by determining transcript levels of *Ucp1* in both epididymal (white) and interscapular (brown) adipose tissue. UCP1 is found in the mitochondria of brown adipose tissue and is used to generate heat from stored metabolic energy in non-shivering thermogenesis (129). In both white and brown fat, *Ucp1* transcript levels in animals fed WD/INH were not different from mice fed only the WD (Figure 7).

To determine if EGFR or neuropeptides involved in feeding and energy were altered in the hypothalamus of mice fed the WD/INH, whole brains were sectioned and

the hypothalamus mechanically removed. qPCR was used to assess transcript levels of *Egfr*, anorexogenic neuropeptide *Pomc*, and orexogenic neuropeptide *Npy*. No differences were observed between groups (Figure 8).

#### *Inhibition of EGFR results in smaller adipocytes*

To determine if reduced EGFR signaling impacted adipocyte histology, fat pads were sectioned and the number of adipocytes counted and normalized to the fat pad weights. Significantly smaller cell area and more adipocytes per fat pad weight were observed in mice administered WD/INH compared to WD alone (Table 2 and Figure 9). To establish possible causes for the difference in adipocyte size and number, qPCR was used to assess transcript levels of adipocyte stage-specific factors in epididymal tissue. Preadipocytes were assessed with *Pref1* while mature adipocytes were assessed with *Cebpa*, *Cebpb*, *Arb3*, and *aP2* in epididymal fat pads of these mice. EGFR inhibition caused a significant decrease in *Cebpb* mRNA levels in mice fed a WD/INH (Figure 10), however other adipocyte-specific markers were not different between groups.

#### *EGFR inhibition leads to improved clinical parameters*

To examine the broader clinical consequences of EGFR inhibition, cholesterol, triglyceride, glucose, insulin, and adipokine levels were analyzed in the blood and serum, and expression levels of *lep* and pro-inflammatory cytokines *Il6* and *Tnfa* in the epididymal fat pads. Compared to the mice fed WD alone, mice fed WD/INH showed a significantly improved clinical profile for cholesterol and glucose as well as decreased *lep* and *Il6* mRNA levels in the fat pads, consistent with lower fat mass in these animals (Table 3; Figure 11). To test whether EGFR inhibition is associated with improved insulin resistance in a DIO mouse model, we evaluated insulin sensitivity through

measuring homeostasis model assessment of insulin resistance (HOMA-IR) and a glucose tolerance test (GTT). Insulin levels were higher in these animals, however intraperitoneal GTT and HOMA-IR levels were not different between groups (Figure 12 and Figure 13, respectively). Consistent with these results, lower cholesterol levels were observed in *Egfr<sup>wa2/wa2</sup>* mice compared to control littermates on WD (data not shown). Although values of other clinical parameters measured were not significant at 20 weeks (PAI-1/SERPINE1, resistin, and adiponectin; data not shown), there was a trend to an overall improved clinical profile for all parameters with EGFR inhibition.

### Discussion

Results reported here demonstrate that pharmacological or genetic inhibition of EGFR leads to a reduced fat mass deposition due to decreased food intake and feeding efficiency. Others have shown that inhibition of an EGFR ligand, EGF, causes an adipocyte-specific weight decrease with no effect on other organ weights (68, 69, 120), similar to what was observed here. The decreased fat mass observed in this study due to pharmacological inhibition is not due to the taste or toxicity of AG1478. We can conclude that this decreased fat mass was not due to the taste of the food because we noted this same weight phenotype using the *Egfr<sup>wa2</sup>* fed only the WD. Also, when male Swiss mice were fed a WD for eight weeks and then administered an EGFR TKI, PD153035 for two weeks afterwards, similar body weight and fat pad weight decreases were noted (68, 69, 120, 121). As for the toxicity of AG1478, our lab has detected no signs of lethargy, dehydration, or ataxia or differences in heart, liver, or kidney weights in wild-type male and female mice fed a control diet with AG1478 for 90 days. Also, this pharmacological treatment did delay weight gain in these animals, although treatment and

control groups gained weight over the course of the experiment (120).

Consistent with this decrease in food intake, EGFR inhibition resulted in less efficient conversion of food intake to body weight gain. However, due to the decrease in feeding efficiency in these animals, a decrease in food intake alone is insufficient to produce this reduced fat mass. Energy homeostasis is regulated through a balance between food intake and energy expenditure. Energy expenditure can be measured indirectly as oxygen consumption and carbon dioxide output (RER) and directly as voluntary wheel running, home cage activity, such as climbing, rearing, foraging and grooming, and heat production or thermogenesis (130). There were no differences in energy expenditure, RER, or voluntary wheel running between groups. We have not measured home cage activity to see if an increase could be a reason why these mice fed WD/INH are leaner than their WD only fed littermates. Wheel running may or may not be a direct reflection of home cage activity in mice fed a HFD since some studies show increased home cage activity with increased wheel running while others show no change in home cage activity but decreases in wheel running (130-132). Therefore this measurement should be determined to see if differences in home cage activity are aiding in this weight loss. In terms of thermogenesis, UCP1 is found in the mitochondria of brown adipose tissue and is used to generate heat from stored metabolic energy by non-shivering thermogenesis in hibernating mammals and in human infants (95, 129). It has been shown in mice with increased expression of *Ucp1* in adipose depots that a lean phenotype occurs even when fed a high-fat diet (95). However, although mice fed WD/INH in this study were leaner than their control littermates, their levels of *Ucp1* in epididymal and interscapular brown fat were not different. Perirenal, inguinal, and other

subcutaneous white adipose depots possess more capacity for brown adipocytes than visceral depots and therefore we should analyze the other fat depots collected for brown adipocytes and *Ucp1* expression (133, 134). This data now however suggests that this body weight and adipose phenotype is due to the decrease in food intake, not to the recruitment of brown adipocytes and increased thermogenesis.

Neuronal signaling within the arcuate nucleus (ARC) of the hypothalamus dictates food intake and energy expenditure. We first wanted to determine if EGFR expression was affected within the hypothalamus in WD/INH fed mice. EGFR is expressed within the hypothalamus however it was not altered by treatment. We next wanted to determine if alterations in neuropeptides in the ARC associated with feeding were different between groups. Two sets of neurons are found in the ARC; one synthesizes orexigenic neuropeptide NPY, which stimulates food intake and decreases energy expenditure, and the other synthesizes anorexigenic neuropeptide POMC, which reduces food intake and increase energy expenditure (32, 92). Insulin and leptin reduce the expression of orexigenic neuropeptides and induce expression of anorexigenic neuropeptides (31, 93). No differences in expression levels of either neuropeptide were observed in the hypothalamus of these mice. This suggests that EGFR inhibition with AG1478 is not enough to alter mRNA expression of *Egfr* within the ARC, nor the neuropeptides associated with feeding and energy. However, AG1478 may alter these neuropeptides and produce this decrease in food intake without measurable differences in mRNA expression. Other possible mechanisms of this decreased food intake without NPY or POMC alteration include AG1478 altering other satiety or appetite

neurotransmitters in the brain such as serotonin, dopamine, or melanocyte-stimulating hormone (135).

Since a decrease in fat mass could be due to a reduction in adipocyte cell size and/or a decrease in cell number, we histologically analyzed fat pads from mice fed the WD or WD/INH. Adipocyte cell size is smaller and cell number per fat pad mass larger in the fat pads of mice fed WD/INH. To determine causes for these differences between groups, we analyzed adipocyte-stage specific genes found in preadipocytes, *Pref1*, and in mature adipocytes, *Cebpa*, *Cebpb*, *Arb3*, and *aP2*. We observed a significant decrease in *Cebpb* mRNA levels however, expression of other adipocyte genes were not different between groups. *Cebpb* is one of the first transcription factors induced after the induction of differentiation and it promotes the transcription of a number of other adipogenic genes such as *Cebpa*, *Arb3*, and *aP2* (49, 58, 59). Although *Cebpb* is essential for the expression of *Cebpa* and other mature adipocyte markers *in vitro* for adipocyte differentiation, *in vivo* it has been shown that these factors can be induced without *Cebpb* expression (49). This suggests that EGFR inhibition does not inhibit differentiation of preadipocytes, rather it may cause an arrested differentiation of these cells, given the smaller droplets noted in the fat pads of these animals. This has been noted in *Cebpb*<sup>-/-</sup> and *Cebpb/Cebpd*<sup>-/-</sup> mice whose epididymal fat pads were significantly smaller than their control littermates, although adipocyte-specific markers *aP2* and *Cebpa* were not different between groups (49).

Obesity is thought to be a state of low-grade systemic inflammation with levels of adipokines such as TNFA and IL6 elevated in serum and adipose tissue. It is a complex metabolic disorder associated with hyperglycemia, insulin resistance, hypertension, and

atherosclerosis. Disruption in the production and circulation of adipokines such as leptin, adiponectin, resistin, PAI1, and insulin, occurs when energy balance is skewed, as in obesity, and when obesity is reduced these adipokines can be brought into balance again (22, 23, 28, 29, 68). Diets high in fat are also known to cause insulin resistance and signs of inflammation which disrupts adipokine levels. It has been reported that an overall better clinical profile such as decreases in serum leptin, resistin, triglycerides, cholesterol, pro-inflammatory cytokines, improvements in insulin sensitivity, and an increase in serum adiponectin is noted with less weight, such as with weight loss in moderate and morbid obesity or in individuals of normal body mass index (21, 22, 28, 105, 106). Our results show a significant delay in the amount of weight gained in animals fed the WD/INH and this weight retardation lead to a significant decrease in serum cholesterol levels. Also observed were significant decreases in mRNA expression levels of *lep* and *I/6* between groups, consistent with less fat mass noted in these animals. This decrease in cholesterol levels could be associated with low density lipoprotein levels (LDLs) and decreased EGFR signaling. LDLs deliver cholesterol to vascular smooth muscle cells subsequently leading to atherosclerosis through cell proliferation involving EGFR. Therefore, a decrease in EGFR signaling could lead to a decrease in cholesterol levels as noted in this study by inhibiting LDL levels and reducing lesion formation (122, 123). Changes in fat mass can also be associated with changes in glucose and insulin homeostasis. With our experiment, glucose levels were significantly lower in mice fed the WD/INH, however in performing the GTT, these animals did not clear glucose differently. However, since insulin levels were higher in mice fed the WD/INH, these glucose levels may be just high enough to alter this homeostasis despite the lower fat

mass and glucose levels in these animals, although increased insulin resistance is not noted (136). Triglycerides, glucose, and serum and expression levels of other adipokines were not significantly altered however these levels were trending towards a better profile. Perhaps if these mice were fed the WD/INH for a longer period of time, this better clinical profile would be noted. Therefore, besides potential cholesterol modulation, these changes are most likely due to less fat mass observed with EGFR inhibition, rather than EGFR directly mediating these changes in clinical parameters.

In conclusion, we have shown that inhibition of EGFR with a small molecule, AG1478, in wild-type B6 mice fed a WD, causes a decrease in body weight due to a decrease in food intake and feeding efficiency. Also observed in mice fed WD/INH is a decrease in adipocyte cell size within the fat pads and decreases in some clinical parameters suggesting a better overall clinical profile. Future experiments include evaluating the role of EGFR in this food intake phenotype by addressing the role of EGFR signaling in energy homeostatic signaling.

Fat pad	Average cell counts/fat pad weight			Average cell area ( $\mu\text{m}^2$ )			
	WD	WD/INH	[INH/WD] (%)	WD	WD/INH	[INH/WD] (%)	Fat pad wt [INH/WD] (%)
Epididymal	79 $\pm$ 10	144 $\pm$ 16*	181	3,364 $\pm$ 273	2,995 $\pm$ 59	89	75**
Inguinal	271 $\pm$ 41	520 $\pm$ 71*	192	2,529 $\pm$ 179	1,715 $\pm$ 179*	68	74*
Perirenal	290 $\pm$ 28	604 $\pm$ 95*	208	3,087 $\pm$ 397	2,869 $\pm$ 185	93	68**

**Table 2.** Effects of EGFR inhibition on adipocyte number and size.

B6 mice fed a WD or WD /INH at 20 weeks of age (N=5-8 animals per fat pad). Results are mean  $\pm$  SEM. Statistical significance: \*  $P < 0.05$  vs. WD.

Parameter	WD	WD/INH
Cholesterol, mg/dL	230 ± 8	184 ± 8**
Triglycerides, mg/dL	89 ± 17	75 ± 9
Blood Glucose, mg/dL	161 ± 18	112 ± 3.7***
Insulin, ng/mL	1.21 ± 0.12	1.66 ± 0.35*
Leptin, ng/mL	14.59 ± 2.6	8.57 ± 1.2
IL6, pg/mL	10.6 ± 4.3	5.69 ± 0.88
TNFA, pg/mL	3.36 ± 0.30	4.52 ± 0.88

**Table 3.** Effects of pharmacological EGFR inhibition on clinical serum parameters.

Measurements at 20 weeks of age. N=8 per group. Results are mean ± SEM. Statistical significance: \*  $P < 0.05$ , \*\*  $P < 0.01$ , and \*\*\*  $P < 0.0001$  vs. WD.

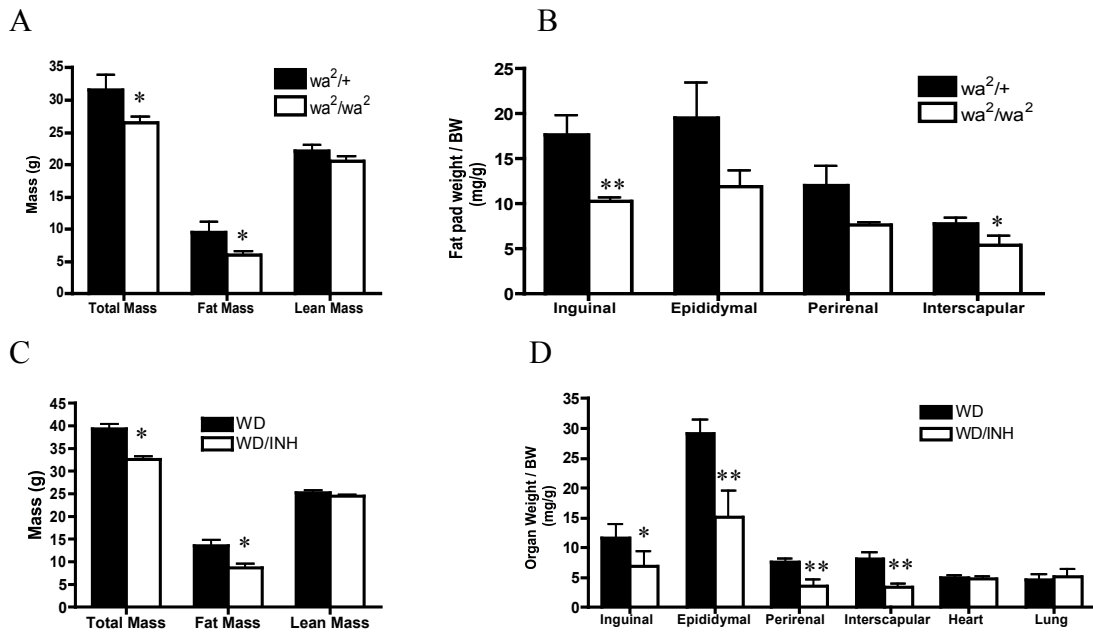


**Figure 5.** Effects of genetic or pharmacological inhibition of EGFR on body weight and fat mass.

Magnetic Resonance Imaging and normalized organ weights of *Egfr*<sup>wa2</sup> littermates (N=7 (*Egfr*<sup>wa2/+</sup>); N=4 (*Egfr*<sup>wa2/wa2</sup>)) (A, B) or wild-type C57Bl/6J (C, D) mice fed a WD (N=8) or WD/INH (N=8). Results are expressed as the mean  $\pm$  SEM. Statistical significance: \* $P < 0.05$  vs. *wa*<sup>2/+</sup> or WD; \*\*  $P < 0.01$  vs. *wa*<sup>2/+</sup> or WD.

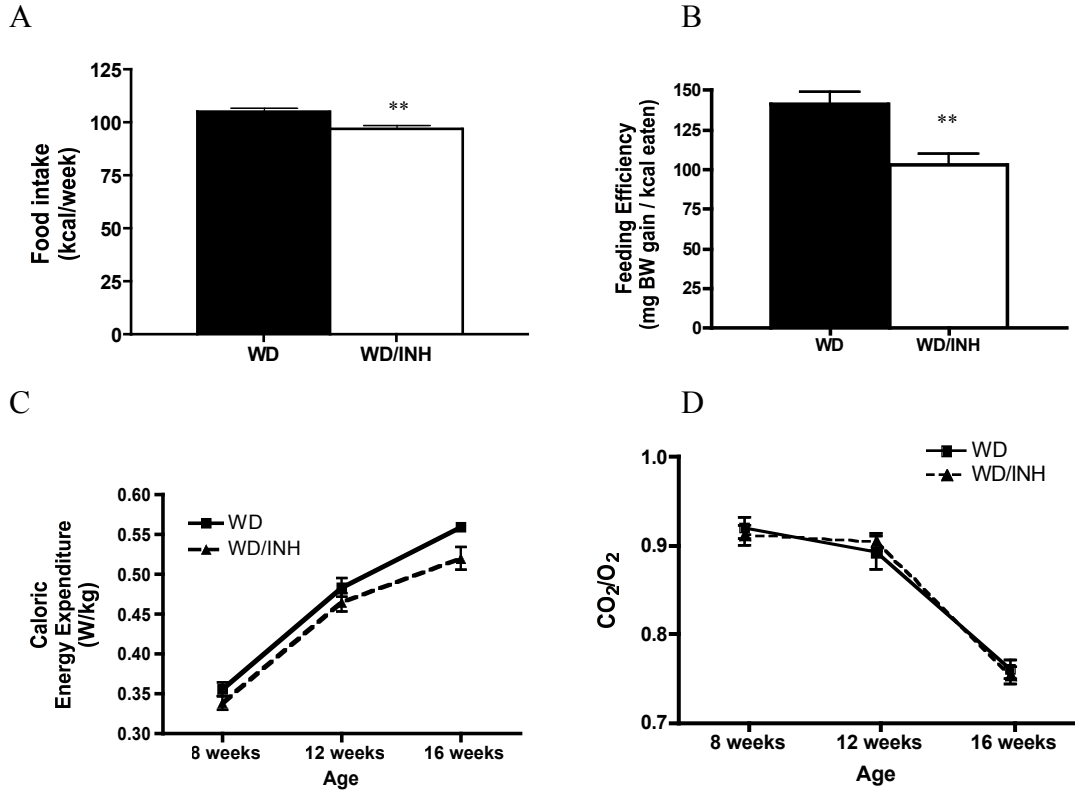


**Figure 6.** Effect of pharmacological EGFR inhibition on feeding and metabolic parameters.

Food intake/week (A), feeding efficiency (B), energy expenditure (C) and RER (D) in wild-type male B6 mice. Mice were placed on a WD (N=8) or WD/INH (N=8) for 3 months. Energy expenditure is in watts of caloric energy expended per kg of body weight. Results are mean  $\pm$  SEM. Statistical significance: \*\*  $P < 0.01$  vs. WD.

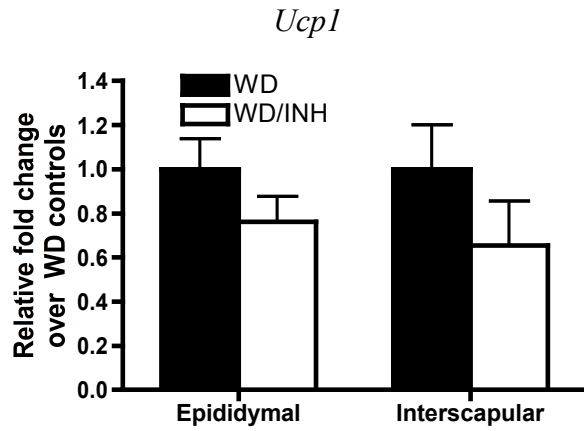


**Figure 7.** Effect of pharmacological EGFR inhibition on uncoupling protein-1 expression.

Epididymal and interscapular fat of B6 mice at 20 weeks of age fed the WD (N=8) or WD/INH (N=8). Results are mean  $\pm$  standard error.

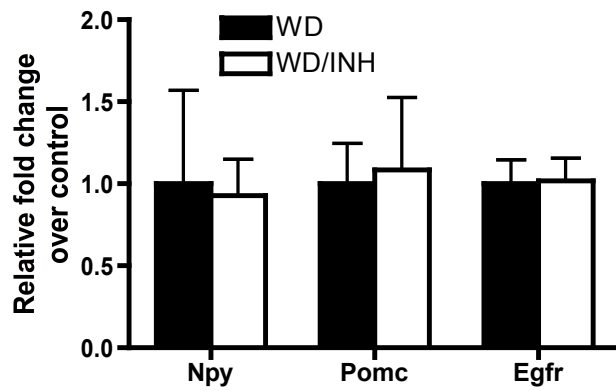
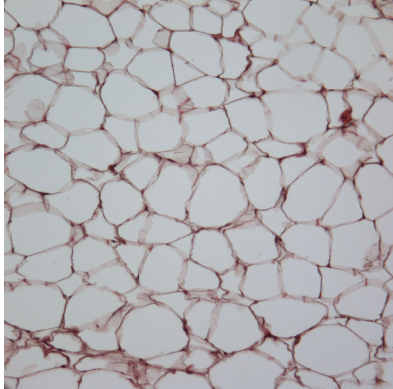


**Figure 8.** Effect of pharmacological EGFR inhibition on hypothalamic *Egfr* and neuropeptide expression.

*Egfr*, *Pomc*, and *Npy* mRNA levels in B6 mice at 20 weeks of age fed the WD (N=8) or WD/INH (N=8). Results are mean  $\pm$  standard error.

A



B

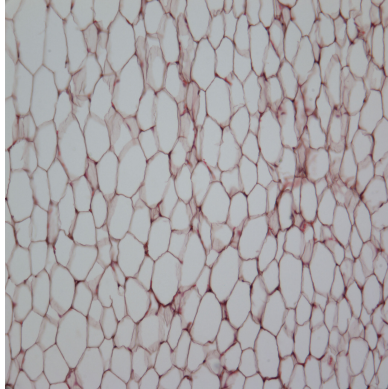


**Figure 9.** Representative inguinal fat pad histology sections from control and EGFR inhibited mice.

Representative images depicting inguinal fat pads of B6 mice fed a WD (A) or WD/INH (B) at 20 weeks of age. 7-10 $\mu$ m sections. 20x magnification.

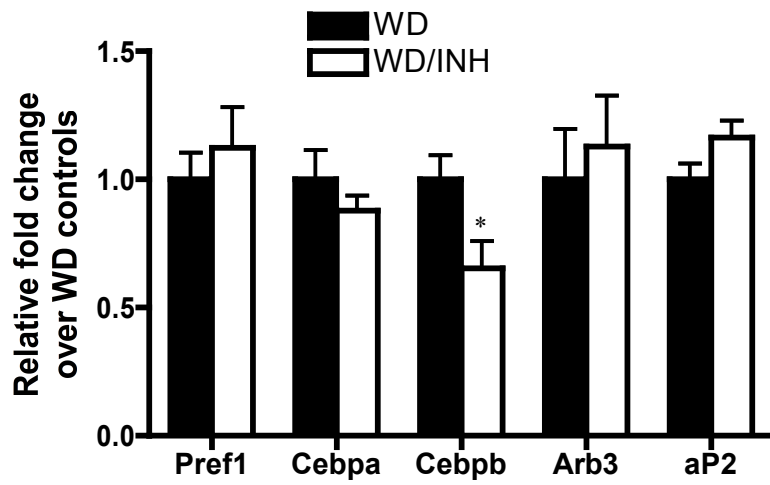


**Figure 10.** Effect of pharmacological EGFR inhibition on adipocyte-specific factors in epididymal fat.

B6 mice at 20 weeks of age fed WD (N=8) or WD/INH (N=8). Results are mean  $\pm$  standard error. Statistical significance: \*  $P < 0.05$  vs. WD.

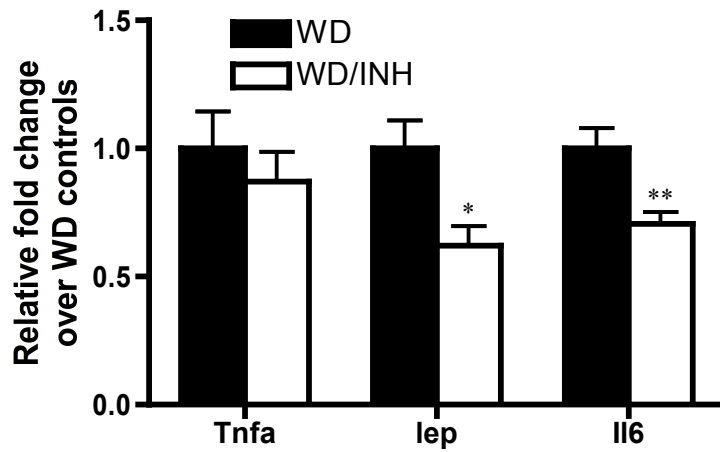


**Figure 11.** Effect of pharmacological EGFR inhibition on adipokine transcript expression in epididymal fat.

20 week old B6 mice fed WD (N=8) or WD/INH (N=8). Results are mean  $\pm$  standard error. Statistical significance: \*  $P < 0.05$  vs. WD, \*\*  $P < 0.01$  vs. WD.

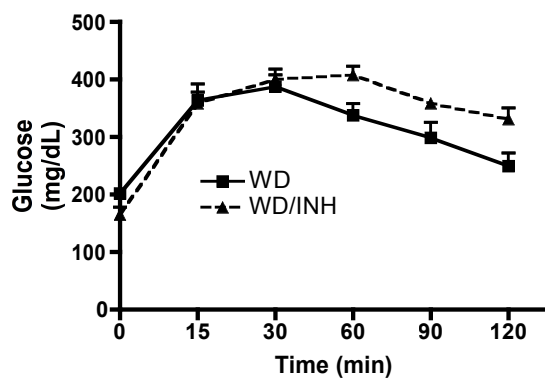


**Figure 12.** Glucose tolerance test measurements from B6 control and EGFR inhibited mice.

20 week old B6 mice fed WD (N=8) or WD/INH (N=8). Results are mean  $\pm$  SEM.

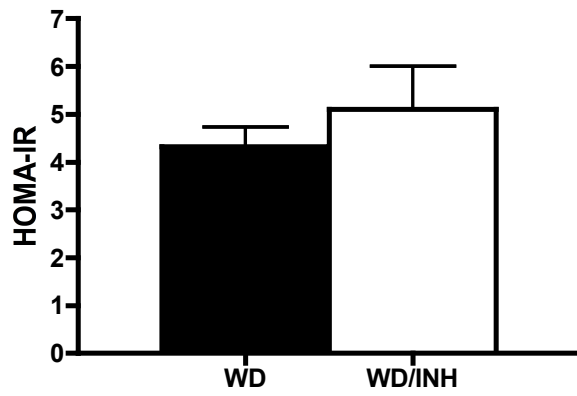


**Figure 13.** Effect of pharmacological EGFR inhibition on HOMA-IR measurements. 20 week old B6 mice fed WD (N=8) or WD/INH (N=8). Results are mean  $\pm$  SEM.

## CHAPTER 3

### EGFR SIGNALING IS IMPORTANT IN THE CENTRAL NERVOUS SYSTEM FOR MAINTAINING ENERGY HOMEOSTASIS

**Melanie B. Weed,<sup>1</sup> Tang-Cheng Lee,<sup>2</sup> Troy Ghashghaei,<sup>3</sup> and David W. Threadgill<sup>1,2</sup>**

<sup>1</sup>*Curriculum in Toxicology, University of North Carolina, Chapel Hill, North Carolina,*

<sup>2</sup>*Department of Genetics, University of North Carolina, Chapel Hill, North Carolina, and*

<sup>3</sup>*Department of Molecular and Biomedical Sciences, College of Veterinary Medicine,*

*North Carolina State University, Raleigh, North Carolina*

#### Abstract

Obesity results from an imbalance between energy intake and energy expenditure and a highly integrated multi-organ system regulates body weight. Signals relaying energy storage and satiety from the periphery are sent to the central nervous system (CNS) where they along with other neuronal signals are used to maintain energy homeostasis. The epidermal growth factor receptor (EGFR) is involved in adipogenesis and therefore may contribute to energy homeostatic regulation. Using a diet-induced obesity mouse model, we found that inhibition of EGFR either genetically with the *Egfr*<sup>wa2</sup> hypomorphic allele or pharmacologically with a small molecule inhibitor against the EGFR tyrosine kinase (AG1478) slows adipose mass deposition due to a decrease in

food intake. To determine the role of EGFR in adipose deposition within energy homeostatic regulation, we deleted *Egfr* specifically in peripheral tissues (intestines and adipocytes) and in the CNS using the *Egfr<sup>tm1Dwt</sup>* conditional allele and the *Villin-Cre*, *aP2-Cre*, and *GFAP-Cre* transgenic lines, respectively. All mice were fed a high-fat western diet over three months. Body weight and MRI measurements were collected monthly and upon sacrifice, heart, liver, and fat depots were dissected, weighed, and stored. Brains were also collected for later hypothalamic extraction. Ablation of EGFR within the intestinal epithelium and adipocytes showed no effect on adipose deposition. However, deletion specifically within the CNS caused a significant reduction in adipose mass with consequent smaller adipocytes in fat pads, hyperphagia, increased energy expenditure, and improved clinical profile. The phenotype is due in part to increases in energy expenditure from hyperactivity, thermogenesis, and white adipose tissue lipolysis.

## **Introduction**

The balance between food intake and energy expenditure is regulated through a highly integrated multi-organ system. Satiety and adiposity signals from the intestines and adipose tissue are sent to the central nervous system (CNS) where they, along with other neuronal signals, are used to maintain this balance. Obesity results from taking in more calories than expended and is just one of the factors associated with metabolic syndrome, which includes such symptoms as hypertension, insulin resistance, and hyperlipidemia. Metabolic syndrome is also known to be associated with increased inflammatory responses such as cytokine and free fatty acid release (26, 27, 124, 125). Being overweight or obese increases the risk of many diseases and health conditions, including type 2 diabetes, atherosclerosis, cancer, and stroke (16, 17). Recent studies

implicating a key role of the epidermal growth factor receptor (EGFR) in adipogenesis suggest signaling through this receptor may contribute to obesity, and therefore in the regulation of energy homeostasis.

The EGFR is the prototypical member of the ERBB family, which are expressed in a wide range of tissues and cell types and regulate a number of cellular processes such as proliferation, differentiation, motility, apoptosis, and survival (1-4). The ERBB family consists of four members: ERBB1 (EGFR), ERBB2, ERBB3, and ERBB4 and upon binding of ligands to the extracellular domain, these receptors homo or heterodimerize to initiate autophosphorylation of tyrosine residues (3-6). Signaling cascades, such as the mitogen-activated protein kinase (MAPK) family of extracellular regulated kinases (ERK)-1 and -2, are then initiated, many of which are involved in adipocyte proliferation and differentiation (9, 72). Lipogenic and lipolytic effects have also been reported for EGFR ligands (68-70, 73). Thus studying EGFR signaling is important for understanding the underlying mechanisms of adipose deposition and obesity.

We have shown that EGFR inhibition, either pharmacologically or genetically, decreases adipose deposition in mice fed a high-fat western diet (WD), but does not affect the mass of other organs. Also, we have shown that this decrease in fat mass is due to a reduction in food intake without changes in energy expenditure. Therefore, given this adipose specificity and feeding phenotype, we examined the molecular mechanisms underlying this reduction in adipose mass. We modeled a typical WD and determined the effect on adipose deposition and energy homeostasis when *Egfr* was specifically deleted in adipocytes, intestines, and the CNS using the *ap2-Cre*, *Villin-Cre*, and *GFAP-Cre* transgenic mouse lines, respectively.

## Methods and Materials

*Animals and treatment.* *ap2-Cre*, *Villin-Cre*, and *GFAP-Cre* transgenic mice were mated with *Egfr*<sup>fllox/+</sup> or *Egfr*<sup>fllox/fllox</sup> mice (137, 138). *ap2-Cre* (and *Villin-Cre* and *GFAP-Cre*) x *Egfr*<sup>fllox/fllox</sup> male mice with their control littermates (*-Cre*, *-CreEgfr*<sup>fllox/+</sup>, *Egfr*<sup>fllox/+</sup>, or *Egfr*<sup>fllox/fllox</sup>) were started on a high-fat western diet (WD, Research Diets, D12079B, New Brunswick, NJ, 40% calories from fat) (113) at eight weeks of age for three months. The WD is nutritionally matched with the STD AIN-93G diet (Research Diets, D10012G) except for increased fat and reduced fiber, calcium, and vitamin D, more consistent with the diets consumed by people in North America. Mice had free access to food and water throughout each study. Body weight and food and water intake measurements were collected at the start of the study and every week thereafter. All mice were sacrificed according to an approved University of North Carolina (UNC) Institutional Animal Care and Use Committee's protocol. Inguinal, epididymal, perirenal, and interscapular fat pads, heart, liver, and skeletal muscle were collected and stored at -80°C. Brains were also collected and stored in cold RNAlater for hypothalamic extraction.

*Genotyping.* Genotyping was performed by PCR to determine presence of *Cre* and floxed alleles. The *Egfr*<sup>fllox</sup> allele was amplified from genomic DNA for 35 cycles (30 s at 94°C, 1 min at 60°C, and 1 min at 72°C). The primers used were lox3s: 5'CTTTGG-AGAACCTGCAGATC-3' and lox3as: 5'CTGCTACTGGCT-CAAGTTTC-3'. A 375 bp PCR product was detected from the *Egfr*<sup>fllox</sup> allele and a 320 bp PCR product from the wild-type allele. For the *Egfr*<sup>Δ</sup> allele showing *Egfr* excision, genomic DNA was amplified for 40 cycles (30 s at 94°C, 20 s at 60°C, and 20 s at 72°C). The primers used were Delta-

3: 5'-CTCAGCCAGATGATGTTGAC-3' and Delta-4: 5'-CCTCGTCTGTGGAAGA-ACTA-3'. A 129 bp PCR fragment was detected from the *Egfr*<sup>A</sup> allele. For the *Cre* transgene, DNA was amplified for 38 cycles (30 s at 94°C, 1 min at 56°C, and 1 min at 72°C) with primers CRE-1: 5'-GTGATGAGGTTTCGCAA-GAAC-3' and CRE-2: 5'AGCATTGCTGTCACTTGGTC-3'. A 278 bp PCR fragment was generated from the *Cre* transgene. All PCR products were run on a 3% agarose gel at 150mV for 25 minutes and all reactions used Taq DNA polymerase (Qiagen, Germantown, MD) and a GeneAmp PCR system 9700 (Applied Biosystems, Foster City, CA).

*Indirect Calorimetry.* 24-hour caloric expenditure, oxygen consumption, and respiratory exchange rate (RER) were measured by indirect calorimetry from *GFAP-Cre Egfr*<sup>lox/lox</sup> mice and their control littermates once a month starting at eight weeks of age (126). Briefly, mice were housed individually with free access to food and water. Indirect calorimetry was performed using the LabMaster System (TSE Systems, Hamburg, Germany). Oxygen (O<sub>2</sub>) consumption and carbon dioxide (CO<sub>2</sub>) production (ml/kg · h) measures were used to calculate the RER (Volume CO<sub>2</sub> / Volume O<sub>2</sub>).

*Activity.* *GFAP-Cre Egfr*<sup>lox/lox</sup> mice and their control littermates were given access to a running wheel for one week after the calorimetry measurements. Mice were housed individually in a cage with a solid-surface running wheel attached (145-mm diameter, Ware Manufacturing, Phoenix, AZ). Total daily distance (m) and total daily exercise time (sec) were recorded every 24 h for each mouse, with average daily running speed (m/sec) being subsequently calculated by dividing distance by duration.

*Acid Steatocrit.* In short, 0.05 g of powdered fecal specimen was mixed in 200 µL of 1 N perchloric acid. One drop of 0.5% oil red O was added and mixed. Specimens

were placed in nonheparinized capillary tubes and spun. Steatocrit was calculated as  $100 \times \text{length of fatty layer} / (\text{length of solid layer} + \text{length of fatty layer})$ .

*Blood Biochemical Analyses.* Blood samples were collected at the beginning of the study and monthly thereafter by tail clip or terminal cardiac puncture. Serum cholesterol and triglycerides were analyzed monthly at the UNC Clinical Chemistry Core. Blood glucose levels were measured using a Freestyle Glucose Monitoring System (Abbott Laboratories, Abbott Park, IL). Adipokine measurements including leptin, insulin, tumor necrosis factor- $\alpha$  (TNFA), plasminogen activator inhibitor-1 (PAI1), and resistin were analyzed using a mouse serum adipokine kit (Linco Research, MADPK-71K, St. Charles, MI) and a BioRad Luminex Instrument (Austin, TX).

*Glucose Tolerance Test.* Mice were fasted overnight prior to administration of the GTT. d-glucose (Sigma, St. Louis, MO) was dissolved in phosphate buffered saline and administered to mice via i.p. injection (2 g/kg). Samples of whole-blood (2–3  $\mu$ l each) were collected from a tail clip bleed immediately before and 15, 30, 60, 90, and 120 minutes after glucose injection. Blood glucose levels were measured using a Freestyle Glucose Monitoring System (Abbott Laboratories, Abbott Park, IL).

*Homeostatic model assessment of insulin resistance.* HOMA-IR calculations were performed using the HOMA Calculator 2.2.2 (University of Oxford, United Kingdom).

*Brain processing.* Whole brains were collected in cold RNAlater and processed within 4 hours. 500  $\mu$ m whole brain sections from control and *GFAP-Cre Egfr<sup>fllox/fllox</sup>* mice were obtained using a vibratome (Leica Instruments, Bannockburn, IL) and collected in RNAlater. The hypothalamus was then microdissected using microforceps

and tissue isolated by mechanical removal was placed in TRIzol (Invitrogen, Carlsbad, CA) for later RNA extraction.

*Gene expression.* Total RNA was extracted from fat pads and brains using TRIzol (Invitrogen). 400 ng of total RNA was reverse transcribed using the AffinityScript™ QPCR cDNA synthesis kit (Stratagene, La Jolla, CA). The expression of pre-adipocyte factor-1 (*Pref1*), CAAT/enhancer binding proteins- $\alpha$  and  $\beta$ , (*Cebpa* and *Cebpb*), adrenergic receptor  $\beta$ 3 (*Arb3*), fatty acid-binding protein (*aP2*), leptin (*lep*), uncoupling protein-1 (*Ucp1*) and *Ucp3*, tumor necrosis factor- $\alpha$  (*Tnfa*), *Egfr*, pro-opiomelanocortin (*Pomc*), and neuropeptide Y (*Npy*) were determined by real-time quantitative PCR (qPCR) using the Brilliant® II QPCR Master Mix (Stratagene) and Assays-on Demand primers and probes (Applied Biosystems). Results are represented as mean fold changes relative to controls. Reactions were run on a Stratagene MX3000P machine and threshold cycles (CT) were determined by an in-program algorithm assigning a fluorescence baseline based on readings prior to exponential amplification. Fold change in expression was calculated using the  $2^{-\Delta\Delta Ct}$  method (127), with ribosomal protein 36B4, 18s rRNA, and  $\beta$ -actin as the endogenous controls for adipose tissue, hypothalamus, and liver, respectively.

*Statistics.* Results are expressed as mean  $\pm$  SEM. Unpaired t-tests were used to determine statistical significance of these measurements between groups using Prism 4.0 (GraphPad). Repeated measures ANOVAs were used to determine statistical significance of caloric energy expenditure, wheel running, and GTT between groups (SPSS). Statistical significant was considered at  $p < 0.05$ .

## Results

### *Egfr* ablation within the CNS results in reduced fat mass deposition

Previously our lab showed that inhibition of EGFR produces lower body weights and fat mass in animals fed a high-fat WD due to a decrease in food intake without changing activity or energy expenditure. To determine the origin of EGFR-mediated fat mass deposition, a *Cre-loxP* strategy was used to specifically ablate *Egfr* activity in selected organs. *Egfr<sup>lox/lox</sup>* mice that contain loxP sites flanking exon 3 of the *Egfr* gene were created in our laboratory and bred to three established transgenic *Cre* lines (*Villin-Cre*, *aP2-Cre*, and *GFAP-Cre*) to delete EGFR within intestines, adipocytes, and CNS, respectively (137). The resulting *Cre Egfr<sup>lox/lox</sup>* mice did not exhibit overt phenotypes when compared to their *Egfr* wild-type littermates and therefore wild-type, *Egfr<sup>lox/+</sup>*, and *Cre* mice were considered as controls (138-140). Eight week-old male littermates from each mating were housed individually and placed on the WD for three months. Ablation of *Egfr* within the intestinal epithelium with *Villin-Cre* or within adipocytes with *aP2-Cre* had no effect on adipose deposition (Figure 14A and Figure 14B). However, deletion of *Egfr* activity in the CNS with *GFAP-Cre* resulted in decreased total and fat mass without an effect on lean mass (Figure 14C and Figure 14D). Brain weights were larger in *GFAP-Cre Egfr<sup>lox/lox</sup>* mice compared to controls, although all other organs weights were unchanged between groups (Figure 14E). Steatocrit was also measured in the feces of these animals and no differences were noted between groups (data not shown). Therefore, *Egfr* signaling within the CNS aids in controlling adipose deposition.

*Use of the GFAP-Cre transgene leads to reduced Egfr and anorexigenic neuropeptide in the hypothalamus*

To determine the physiological mechanisms behind the fat mass phenotype with deleted *Egfr* in the CNS, *GFAP-Cre Egfr<sup>fllox/fllox</sup>* mice and their control littermates were placed in individual calorimeter cages three days per month for three months to measure RER and caloric energy expenditure, fed the WD as before. CNS deletion of *Egfr* with *GFAP-Cre* resulted in significantly increased food and water intake and decreased feeding efficiency as compared to control littermates (Figure 15). We also observed an increase in caloric energy expenditure and oxygen consumption in these mice (Figure 16A and Figure 16B). However, no differences in activity, measured by voluntary wheel running (Figure 16C and Figure 16D), or in RER (data not shown) were observed between groups.

In addition to measuring energy expenditure indirectly with calorimetry, energy usage was also measured by determining transcript levels of uncoupling protein-1 (*Ucp1*) in both epididymal (white) and interscapular (brown) adipose tissue. UCP1 is found in the mitochondria of brown adipose tissue and is used to generate heat from stored metabolic energy in non-shivering thermogenesis (129). In both white and brown fat, *Ucp1* transcript levels were not different between groups, although levels in white fat trended higher in *GFAP-Cre Egfr<sup>fllox/fllox</sup>* mice than control littermates (Figure 17A). Expression of *Ucp3* was also measured in skeletal muscle but no difference was observed between groups (Figure 17B).

To verify that *Egfr* was deleted in the hypothalamus with *GFAP-Cre* and to identify changes in feeding peptides within this area, whole brains were sectioned and the

hypothalamus mechanically removed. qPCR was used to assess transcript levels of *Egfr*, anorexigenic neuropeptide *Pomc*, and orexigenic neuropeptide *Npy*. Levels of *Pomc* and *Egfr* were significantly decreased in *GFAP-Cre Egfr<sup>lox/lox</sup>* mice compared to their control littermates (Figure 18).

#### *Ablation of EGFR results in smaller adipocytes*

To determine if CNS deletion of EGFR impacted adipocyte histology, fat pads were sectioned and the number of adipocytes counted and normalized to the fat pad weights. Significantly smaller cell area and more adipocytes per fat pad weight were observed in *GFAP-Cre Egfr<sup>lox/lox</sup>* mice compared to control littermates (Table 4 and Figure 19). To establish possible causes for the difference in adipocyte size and number, qPCR was used to assess transcript levels of adipocyte stage-specific factors.

Preadipocytes were assessed with *Pref1* while mature adipocytes were assessed with *Cebpa*, *Cebpb*, *Arb3*, and *aP2* in epididymal fat pads of these mice. A significant increase in *Arb3* mRNA levels was observed in *GFAP-Cre Egfr<sup>lox/lox</sup>* mice compared to controls (Figure 20); no other adipocyte-specific markers were different between groups.

#### *Egfr deletion in the CNS leads to improved clinical parameters*

To examine the broader clinical consequences of *Egfr* deletion in the CNS, cholesterol, triglyceride, glucose, insulin, and adipokine levels were analyzed in the blood and serum, and expression levels of *lep* and pro-inflammatory cytokine *Tnfa* in epididymal fat pads. *GFAP-Cre Egfr<sup>lox/lox</sup>* mice showed a significantly improved clinical profile for cholesterol, triglycerides, leptin, and insulin in the serum as well as decreased *lep* mRNA levels in the fat pads, consistent with lower fat mass in these animals. Although not significant, an increase in serum and mRNA expression levels of

TNFA were observed (Table 5). To test whether *Egfr* deletion in the CNS is associated with improved insulin resistance in a DIO mouse model, we evaluated insulin sensitivity through measuring homeostasis model assessment of insulin resistance (HOMA-IR) and a glucose tolerance test (GTT). Intraperitoneal GTT were not different between groups, however HOMA-IR was significantly decreased in *GFAP-Cre Egfr<sup>flox/flox</sup>* mice (Figure 21 and Figure 22, respectively).

### Discussion

The body maintains a balance between energy intake and energy expenditure and obesity results from taking in more calories than expended. Obesity is just one of the factors associated with metabolic syndrome, which includes such symptoms as hypertension, insulin resistance, and hyperlipidemia (26, 27, 124, 125). Recent studies implicating a key role for EGFR in adipogenesis suggest signaling through this receptor may contribute to obesity. Using a diet-induced obesity mouse model, our lab previously found that genetic and pharmacological inhibition of EGFR caused a retardation in weight gain and adipose deposition due to a reduction in food intake. Others have also shown adipocyte-specific weight decreases with EGFR downregulation (68, 69, 120, 121).

To determine the role of EGFR in energy homeostasis, we employed the *Cre-loxP* system to delete *Egfr* specifically in the periphery (intestines and adipocytes) and in the CNS. Although deletion of *Egfr* within intestines or adipocytes had no effect on fat mass, deletion of *Egfr* in the CNS results in decreased total and fat mass, showing that EGFR signaling within the CNS is important for normal adipose deposition. Brain weights normalized to body weight in *GFAP-Cre Egfr<sup>flox/flox</sup>* mice were increased

compared to control littermates, while other organ weights were not different. Since brains from *GFAP-Cre Egfr<sup>lox/lox</sup>* mice do not show any morphological changes relative their control littermates (138) the increase in brain weight may be a consequence of the low body weight in these animals since no differences are noted on a wet brain weight basis.

Since the balance of energy homeostasis is dependent on both energy intake and energy expenditure, we evaluated these two components to determine the physiological mechanism of the *Egfr* mutant phenotype. We demonstrate an increase in food intake and a decrease in feeding efficiency in *GFAP-Cre Egfr<sup>lox/lox</sup>* mice compared to their control littermates. Due to the difference in feeding efficiency between groups, perhaps energy expenditure is also affected, producing lower body weights. Energy expenditure can be measured indirectly as oxygen consumption and carbon dioxide output (RER and caloric energy expenditure) or directly as voluntary wheel running, home cage activity, such as climbing, rearing, foraging and grooming, and heat production or thermogenesis. Consistent with an increase in food intake, deletion of *Egfr* with *GFAP-Cre* resulted in an increased conversion of food energy to heat energy and increased oxygen consumption as measured by indirect calorimetry, suggesting hyperkinesia in these animals. However, no differences in RER or voluntary wheel running were observed between groups. The control mice did decrease the distance ran over time as they became obese, possibly because they found it harder to move around, which could be responsible for their further increase in obesity. We have not measured home cage activity to see if an increase could be a reason why *GFAP-Cre Egfr<sup>lox/lox</sup>* mice are leaner than their control littermates. Wheel running may or may not be a direct reflection of home cage activity in mice fed a

HFD since some studies show increased home cage activity with increased wheel running while others show no change in home cage activity but decreases in wheel running (130-132). Home cage activity should then be measured to assess if it is increased and aiding in this decrease in body weight and fat mass. Therefore this data suggests that deletion of *Egfr* using *GFAP-Cre* regulates appetite and metabolism in these animals but not their activity through wheel running activity.

Other studies have also shown this increase in food intake and energy expenditure with a decrease in body weight and have attributed it in part to an increase in thermogenesis (25, 129). Adaptive thermogenesis is the dissipation of heat energy in response to external stimuli and it has been implicated in the regulation of energy balance and body temperature. In rodents, adaptive thermogenesis in response to cold-exposure and high-fat feeding activates brown adipose tissue. UCP1 is found in the mitochondria of brown adipose tissue and is used to generate heat from stored metabolic energy by non-shivering thermogenesis in hibernating mammals and in human infants. In mice with increased expression of *Ucp1* and increased food intake, a lean phenotype occurs even when fed a high-fat diet (25, 95, 129). *Ucp1* expression levels in interscapular tissue were not different between groups, however levels in epididymal tissue were increased although not significantly in *GFAP-Cre Egfr<sup>fllox/fllox</sup>* animals. Perirenal, inguinal, and other subcutaneous white adipose depots possess more capacity for brown adipocytes than visceral depots and therefore they should be analyzed for brown adipocytes and *Ucp1* expression (133, 134). Recent data has shown that brown and white adipocytes are present together in the same depots and may convert to the other type depending on energy needs (52, 53). Therefore, increased *Ucp1* expression in the epididymal or other

fat pads of these animals suggests more brown adipocytes in the white adipose tissue of these animals. Promotion of brown fat adipogenesis in these depots could therefore contribute to increased thermogenesis and the decreased fat mass observed. Another uncoupling protein thought to be associated with energy metabolism is UCP3. It is expressed predominantly in skeletal muscle and similar to UCP1 in brown adipose tissue, is upregulated after the consumption of a high-fat diet in rodents and humans(141). Mice overexpressing UCP3 eat considerably more than their wild-type littermates, but do not become obese, suggesting that metabolic rate is increased in these animals. In this study no difference in *Ucp3* expression was observed between groups, suggesting that *Ucp3* expression in skeletal muscle does not affect energy metabolism with perturbed EGFR in the CNS (141-143).

Neuronal signaling within the arcuate nucleus (ARC) of the hypothalamus evaluates energy intake and energy expenditure. GFAP-labeled astrocytes implicated in feeding are found within the ARC. These astrocytes play an important role in regulating food intake by monitoring fat stores and lipid metabolism. Hypothalamic astrocytes have been shown to express EGFR and this is well preserved between rodents and humans (10, 103, 138, 144). *Egfr* expression was significantly reduced within the hypothalamus in *GFAP-Cre Egfr<sup>fllox/fllox</sup>* mice. Thus deletion of *Egfr* using the GFAP promoter in the ARC is possibly responsible for the alteration in feeding and energy expenditure. Two key sets of neurons important for conveying appetite and energy are found in the ARC; one synthesizes orexigenic NPY, which stimulates food intake and decrease energy expenditure, and the other synthesizes anorexigenic neuropeptide POMC, which reduces food intake and increases energy expenditure. Insulin and leptin reduce the expression of

orexigenic neuropeptides and induce expression of anorexigenic neuropeptides (31, 32, 92, 93). Other studies have shown that diet-induced obesity and weight loss alter neuropeptide expression in the ARC to increase or decrease feeding and energy expenditure (78, 145). Expression levels of anorexigenic neuropeptide *Pomc* in the hypothalamus of *GFAP-Cre Egfr<sup>fllox/fllox</sup>* mice was reduced compared to control littermates. Since stimulation of POMC neurons decrease food intake, with decreased expression we see an increase in food intake in *GFAP-Cre Egfr<sup>fllox/fllox</sup>* mice. Also consistent with this downregulation of *Pomc* is the significant decrease in insulin and leptin levels. This suggests that this reduction in *Egfr* expression within the hypothalamus of *GFAP-Cre Egfr<sup>fllox/fllox</sup>* mice leads to an increase in food intake by downregulating anorexigenic neuropeptide *Pomc*, further evidenced by the reduction of leptin and insulin.

Since a decrease in fat mass could also be due to a reduction in adipocyte cell size and/or a decrease in cell number, we analyzed fat pads from these animals. Adipocyte cell size is smaller and cell number per fat pad mass larger in the fat pads of the *GFAP-Cre Egfr<sup>fllox/fllox</sup>* mice compared to control littermates. To determine causes for these differences in the *GFAP-Cre Egfr<sup>fllox/fllox</sup>* fat pads, we analyzed adipocyte-stage specific genes found in preadipocytes, *Pref1*, and in mature adipocytes, *Cebpa*, *Cebpb*, *Arb3*, and *aP2*. We observed a significant increase in *Arb3* mRNA levels, although expression of other adipocyte genes were not different between groups. This increase in *Arb3* may not be related to the amount of mature adipocytes in the fat pads. Rather this increased expression may be involved in increasing lipolysis in these depots, leading to a decrease in fat mass.

White adipose tissue stores triglycerides in periods of energy excess and in times of energy need, lipolysis of triglycerides occurs. ARB3 is a member of the large family of G protein-coupled receptors (GPCRs) that couple to members of the heterotrimeric G proteins to activate adenylyl cyclase and cAMP-dependent protein kinase A (PKA). PKA then phosphorylates hormone sensitive lipase, which then aids in lipase access to lipid droplets and triglyceride breakdown by altering proteins on the droplet's surface. Stimulation of the ARBs leads to lipolysis in white adipocytes and non-shivering thermogenesis in brown adipocytes and ARB3 activation of the MAPK pathway accounts for 15 to 25% of total lipolysis in white adipocytes in rodents (95, 96, 99, 146). In *GFAP-Cre Egfr<sup>lox/lox</sup>* mice, a significant decrease in body fat and serum triglycerides is observed with increases in energy expenditure and possible thermogenesis in white adipose tissue, suggesting increased fatty acid oxidation within the epididymal depots. This phenotype is also observed in mice that overexpress a triglyceride hydrolase in white adipose tissue or are treated with an orexigenic melanin-concentrating hormone-1 (MCH1) receptor antagonist (147, 148). In both of these models, increased lipolysis is specific to white adipose tissue without increased circulating levels of fatty acids. Therefore, the increased *Arb3* expression may cause mobilization of triglycerides from white adipose tissue or increased thermogenesis in brown adipocytes leading to a reduction of body fat mass. These fatty acids could either be brought back into the adipocyte for oxidation and energy or could be liberated into the serum. The fatty acids liberated from white adipose depots into the serum could have detrimental effects on metabolism and cause ectopic lipid storage on other organs however and therefore where these fatty acids are going in this model needs to still be determined. We do not see

excess fat in the feces of these animals however we do need assess other locations for increased fatty acids such as in the liver and around other organs. Increased delivery of fatty acids into the portal venous system could affect liver metabolism through alterations in glucose production, lipoprotein secretion, and insulin clearance (149). Therefore increased adipocyte oxidation with or without increased serum fatty acids may play a significant role in the adiposity and energy metabolism phenotypes observed in these *GFAP-Cre Egfr<sup>lox/lox</sup>* mice (147, 148, 150, 151).

Obesity is thought to be a state of low-grade systemic inflammation with levels of adipokines such as TNFA and IL6 elevated in serum and adipose tissue. It is a complex metabolic disorder associated with hyperglycemia, insulin resistance, hypertension, and atherosclerosis (21, 23, 25, 152). Disruption in the production and circulation of adipokines such as leptin, adiponectin, and insulin, occurs when energy balance is skewed, as in obesity, and when obesity is reduced these adipokines can be brought into balance again. Diets high in fat are also known to cause insulin resistance and signs of inflammation which disrupts adipokine levels (22, 28, 29). It has been reported that an overall better clinical profile such as decreases in serum leptin, triglycerides, and cholesterol levels, and improvements in insulin sensitivity is observed with weight loss in moderate and morbid obesity or in individuals of normal body mass index (21, 22, 28, 105, 106). Our results show a significant delay in the amount of weight gained in *GFAP-Cre Egfr<sup>lox/lox</sup>* animals and this weight retardation lead to a significant decrease in serum cholesterol, triglyceride, leptin, and insulin levels. Also observed were significant decreases in mRNA expression levels of *lep* in epididymal fat pads between groups, consistent with less fat mass noted in these animals. In overweight or obese people,

decreased serum levels of many pro-inflammatory cytokines are observed with less weight. TNFA levels in the serum and mRNA expression in white adipose tissue were increased in the *GFAP-Cre Egfr<sup>lox/lox</sup>* animals, however not significantly. As mentioned previously, the phenotypes observed in the *GFAP-Cre Egfr<sup>lox/lox</sup>* mice may be due to an increase in lipolysis in white adipose tissue. Adipocytes regulate lipolysis locally by releasing TNFA, which inhibits anti-lipolytic pathways, and perhaps this increase in *Tnfa* expression in adipocytes is for this process (146, 153). Changes in fat mass can also be associated with changes in glucose and insulin homeostasis. In this model, deletion of EGFR in the CNS attenuated insulin resistance as shown by improved HOMA-IR values and, although not significant, decreased glucose levels and improved glucose tolerance (136). Therefore, this overall better profile is most likely due to less fat mass observed with EGFR CNS deletion, rather than EGFR directly mediating these changes in clinical parameters.

In conclusion, EGFR signaling is important in the balance of energy homeostasis within these animals by affecting their appetite and metabolism. The deletion of *Egfr* with *GFAP-Cre* leads to an increase in food intake by altering hypothalamic neuropeptide levels important in feeding, yet a lower body weight is observed. The lower body weight may be due to an environment produced within adipocytes for increased lipolysis by upregulating the expression of genes that aid in this process or by increasing the amount of brown adipocytes within white adipose tissue. The decrease in body weight and fat mass observed in *GFAP-Cre Egfr<sup>lox/lox</sup>* animals also produces mice with a better overall clinical profile and increased insulin sensitivity. Ultimately, the question as to how this decrease in *Egfr* within the hypothalamus alters neuropeptide expression and how these

alterations signal to the periphery for decreased body weight and perhaps increased fatty acid oxidation remains. Future directions include determining if lipolysis is occurring within white adipose stores and the effect on fatty acid levels. If fatty acids are taken back into the adipocyte for oxidation or use in triglyceride synthesis, then they would not be liberated into the circulation to cause detrimental effects on glucose and insulin metabolism. Also, it will be important to evaluate if more brown adipocytes are observed in the white fat depots of *GFAP-Cre Egfr<sup>flox/flox</sup>* animals. These measures will aid in our understanding of EGFR signaling within the CNS with respect to appetite and metabolism regulation.

Fat pad	Average cell counts/fat pad weight			Average cell area ( $\mu\text{m}^2$ )			
	Control	<i>Gfap-Cre</i>	[ <i>Cre/ctrl</i> ] (%)	Control	<i>Gfap-Cre</i>	[ <i>Cre/ctrl</i> ] (%)	Fat pad wt [ <i>Cre/ctrl</i> ] (%)
Epididymal	49 $\pm$ 6.9	265 $\pm$ 48*	543	6,785 $\pm$ 133	3,264 $\pm$ 107***	48	36***
Inguinal	191 $\pm$ 16	933 $\pm$ 212**	490	3,591 $\pm$ 139	2,248 $\pm$ 284*	63	56

**Table 4.** Effects of *Egfr* CNS deletion with *GFAP-Cre* on adipocyte number and size. *GFAP-Cre Egfr<sup>lox/lox</sup>* mice and their control littermates were fed a WD for 3 months (N=3-8 animals per fat pad). Results are mean  $\pm$  SEM. Statistical significance: \*  $P < 0.05$ , \*\*  $P < 0.01$  and \*\*\*  $P < 0.0001$  vs. control.

Parameter	Control	<i>GFAP-Cre Egfr<sup>lox/lox</sup></i>
Cholesterol, mg/dL	222 ± 17	152 ± 27*
Triglycerides, mg/dL	135 ± 9.5	89 ± 16*
Blood Glucose, mg/dL	214 ± 16	163 ± 23
Leptin, ng/mL	31.1 ± 3.2	10 ± 5.2**
Leptin, fold change/control	1 ± 0.14	0.29 ± 0.17**
Insulin, ng/mL	1.46 ± 0.19	0.73 ± 0.25*
PAI-1, ng/mL	4.37 ± 0.86	4.45 ± 1.1
Resistin, ng/mL	5.23 ± 0.51	4.39 ± 1.4
TNFA, pg/mL	9.89 ± 2.5	31.9 ± 11
TNFA, fold change/control	1 ± 0.2	2.66 ± 1.1

**Table 5.** Clinical serum and expression data from control and *GFAP-Cre Egfr<sup>lox/lox</sup>* mice.

Measurements are at 20 weeks of age for control (N=10) and *GFAP-Cre Egfr<sup>lox/lox</sup>* (N=6) mice. Results are mean ± SEM. Statistical significance: \*  $P < 0.05$  and \*\*  $P < 0.01$  vs. control.

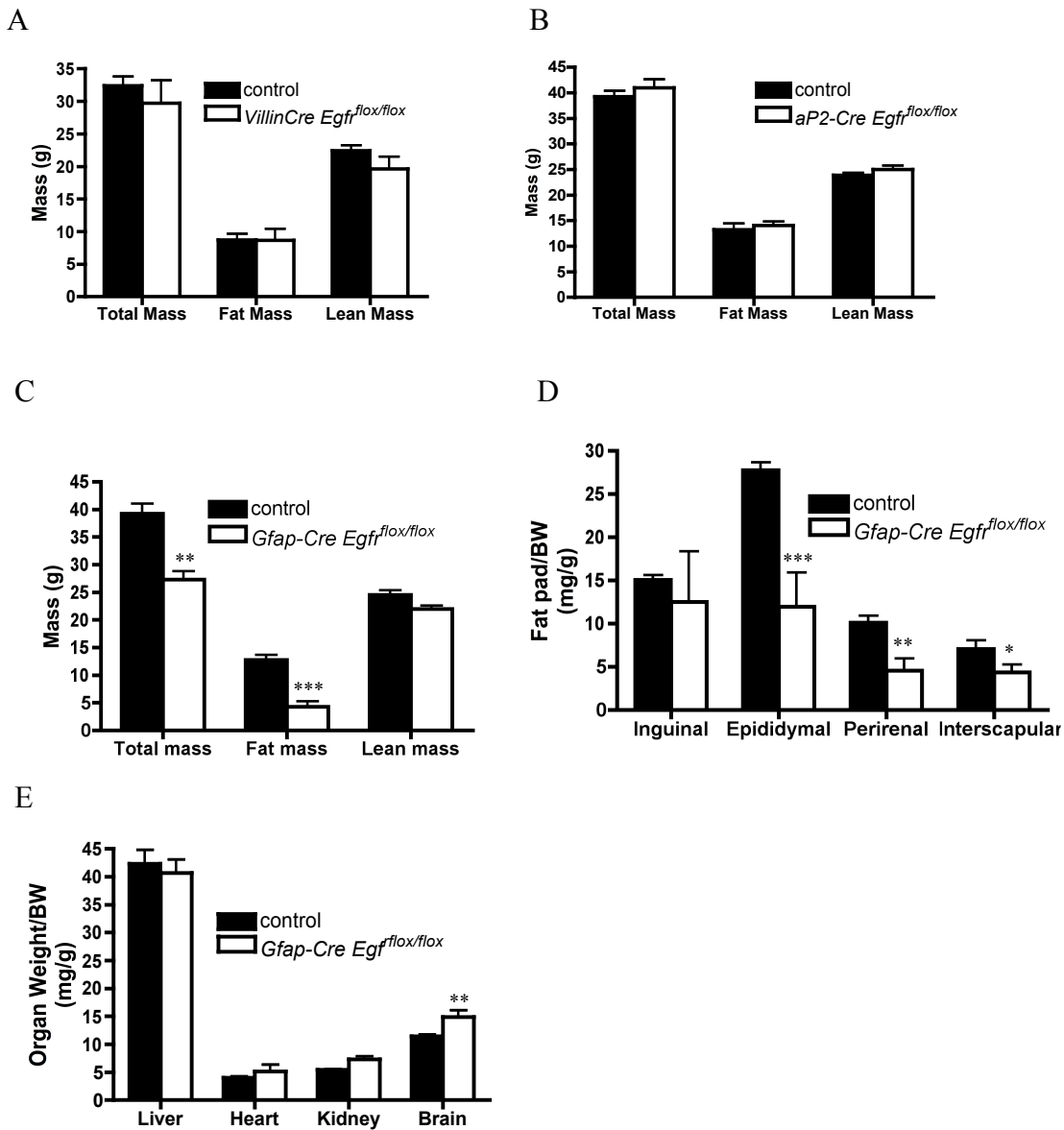


**Figure 14.** Effects of conditional deletion of *Egrf* on body masses and organ weights.

MRI data of *Villin-Cre Egrf<sup>flx/flx</sup>* (A), *aP2-Cre Egrf<sup>flx/flx</sup>* (B), and *GFAP-Cre Egrf<sup>flx/flx</sup>* (C) and their control littermates fed a WD. Normalized organ weights in *GFAP-Cre Egrf<sup>flx/flx</sup>* mice (D, E). N=4 *Villin-Cre Egrf<sup>flx/flx</sup>*; N=6 *Villin-Cre* controls; N=10 *aP2-Cre Egrf<sup>flx/flx</sup>*; N=12 *aP2-Cre* controls; N=6 *GFAP-Cre Egrf<sup>flx/flx</sup>*; N=10 *GFAP-Cre* controls. Results are expressed as mean  $\pm$  SEM. Statistical significance: \*  $P < 0.05$ , \*\*  $P < 0.01$ , and \*\*\*  $P < 0.0001$  vs. control.

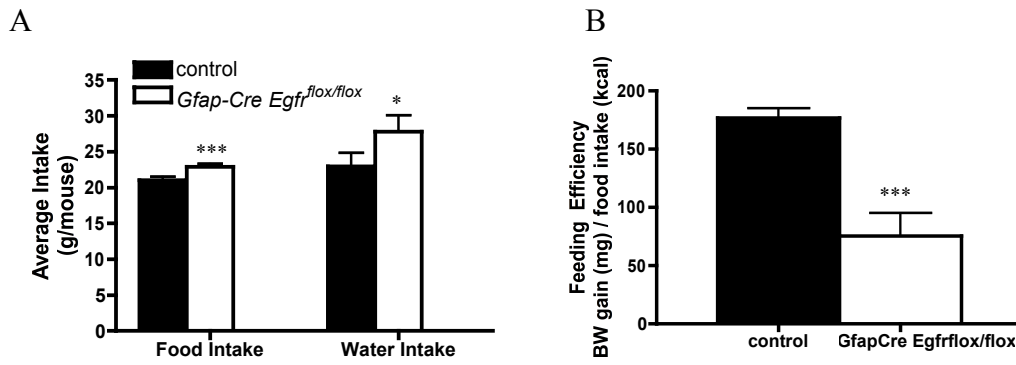


**Figure 15.** Effects of *Egfr* CNS deletion with *GFAP-Cre* on food and water intake and feeding efficiency.

Food and water intake (A) and feeding efficiency (B) in *GFAP-Cre Egfr<sup>flx/flx</sup>* mice (N=6) and their control littermates (N=10) fed a WD. Results are expressed as mean  $\pm$  SEM. Statistical significance: \*  $P < 0.05$  and \*\*\*  $P < 0.0001$  vs. control.

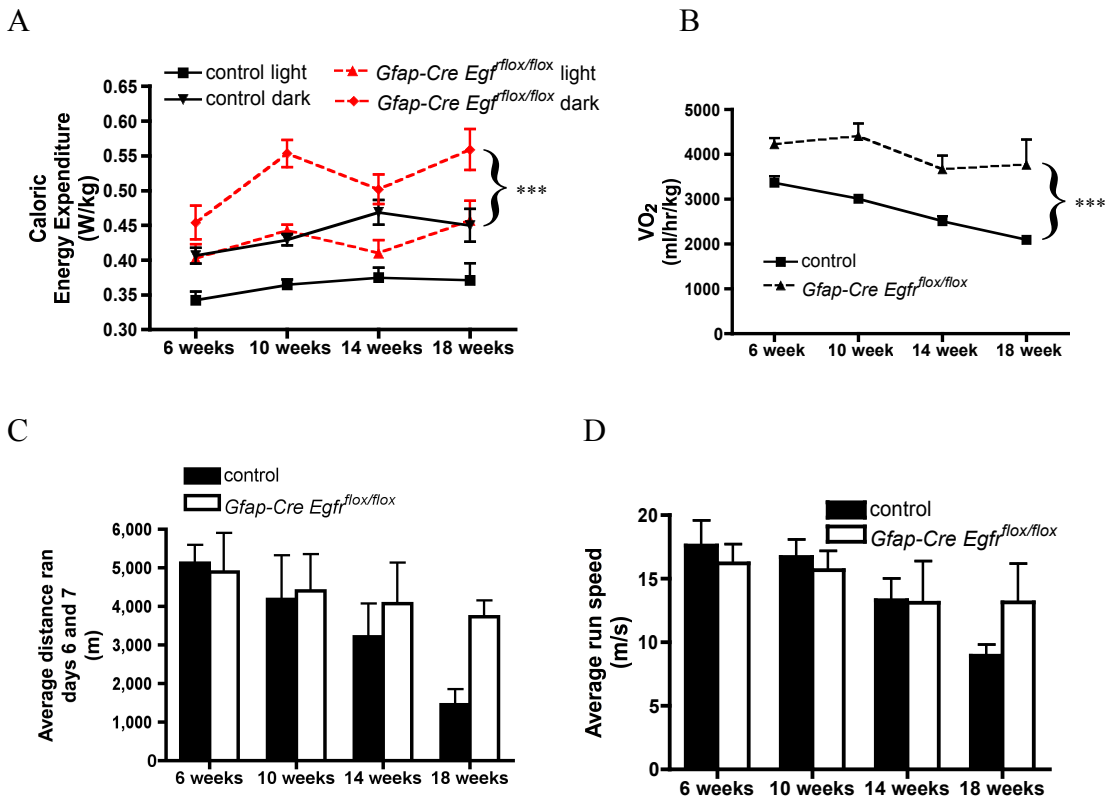


**Figure 16.** Effects of *Egfr* CNS deletion with *GFAP-Cre* on energy expenditure and activity.

Caloric energy expenditure (A), oxygen consumption, (B), distance ran (C), and speed during running (D) in *GFAP-Cre Egfr<sup>flox/flox</sup>* mice (N=6) and their control littermates (N=10) fed a WD. Energy expenditure is in watts of caloric energy expended per kg of body weight. Results are expressed as mean  $\pm$  SEM. Statistical significance: \*\*\*  $P < 0.0001$  vs. control.

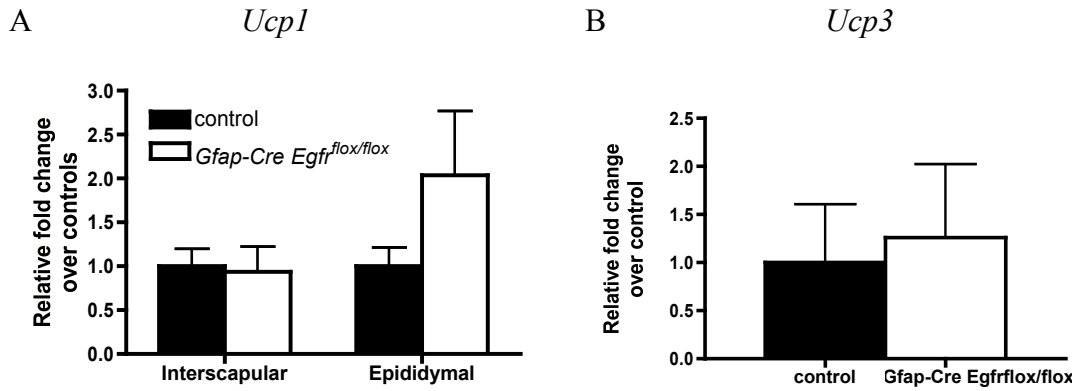


**Figure 17.** Effects of *Egfr* CNS deletion with *GFAP-Cre* on uncoupling proteins-1 and 3 expression.

Uncoupling protein-1 expression interscapular and epididymal fat (A) and uncoupling protein-3 expression in skeletal muscle (B) of control (N=10) and *GFAP-Cre Egfr<sup>flox/flox</sup>* (N=6) mice at 20 weeks of age fed the WD. Results are mean  $\pm$  standard error.

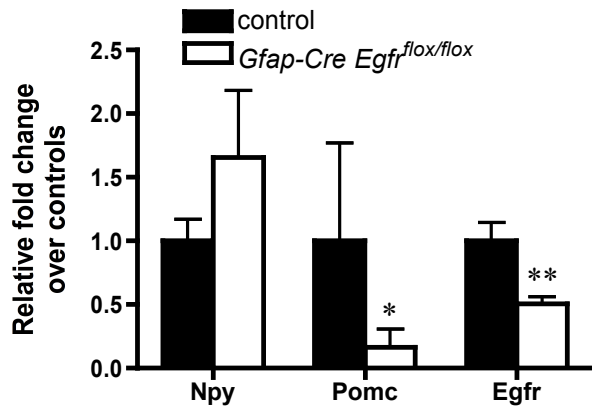
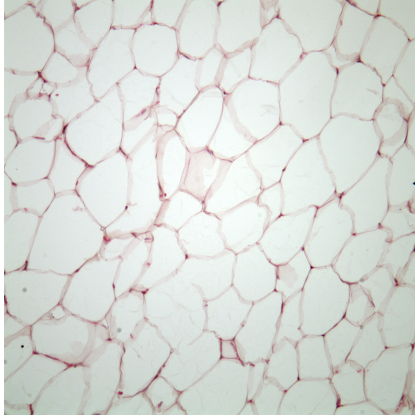


**Figure 18.** Effects of *Egfr* CNS deletion with *GFAP-Cre* on hypothalamic neuropeptide and *Egfr* expression levels.

Results are from control (N=10) and *GFAP-Cre Egfr<sup>flox/flox</sup>* (N=6) mice at 20 weeks of age. Results are mean ± standard error. Statistical significance: \* $P < 0.05$  and \*\* $P < 0.01$  vs. control.

A



B

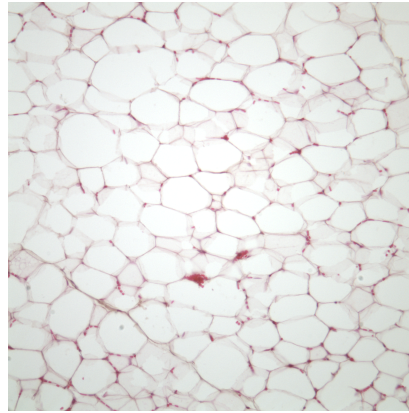


**Figure 19.** Representative inguinal fat pad histology from control and *GFAP-Cre Egf<sup>flox/flox</sup>* mice.

Control (A) and *GFAP-Cre Egf<sup>flox/flox</sup>* mice (B) at 20 weeks of age. 7-10 $\mu$ m sections. 20x magnification.

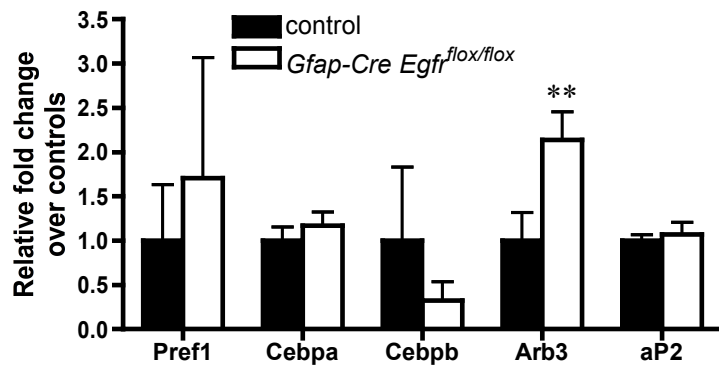


**Figure 20.** Effects of *Egfr* CNS deletion on adipocyte-specific factors in epididymal fat pads.

Results are from control (N=10) and *GFAP-Cre Egfr<sup>flox/flox</sup>* (N=6) mice at 20 weeks of age fed the WD. Results are mean  $\pm$  standard error. Statistical significance: \*\*  $P < 0.01$  vs. control.

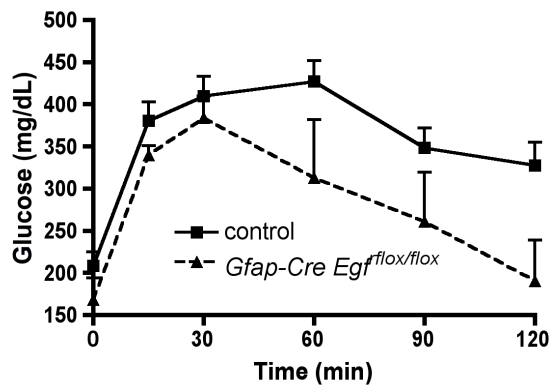


**Figure 21.** Glucose tolerance test measurements from control and *GFAP-Cre Egfr<sup>lox/lox</sup>* mice.

Results are from 20 week old control (N=10) and *GFAP-Cre Egfr<sup>lox/lox</sup>* (N=6) mice. Results are mean  $\pm$  SEM.

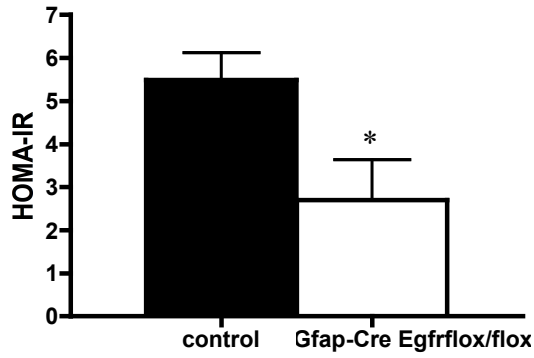


**Figure 22.** Average HOMA-IR measurements from control and *GFAP-Cre Egfr<sup>flox/flox</sup>* mice.

Results are from 20 week old control (N=10) and *GFAP-Cre Egfr<sup>flox/flox</sup>* (N=6) mice. Results are mean ± SEM. \*  $P < 0.05$  vs. control.

## CHAPTER 4

# THE EPIDERMAL GROWTH FACTOR RECEPTOR IS NOT REQUIRED IN ADIPOCYTES FOR ADIPOSE DEPOSITION BUT IS REQUIRED FOR NORMAL GROWTH IN MICE

Melanie B. Weed,<sup>1</sup> Tang-Cheng Lee,<sup>2</sup> and David W. Threadgill<sup>1,2</sup>

<sup>1</sup>*Curriculum in Toxicology, University of North Carolina, Chapel Hill, North Carolina;*

<sup>2</sup>*Department of Genetics, University of North Carolina, Chapel Hill, North Carolina*

### Abstract

As a result of the worldwide rise in obesity and obesity-related complications such as diabetes, stroke, and cardiovascular disease, understanding the mechanisms associated with this disease and determining treatment options is necessary. The epidermal growth factor receptor (EGFR) is involved in adipogenesis and therefore may contribute to the regulation of energy homeostasis. Using a diet-induced obesity mouse model, we found that inhibition of EGFR either genetically with the *Egfr*<sup>wa2</sup> hypomorphic allele or pharmacologically with a small molecule inhibitor against the EGFR tyrosine kinase (AG1478) slows adipose mass deposition. Therefore, due to this adipose phenotype and to determine the role of EGFR in adipose deposition, we deleted *Egfr* specifically in adipocytes using the *Egfr*<sup>tm1Dwt</sup> conditional allele and the *aP2-Cre*

transgenic line. Mice were fed a high-fat western diet over three months. Body weight and MRI measurements were collected monthly and upon sacrifice, heart, liver, and adipose depots were dissected, weighed, and stored. Ablation of EGFR within adipocytes showed no effect on adipose deposition. However an overall increase in the growth rate of these animals was observed, possibly due to a compensatory mechanism through the insulin-like growth factor receptor.

### **Introduction**

As a result of the worldwide rise in obesity and obesity-related complications such as diabetes, stroke, and cardiovascular disease, understanding the *in vivo* mechanisms associated with this disease and determining treatment options is necessary. Obesity is just one of the factors associated with metabolic syndrome, which includes such symptoms as hypertension, insulin resistance, and hyperlipidemia. Metabolic syndrome is also associated with increased inflammatory responses such as cytokine and free fatty acid release (26, 27, 124, 125). Recent studies implicating a key role of the epidermal growth factor receptor (EGFR) in adipogenesis suggest activation of this signaling pathway may contribute to obesity.

The EGFR and other ERBB family members are expressed in a wide range of tissues and cell types that regulate a number of cellular processes such as proliferation, differentiation, motility, apoptosis, and survival (1-4). The ERBB family consists of four members: EGFR (ERBB1), ERBB2, ERBB3, and ERBB4 that all contain an extracellular ligand binding domain, a transmembrane region, and an intracellular tyrosine kinase domain. Upon binding of ligands to the extracellular domain, these members form homo or heterodimers that initiate autophosphorylation of tyrosine residues and signaling

cascades (3-6). We have previously shown that that male and female wild-type B6 mice chronically exposed to small molecule EGFR inhibitors and mice homozygous for the waved-2 (*Egfr<sup>wa2</sup>*) hypomorphic allele exhibit delayed weight gain over the course of exposure compared to controls, with the mass of other organs not affected (120).

Therefore, we determined if EGFR signaling was important within adipocytes for adipose deposition. We examined the molecular mechanisms underlying the reduction in adipose mass by modeling a typical high-fat western diet (WD) and analyzing the morphological and metabolic parameters associated with adipose deposition when *Egfr* is specifically deleted in adipocytes using the *ap2-Cre* transgenic mouse model. We found that deleting EGFR within adipocytes did not result in an adipose phenotype; rather we found an increased growth rate in these animals compared to control littermates.

## Materials and Methods

*Animals and treatment.* *ap2-Cre* mice were mated with *Egfr<sup>lox/+</sup>* or *Egfr<sup>lox/lox</sup>* mice. *ap2-Cre Egfr<sup>lox/lox</sup>* male mice with their control littermates (*ap2-Cre*, *ap2-CreEgfr<sup>lox/+</sup>*, *Egfr<sup>lox/+</sup>*, or *Egfr<sup>lox/lox</sup>*) were started on a high-fat western diet (WD) (Research Diets D12079B, New Brunswick, NJ, 40% calories from fat) at eight weeks of age for three months (113). The WD is nutritionally matched with the STD AIN-93G diet (Research Diets, D10012G) except for increased fat and reduced fiber, calcium, and vitamin D, more consistent with the diets consumed by people in North America. Mice had free access to food and water throughout each study. Body weight and food and water intake measurements were collected at the start of the study and every week thereafter. All mice were sacrificed according to an approved University of North Carolina (UNC) Institutional Animal Care and Use Committee's protocol. Inguinal,

epididymal, perirenal, and interscapular fat pads, heart, liver, and skeletal muscle were collected and stored at -80°C.

*Genotyping.* Genomic DNA was extracted from ear tissue using 25mM NaOH/0.2mM EDTA and 40mM Tris HCL for use in PCR reactions in all genotyping assays. The *Egfr<sup>fllox</sup>* allele was amplified using 1 uL DNA in each PCR reaction for 35 cycles (30 s at 94°C, 1 min at 60°C, and 1 min at 72°C). The primers were lox3s: 5'CTTTGGAGAACCTGCAGATC-3' and lox3as: 5'CTGCTACTGGCTCAAGTTTC-3'. A 375 bp PCR product was detected from the *Egfr<sup>fllox</sup>* allele and a 320 bp PCR product from the wild-type allele. For the *Egfr<sup>Δ</sup>* allele, DNA was amplified for 40 cycles (30 s at 94°C, 20 s at 60°C, and 20 s at 72°C). The primers for this reaction were Delta-3: 5'CTCAGCCAGATGAT-GTTGAC-3' and Delta-4: 5'CCTCGTCTGTGGAAGA-ACTA-3' and a 129 bp PCR fragment was detected for the *Egfr<sup>Δ</sup>* allele. For the *aP2-Cre* transgene, DNA was amplified for 38 cycles (30 s at 94°C, 1 min at 56°C, and 1 min at 72°C) with primers CRE-1: 5'-GTGATGAGGTTTCGCAAGAAC-3' and CRE-2: 5'AGCATTGCTGTCACTTGGTC-3'. A 278 bp PCR fragment was generated from the *Cre* transgene. All PCR products were run on a 3% agarose gel at 150mV for 25 minutes and all reactions used Taq DNA polymerase (Qiagen, Germantown, MD) and a GeneAmp PCR system 9700 (Applied Biosystems, Foster City, CA).

*MRI.* Body composition was collected by magnetic resonance imaging (MRI) (EchoMRI, Houston, TX) once a month starting at eight weeks of age for three months.

*Glucose Tolerance Test.* Mice were fasted four hours prior to administration of the GTT. d-glucose (Sigma, St. Louis, MO) was dissolved in phosphate buffered saline and administered to mice via i.p. injection (2 g/kg). Samples of whole-blood (2–3 µl

each) were collected from a tail clip bleed immediately before and 15, 30, 60, 90, and 120 minutes after glucose injection. Blood glucose levels were measured using a Freestyle Glucose Monitoring System (Abbott Laboratories, Abbott Park, IL).

*Homeostatic model assessment of insulin resistance.* HOMA-IR calculations were performed using the HOMA Calculator 2.2.2 (University of Oxford, United Kingdom).

*Gene expression.* Total RNA was extracted from fat pads of control and *aP2-Cre Egfr<sup>flox/flox</sup>* mice using TRIzol (Invitrogen, Carlsbad, CA). 400 ng of total RNA was reverse transcribed using the AffinityScript™ QPCR cDNA synthesis kit (Stratagene, La Jolla, CA). The expression of insulin growth factor-1 (*Igf1*), IGF1 receptor (*Igflr*), growth hormone receptor (*Ghr*), insulin growth factor binding protein-3 (*Igfbp3*), leptin (*lep*), and tumor necrosis factor- $\alpha$  (*Tnfa*) were determined by real-time quantitative PCR (qPCR) using the Brilliant® II QPCR Master Mix (Stratagene) and Assays-on Demand primers and probes (Applied Biosystems). Results are represented as mean fold changes relative to control groups. Reactions were run on a Stratagene MX3000P machine with analysis software. Threshold cycles (CT) were determined by an in-program algorithm assigning a fluorescence baseline based on readings prior to exponential amplification. Fold change in expression was calculated using the  $2^{-\Delta\Delta Ct}$  method (127), with 36B4 as the endogenous control.

*Blood Biochemical Analyses.* Blood samples were collected at the beginning of the study and monthly thereafter by tail clip or terminal cardiac puncture. Serum cholesterol and triglycerides were analyzed at UNC's clinical chemistry core. Blood glucose levels were measured using a Freestyle Glucose Monitoring System (Abbott Laboratories). Adipokine measurements including leptin, adiponectin, insulin,

plasminogen activator inhibitor-1 (PAI-1), and resistin were analyzed using a mouse serum adipokine kit (Linco Research, MADPK-71K, St. Charles, MI) and a BioRad Luminex Instrument (Austin, TX). Serum IGF1 levels were analyzed by ELISA (Immunodiagnostic Systems, Scottsdale, AZ).

*Statistics.* Results are expressed as mean  $\pm$  SEM. Unpaired t-tests were used to determine statistical significance of these measurements between treated and control groups using Prism 4.0 (GraphPad). Linear regression analysis for growth curves was also performed using Prism 4.0. Group means were considered statistically significant at  $p < 0.05$ .

## Results

### *aP2-Cre Egfr<sup>lox/lox</sup> mice grow faster than controls but do not have higher adiposity*

To investigate the role of EGFR within adipocytes, *Egfr* was deleted specifically in adipocytes by crossing loxP-flanked *Egfr* mice (*Egfr<sup>lox/lox</sup>*) (137) with transgenic mice expressing the *Cre* recombinase under control of the adipose fatty acid binding protein (*aP2*) promoter (138). *Cre* expression was observed in adipose tissue, as expected, however deletion of EGFR in the liver is also noted (Figure 23A). qPCR of EGFR mRNA expression in the liver however showed no change between groups (Figure 23B). Wild-type, *Egfr<sup>lox/+</sup>*, and *aP2-Cre* mice displayed similar phenotypes and therefore were considered as controls.

*aP2-Cre Egfr<sup>lox/lox</sup>* mice displayed similar body and organ weights and fat and lean mass as their control littermates when fed a WD for three months (Figure 24). Also, no differences in adipose cell number or area were observed between fat pads of control

and *ap2-Cre Egfr<sup>flx/flx</sup>* mice (data not shown), consistent with no changes in fat mass between groups. However, *ap2-Cre Egfr<sup>flx/flx</sup>* mice did show a greater postnatal growth rate compared to their control littermates (Figure 25A) that was not due to an increase in fat mass (Figure 24A) or an increase in food intake (Figure 25B).

#### *Increased serum IGF1 levels in aP2-Cre Egfr<sup>flx/flx</sup> mice*

Given the observed growth phenotype, we investigated why deletion of EGFR specifically in adipocytes would cause an increase in overall growth rate. The insulin growth factor (IGF)-1 receptor (IGF1R) is a tyrosine kinase receptor similar to EGFR and the insulin receptor that controls proliferation and differentiation in many tissues and cells when bound by its ligands. IGF1 is structurally similar to insulin and increased IGF1 levels in the body lead to increased overall growth (154-156). Therefore, we determined if the overall growth rate increase could be due to an increase in IGF1 levels. At eight weeks of age, IGF1 serum levels in *aP2-Cre Egfr<sup>flx/flx</sup>* mice were significantly greater than controls (Figure 26A). However, we did not observe any changes in *Igf1* or *Igf1r* mRNA expression in the epididymal fat pads or liver at sacrifice between these groups (Figure 26B; data not shown). Also, there were no changes in mRNA expression of growth hormone receptor (*Ghr*) in the epididymal fat depot or liver (Figure 27) or *Igfbp3* mRNA expression in this epididymal fat depot (data not shown).

#### *Deletion of Egfr in adipocytes causes a decrease in serum cholesterol levels*

To determine the metabolic consequences of *Egfr* deletion within adipocytes, cholesterol, triglyceride, glucose, and adipokine levels were analyzed in the blood and serum of these mice. Expression levels of *Tnfa* and *lep* were also analyzed in epididymal fat pads. A decrease in cholesterol levels in *aP2-Cre Egfr<sup>flx/flx</sup>* mice compared to

controls was observed however no other differences were noted between groups (**Table 6**). To test whether EGFR deletion within adipocytes is associated with changes in insulin resistance in a diet-induced obesity mouse model, we evaluated insulin sensitivity through measuring homeostasis model assessment of insulin resistance (HOMA-IR) and a glucose tolerance test (GTT). There were not differences in intraperitoneal GTT or HOMA-IR between groups (**Figure 28** and Figure 29, respectively).

### **Discussion**

The EGFR and other ERBB receptors are expressed in a wide range of tissues and cell types that regulate a number of cellular processes such as proliferation, differentiation, motility, apoptosis, and survival (1-4). From work performed in our and other labs, we know the EGFR has important functions in intestinal, heart, central nervous system, and placental development and EGFR deficient mice show pre- and postnatal lethality (120, 135, 157, 158). It has also been shown that EGFR signaling plays a role in adipose deposition. By increasing concentrations of EGF, a ligand to EGFR, an increase in adiposity of adult female mice and in 3T3-L1 mature adipocytes occurs by increasing triglyceride synthesis. This effect is inhibited by treating these animals with either anti-EGF or by removing the submandibular gland from the mouse, which produces high levels of EGF (68-70), without changes in other organ weights. Our lab observed a similar adipocyte-specific phenotype with the use of AG1478, an EGFR tyrosine kinase inhibitor, in the chow of male C57BL/6J mice. We therefore hypothesized that EGFR signaling within adipocytes would be important for adipose deposition and deleted *Egfr* specifically within adipocytes to address this hypothesis.

To target adipocytes specifically, we obtained mice expressing *Cre* recombinase under the *aP2* promoter. The *aP2* promoter is used in most adipose-specific inactivations being expressed highly in differentiated adipocytes; however, it is also expressed in macrophages and shows non-adipose tissue specificity in the embryo (88, 89, 159).

EGFR expression was unaffected in most tissues of control animals, indicating that the modified EGFR locus with loxP or the transgene did not affect EGFR expression. EGFR expression using PCR showed downregulation in the liver of control animals, however qPCR did not verify this on an mRNA level.

*aP2-Cre Egfr<sup>lox/lox</sup>* mice were fertile and viable and expressed no differences in body weight, organ weights, or in adipocyte histology as compared to control littermates at 20 weeks of age. Cholesterol levels were significantly lower in *aP2-Cre Egfr<sup>lox/lox</sup>* mice at 20 weeks of age, while no other metabolic consequences were noted between groups. We do not see decreased fat mass with deletion of EGFR in adipocytes like we do in the whole animal downregulation of EGFR using AG1478. This could be due to the differences in the timing of altered EGFR signaling. Wild-type C57BL/6J mice were eight weeks of age when they were administered AG1478. At this age these mice already possess preadipocytes and mature adipocytes with normal EGFR signaling. With inhibition of EGFR, effects on both proliferation and differentiation of cells would occur challenging the normal development of adipose mass. However, with the *aP2-Cre* model, EGFR is deleted from birth in cells that are programmed for adipocyte lineage, leaving pluripotent cells with normal EGFR signaling able to produce adipocytes. Also, in these cells with decreased EGFR signaling, IGF1 may compensate for normal growth.

Although we did not observe an adipose-related phenotype in *aP2-Cre Egfr<sup>lox/lox</sup>*

mice at 20 weeks of age, we did see one related to growth rate. An increase in the growth rate of *aP2-Cre Egfr<sup>lox/lox</sup>* mice over controls was observed between eight and 20 weeks of age. As noted previously, this increase in growth is not due to larger, heavier mice or to an increase in food intake. To account for this increase in growth, other mechanisms may exist that compensate for downregulation of EGFR signaling within adipocytes. One such compensatory mechanism could be through the IGF1R pathway.

The IGF1R is a tyrosine kinase receptor similar to EGFR and signaling through this receptor by its ligands (i.e., IGF1 and IGFII) controls proliferation and differentiation in many tissues and cell types. Bioavailability of these ligands is through binding to IGFbps, which bind IGFs locally or removes them from circulation (138, 154-156, 160). Increased IGF1 levels in circulation increase overall growth while a decrease in IGF1 leads to growth retardation. Tissue specific overproduction leads to only that tissue or organ growing larger, even with higher IGF1 in the serum (154, 161). In this study, we do see increased IGF1 levels in the serum of *aP2-Cre Egfr<sup>lox/lox</sup>* mice at eight weeks of age. This is similar to what was noted in a study with IGF1R deletion in adipocytes of mice using the *aP2-Cre* transgene. These researchers observed an increase in serum IGF1 levels; however they also noted an overall increase in growth and fat pad weights, concluding that IGF1R in adipocytes was important in regulating serum IGF1 levels (138). In our study however, we do not see an increase in fat pad weights at 20 weeks of age even with the increase in IGF1 serum levels.

To establish potential causes for an increase in serum IGF1 levels, we determined mRNA expression levels of *Igf1*, *Igf1r*, and *Ghr* in the fat pads and liver of *aP2-Cre Egfr<sup>lox/lox</sup>* mice and their control littermates. *Egfr* deletion within adipocytes caused no

changes in *Igf1*, *Igf1r*, or *Ghr* mRNA expression in adipose tissue or liver. The liver produces and secretes IGF1 into the circulation (154). Therefore, since there is no difference in *Igf1* or *Igf1r* mRNA expression in liver, the systemic increase of IGF1 noted is not due to liver production. This suggests that this increase is due to the production from the adipose tissue. Others have abolished *Igf1* from the liver using conditional gene targeting and observed low plasma IGF1 levels; however postnatal growth of these mice did not differ from controls, suggesting IGF1 is also generated by other tissues. Also, IGF1 is necessary for differentiation in 3T3-L1 preadipocytes and to stimulate cellular growth and lipogenesis in differentiated adipocytes by acting in an autocrine/paracrine fashion (138, 155). Presumably, local adipocyte production of IGF1 could then lead to an increase in serum IGF1 levels and an overall increased growth rate.

The question as to why downregulation of EGFR signaling in adipocytes would lead to increased IGF1 serum levels and overall growth resides within the transactivation potential of EGFR. EGFR is the point of convergence of growth signals from different stimuli such as G-protein coupled receptors, the IGF1R pathway, and cytokine receptors (155). With regards to adipose development, both IGF1R and EGFR activate similar downstream signaling pathways such as MAPK for growth, and are required for preadipocyte proliferation and adipocyte differentiation (66, 163). It has been suggested that crosstalk between EGFR and IGF1R is due to an autocrine mechanism of proteolytic cleavage of an EGFR ligand HBEGF in COS-7 cells that leads to signaling through the MAPK pathway (75, 164). One study employed 3T3-L1 preadipocytes to decipher the relationship between the IGF1R and EGFR pathways in adipocyte differentiation. Cells were treated with an EGFR tyrosine kinase inhibitor, AG1478, with or without EGF or

IGF1 ligands. They found no inhibition of IGF1 stimulated MAPK activity, however there was inhibition of this pathway with EGF stimulation (66). Therefore the IGF1 receptor pathway does stimulate mitogenesis through MAPK signaling in this cell culture model and a compensatory mechanism could occur without EGFR as in the fat pads of the *aP2-Cre Egfr<sup>flax/flax</sup>* mice (156).

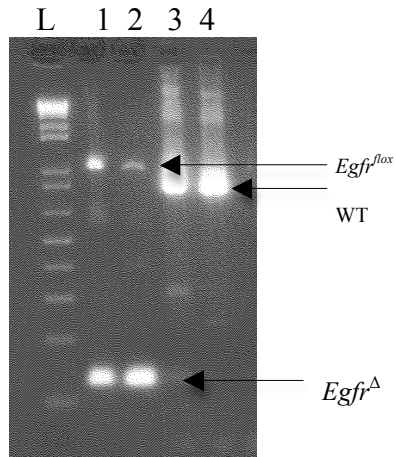
In conclusion, deletion of EGFR in adipocytes using *ap2-Cre* results in an increased postnatal growth rate and lower cholesterol levels compared to controls with no changes in glucose homeostasis. Autocrine/paracrine regulation of IGF1 may be occurring to produce the growth phenotype and the IGF1R pathway may be compensating for the lack of EGFR in adipocytes to produce normal adipose mass. Additional experiments will be needed to fully understand what is occurring in adipocytes and if there is indeed a compensatory mechanism due to downregulation of EGFR signaling *in vivo* since EGFR and IGF1R share many common pathways.

Parameter	Control	<i>aP2-Cre Egfr<sup>lox/lox</sup></i>
Cholesterol, mg/dL	240	162*
Triglycerides, mg/dL	107	112
Blood Glucose, mg/dL	186	194
Leptin, ng/mL	21.7 ± 4.1	20.9 ± 3.7
Leptin, fold change/control	1 ± 0.19	0.95 ± 0.12
Insulin, ng/mL	2.52 ± 0.5	2.84 ± 0.3
PAI-1, ng/mL	3.29 ± 0.7	3.60 ± 0.7
Resistin, ng/mL	5.20 ± 0.7	4.75 ± 0.7
TNFA, fold change/control	1 ± 0.47	1.24 ± 0.5
Adiponectin, ng/mL	2.66 ± 0.06	2.08 ± 0.11

**Table 6.** Serum and expression clinical data from control and *aP2-Cre Egfr<sup>lox/lox</sup>* mice.

Results are from 20 week old control (N=12) and *aP2-Cre Egfr<sup>lox/lox</sup>* (N=10) mice fed a WD for 3 months. Results are mean ± SEM. Statistical significance: \**P* < 0.05 vs. control.

(A)



(B)

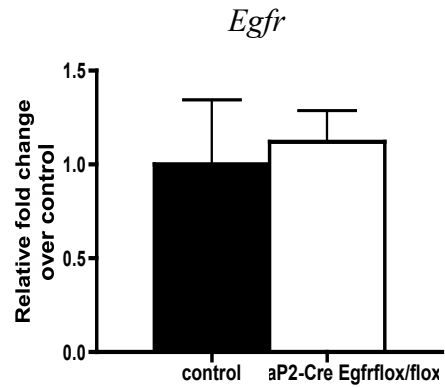


**Figure 23.** PCR analysis of DNA and expression of EGFR in liver of control and *aP2-Cre Egfr<sup>lox/flox</sup>* mice.

(A) DNA from the epididymal fat depot (1) and liver (2) from *aP2-Cre Egfr<sup>lox/flox</sup>* (N=10) and in epididymal fat depot (3) and liver (4) from control mice (N=12). The *Egfr<sup>Δ</sup>* allele is the recombination between the loxP sites resulting in *Egfr* removal. The wild-type allele is 320 bp, the *Egfr<sup>lox</sup>* allele is 375 bp, and *Egfr<sup>Δ</sup>* allele is 129 bp. L= 1 kb ladder. (B) mRNA expression of EGFR in liver from control and *aP2-Cre Egfr<sup>lox/flox</sup>* mice.

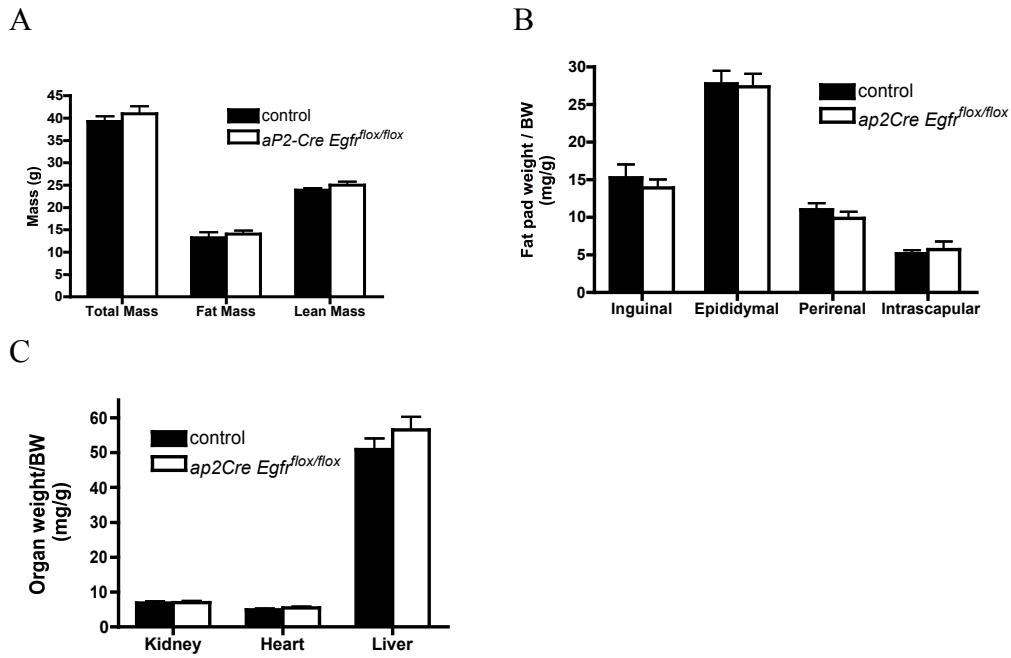
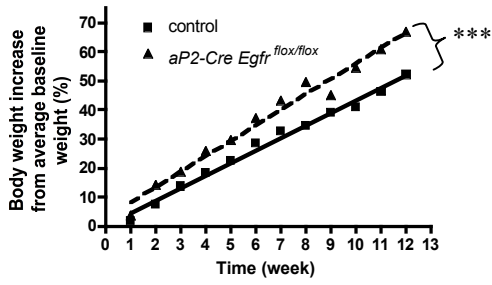


**Figure 24.** Effect of *Egrf* deletion with in adipocytes on organ weights fat mass.

Magnetic Resonance Imaging (A), normalized fat pad/BW data (B) and normalized organs weight/BW data (C) from *ap2-Cre Egrf<sup>flox/flox</sup>* (N=10) mice and their control littermates (N=12) at 20 weeks of age. Results are expressed as the mean  $\pm$  SEM.

A



B

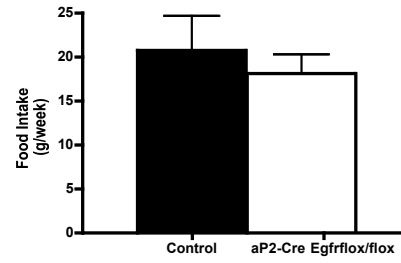
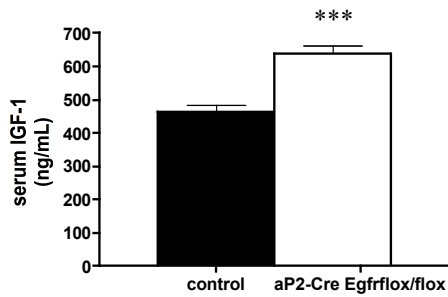


**Figure 25.** Effect of adipocyte-specific *Egfr* deletion on growth and food intake.

Growth rate (A) and food intake (B) from control (N=12) and *aP2-Cre Egfr*<sup>flox/flox</sup> (N=10) mice. Eight week old mice were placed on a WD for 3 months. Results are mean  $\pm$  SEM. Statistical significance: \*\*\*  $P < 0.001$  vs. control.

A



B

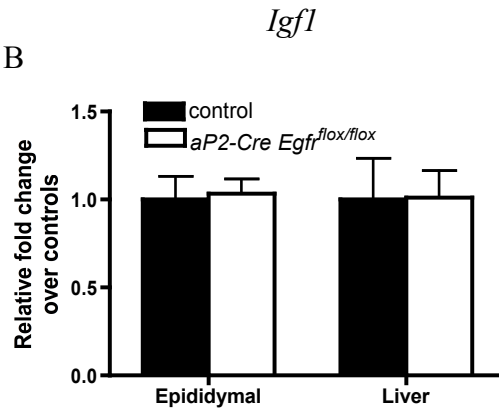


**Figure 26.** IGF1 serum levels and *Igf1* mRNA expression levels in control and *aP2-Cre Egfr<sup>flox/flox</sup>* mice.

IGF1 serum levels (8 weeks of age) (A) and *Igf1* mRNA expression levels (20 weeks of age) (B) in control (N=12) and *aP2-Cre Egfr<sup>flox/flox</sup>* (N=10) mice. Results are expressed as the mean  $\pm$  SEM. Statistical significance: \*\*\*  $P < 0.0001$  vs. control.

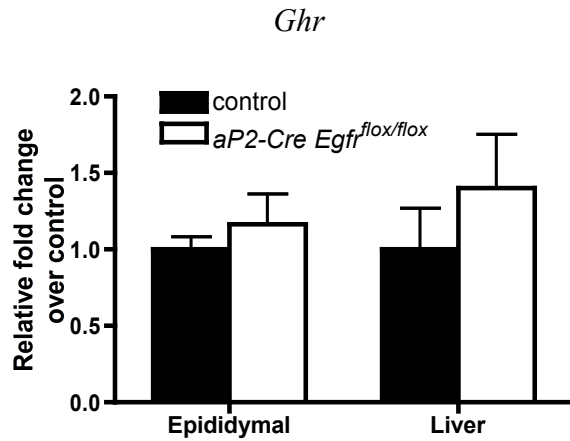


**Figure 27.** Effects of *Egfr* deletion in adipocytes on growth hormone receptor mRNA levels in epididymal fat depot and the liver.

Results are from control (N=12) and *aP2-Cre Egfr<sup>flox/flox</sup>* (N=10) mice fed a WD. Results are mean  $\pm$  SEM.

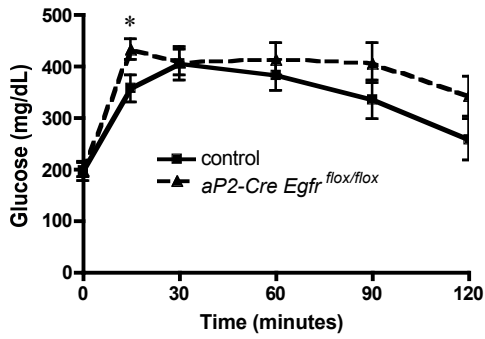


**Figure 28.** Glucose tolerance test measurements in control and *aP2-Cre Egfr<sup>flox/flox</sup>* mice.

Results are from 20 week old control (N=12) and *aP2-Cre Egfr<sup>flox/flox</sup>* (N=10) mice fed a WD for 3 months. Results are mean  $\pm$  SEM. Statistical significance: \* $P < 0.05$  vs. control.

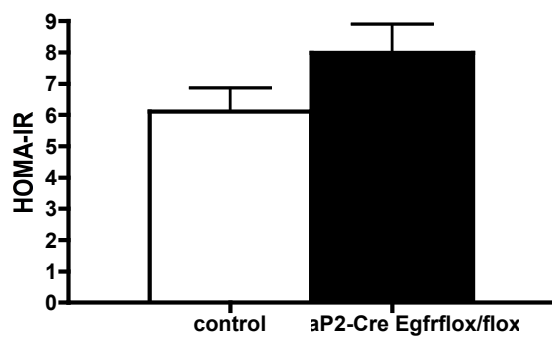


**Figure 29.** Average HOMA-IR measurements from control and *aP2-Cre Egfr<sup>flox/flox</sup>* mice. Results are from 20 week old control (N=12) and *aP2-Cre Egfr<sup>flox/flox</sup>* (N=10) mice fed a WD for 3 months. Results are mean  $\pm$  SEM.

## CHAPTER 5

### CONCLUSIONS AND FUTURE DIRECTIONS

The ERBB family is expressed in a wide range of tissues and cell types that regulate a number of cellular processes such as proliferation, differentiation, motility, apoptosis, and survival (1-4). Regulation of these signaling cascades is a complex process, with regards to duration and potency of activation, and aiding in the complexity is the different heterodimer combinations within the family and the transactivation potential by different mediators. EGFR signaling in adipogenesis has been studied *in vitro* and *in vivo*, using cell lines already committed to the adipocyte lineage or by perturbing EGFR signaling with ligands to the receptor, respectively. These studies revealed that peptides such as the growth factor EGF possesses both lipogenic and lipolytic effects; with increased amounts increasing adiposity in mature female mice and in 3T3-L1 mature adipocytes but decreasing adiposity when EGF is given to neonatal mice (62, 69, 71). Also, Phase I clinical trials evaluating EGFR TKIs EKB-569 and gefinitib for tumors associated with EGFR pathway activation report grade 1/2 anorexia in approximately 20-30% of patients (166, 167). Given these mechanisms of EGFR signaling in adiposity and anorexia, we explored the consequences of chronic EGFR inhibition *in vivo*. This research is relevant and timely due to the overall rise in overweight and obesity over these past few decades and the need for understanding the underlying mechanisms for therapy. Obesity drugs that block lipid absorption or increase

satiety signals have been generated, however side effects such as cardiovascular complications and gastrointestinal effects may limit their usage (104, 108-110).

We have previously shown that female wild-type B6 mice chronically exposed to small molecule EGFR inhibitors exhibit decreased weight gain over the course of exposure compared to controls, with no signs of toxicity (120). Others have also observed *in vivo* this adipocyte-specific decrease in weight with inhibition of EGF, with no effect on other organ weights (68, 69, 120, 121). Therefore, our first experiment sought to determine the mechanisms behind this phenotype by characterizing the metabolic and developmental consequences of EGFR inhibition in diet-induced obesity models. Using both genetic and pharmacological models of EGFR inhibition *in vivo*, we found a decrease in body weight and fat mass due to decreases in food intake and feeding efficiency, along with smaller adipocytes within fat depots and an overall improved clinical profile compared to control littermates. However, no differences in RER, caloric energy expenditure, activity, or thermogenesis were observed between groups. Next we wanted to determine the mechanisms for this decrease in food intake and feeding efficiency with fat mass reduction. Since energy balance depends on the regulation of a peripheral system sensing satiety and energy storage and the CNS using these signals to regulate homeostasis (90, 91), we ablated EGFR within the periphery (intestinal epithelium and adipocytes) and in the CNS using the *Egfr<sup>tm1Dwt</sup>* conditional allele and the *Villin-Cre*, *aP2-Cre*, and *GFAP-Cre*, transgenic lines, respectively and fed these animals a high-fat diet. Ablation of EGFR within the intestinal epithelium and adipocytes showed no effect on adipose deposition, however an overall increase in the growth rate of *aP2-Cre Egfr<sup>lox/lox</sup>* animals was observed. Deletion specifically within the CNS caused a

significant reduction in body weight and adipose mass, similar to the phenotype noted in the previous experiments. Therefore, we evaluated the metabolic, histological, and clinical consequences of this phenotype. Similar to the B6 mice fed the WD with an EGFR inhibitor (WD/INH), a decrease in feeding efficiency, smaller adipocytes per fat depot, improved clinical chemistry, and no differences in wheel running or RER were observed in *GFAP-Cre Egfr<sup>lox/lox</sup>* mice compared to controls. However, an increase in food intake, caloric energy expenditure, and oxygen consumption were noted in these animals, contrasting the B6 DIO model. We next evaluated hypothalamic neuropeptides NPY and POMC to determine mechanisms for this alteration in feeding and energy. We found decreases in anorexigenic neuropeptide *Pomc* mRNA expression in *GFAP-Cre Egfr<sup>lox/lox</sup>* mice. We also observed a decrease in hypothalamic *Egfr* mRNA expression in these mice, suggesting that EGFR downregulation in the hypothalamus is partly responsible for the metabolic phenotype observed. We also evaluated transcript levels of adipocyte stage-specific factors within the fat depots of each group and found increased *Arb3* mRNA expression and a trend for increased *Ucp1* mRNA expression in the *GFAP-Cre Egfr<sup>lox/lox</sup>* mice. This suggests that increased energy expenditure from hyperphagia, hyperkinesia, thermogenesis, and adipocyte oxidation is involved in the reduced body weight observed in these *GFAP-Cre Egfr<sup>lox/lox</sup>* mice.

*In vivo* studies of obesity have determined that, along with alterations in feeding, increases in energy expenditure, measured by home cage activity, body temperature, and increased brown adipocytes within white adipose depots, account for the observed weight loss (150, 168). To better evaluate reasons for the weight loss noted with EGFR inhibition, pair-fed experiments and those relating to the above mentioned mechanisms

should be performed, on both the B6 DIO mouse model and the *GFAP-Cre Egfr<sup>flx/flx</sup>* mice and their control littermates. If EGFR inhibition is to be used as a potential therapy for obesity, the use of an inhibitor is more relevant. However, examining the specific CNS effect with EGFR deletion is also useful. First, in order to distinguish the effects of caloric intake on the AG1478-induced fat mass decrease, pair fed experiments where control animals are fed the same amount of chow consumed by the animals fed the WD/INH should be performed. If the pair-fed animals show a higher fat mass compared to the WD/INH fed group this could indicate that the anti-obesity effects of EGFR inhibition are not only due to suppression of feeding, but some other effect such as energy expenditure, further evidenced by the decrease in feeding efficiency in both models.

Conventional treatment of obesity includes weight loss through reduced caloric intake and increasing physical activity (38, 48). In our studies, mice with EGFR inhibition or CNS ablation showed less body weight and fat mass, however their activity measured by voluntary wheel running was not different between groups. In *GFAP-Cre Egfr<sup>flx/flx</sup>* mice, increased oxygen consumption was also noted, evidence of potential increased home cage activity. Wheel running may or may not be a direct reflection of home cage activity in mice fed a HFD since some studies show increased home cage activity with increased wheel running while others show no change in home cage activity but decreases in wheel running (130-132). Therefore, analyzing their locomotor home cage activity may provide evidence of increased energy expenditure associated with EGFR downregulation. To determine this, locomotor activity should be assessed by placing individual animals into open-field boxes equipped with infrared beams to monitor

activity throughout the study. Increased locomoter activity with reductions in body fat has been observed in both obese Zucker and DIO rats, supporting that increased locomoter activity would translate into increased energy expenditure and loss of body fat (168). Also interesting would be to determine if body temperature differed between groups since it has been observed in other DIO animal models that a higher rectal temperature is related to weight loss (150, 169). Another measure of increased energy expenditure is to evaluate evidence for increased thermogenic brown fat within white adipose depots. Although B6 mice fed WD/INH did not show increased *Ucp1* expression in epididymal fat pads, *GFAP-Cre* transgenic mice showed a trend for increased *Ucp1*, suggesting increased brown adipocytes in this white adipose depot. However, since perirenal, inguinal, and other subcutaneous white adipose depots possess more capacity for brown adipocytes than this visceral depot, we should analyze the other fat depots collected for brown adipocytes and *Ucp1* expression (139, 140). Increased *Ucp1* expression in the other fat pads of these animals would then suggest more brown adipocytes in the white adipose tissue. Promotion of brown fat adipogenesis in these depots could therefore contribute to increased thermogenesis and the decreased fat mass observed. Therefore, enhanced energy expenditure may represent a peripheral mechanism contributing to weight loss in the form of increased locomoter activity, rectal temperature, and/or increased brown adipocytes within white adipose tissue in B6 mice fed WD/INH or in the *GFAP-Cre Egfr<sup>fllox/fllox</sup>* mice.

From the data collected in this study and other studies, it seems that an increase in fatty acid oxidation within white adipocytes may be another mechanism whereby *GFAP-Cre Egfr<sup>fllox/fllox</sup>* mice have lower fat mass than their control littermates. This phenotype

has been observed in mice that overexpress a triglyceride hydrolase in white adipose tissue or are treated with an orexigenic melanin-concentrating hormone-1 receptor antagonist. In both of these models, increased lipolysis is specific to white adipose tissue without increased circulating levels of fatty acids (148-150). The fatty acids liberated from white adipose depots could have detrimental effects on metabolism by causing ectopic lipid storage in liver, skeletal muscle, heart, and other organs and therefore where these fatty acids are going needs to still be determined in these models. Increased delivery of fatty acids to the liver would affect metabolism through alterations in glucose production, lipoprotein secretion, and insulin clearance. Also, increased lipid in skeletal muscle could decrease insulin-stimulated peripheral glucose disposal (147, 170). Excess lipid in the heart can also lead to adverse alterations in cardiac function (157). First, to evaluate if lipolysis is occurring in the fat depots of these animals, adipose tissue explants should be collected from both WD/INH and *GFAP-Cre Egfr<sup>lox/lox</sup>* mice and their control littermates and glycerol release measured in culture. Higher glycerol amounts would indicate higher lipolysis in the adipose depots. Next, expression of lipid metabolism genes in the white adipose tissue and the liver of these mice should be assessed to provide for further evidence that increased oxidation is occurring leading to a lower weight loss. Determining the levels of fatty acids in serum and in organs such as the liver, heart, and skeletal muscle should also be performed to assess if an increased oxidation in adipose tissue lead to increases in circulating lipid or in ectopic lipid storage in *GFAP-Cre Egfr<sup>lox/lox</sup>* mice compared to their control littermates. We demonstrate that excreted fat is not different in *GFAP-Cre Egfr<sup>lox/lox</sup>* mice compared to their control littermates, therefore some evidence that circulating fatty acids may not be increased.

Ultimately, the question as to how this decrease in *Egfr* within the hypothalamus alters neuropeptide expression and how these alterations signal to the periphery for decreased body weight and perhaps increased fatty acid oxidation remains. Perhaps EGFR in the hypothalamus is affecting lipid oxidation activity within the ARC, which is sensed by appetite or energy homeostatic neurons to alter food intake and energy signaling to the periphery. This has been noted in studies of an inhibitor to fatty acid synthase in the hypothalamus (151). Decreased body weight was observed, which was due in part to the inhibitor altering AMP-activated protein kinase (AMPK) activity, a sensor of peripheral energy balance within the hypothalamus (151). Future studies could look at AG1478's effect on AMPK levels in neuronal cultures and determine if activity is altered thereby demonstrating a link between the hypothalamus and the periphery with EGFR deletion using *GFAP-Cre*.

Although both the DIO B6 model and the *GFAP-Cre* transgenic model produced fat mass reductions the genetic model is phenotypically more severe. The opposite feeding behavior and alterations in hypothalamic neuropeptides noted between these two models imply that this effect is due to CNS alternations. To better determine the mechanism of these phenotypes, we first need to understand why behavior changes are occurring in our animals with AG178 treatment or EGFR deletion with *GFAP-Cre*. To assess changes in behavior relating to diet or treatment, microarray technology is often employed (172, 173). This same technique could be applied to our study to evaluate the effects of AG1478 administration or EGFR deletion with *GFAP-Cre* in the hypothalamus, where central appetite regulatory genes are enriched; validating changes of gene expression levels using quantitative RT-PCR. Altered expression of genes in the

hypothalamus of mice fed the WD/INH or *GFAP-Cre Egfr<sup>flx/flx</sup>* mice might therefore be understood as the underlying mechanism behind the phenotypes observed. Also, this analysis could confirm or deny the role of EGFR in the hypothalamus in appetite and energy homeostasis. Altered genes could include those involved in lipid metabolism, glucose homeostasis, satiety, or inflammation.

Off-targets effects have been observed in female wild-type B6 mice chronically exposed to small molecule EGFR inhibitors with decreased weight gain compared to controls. No significant differences were observed in wet heart weight or cardiomyocyte size in these animals. However, histological analysis revealed an increase in fibrosis and decreased expression of an anti-apoptotic gene in these hearts (120). Although the wet weights of hearts in the B6 mice fed the WD/INH or *GFAP-Cre* genetic studies did not differ between groups, heart histology should be performed to evaluate these findings.

Given the complexity of EGFR signaling and heterodimers that occur between family members, perhaps alterations of other family members are also involved in the decreased fat mass phenotype. Microarrays performed on the hypothalamuses of the animals may provide evidence of their involvement. ERBB2 does not bind a ligand and therefore heterodimerization with other ERBB members is required, with EGFR being the preferred partner (72, 75). ERBB2 expression increases during the proliferation and growth arrest phases of adipogenesis. However, progression through differentiation leads to a decrease in expression, similar to EGFR. When serum-starved 3T3-L1 cells are treated with EGF, an increase in ERBB2 activation is noted showing that EGF could activate ERBB2 in these cells through heterodimerization with EGFR (72, 75). Although AG1478 is a tyrosine kinase inhibitor that is highly selective for EGFR (IC<sub>50</sub>, 3 nM

EGFR versus  $> 100 \mu\text{M}$  ERBB2) (2, 5, 119), EGFR and ERBB2 have a high sequence homology in their catalytic domains and therefore AG1478 could suppress the activity of both receptors (158). To determine if AG1478 is suppressing ERBB2 in this model, ERBB2 expression could be assessed in the fat pads of the B6 mice fed the WD/INH and their control littermates. To further evaluate the potential role of ERBB2 in weight loss phenotypes, similar experiments with wild-type B6 mice could be performed with an ERBB2 selective inhibitor or the Cre/loxP system could be utilized for hypothalamic-specific deletion. With respect to ERBB3 and ERBB4 and their role in the body weight phenotype, both are expressed in the hypothalamus (144) and experiments with their deletion in this region or with inhibitors could be performed. Our lab has generated mice with a conditional brain deletion of ERBB3 (*ERBB3<sup>tm2Dwt</sup>*) using the *Nestin-Cre* transgene (*Nestin-Cre Erbb3<sup>lox/lox</sup>*). Male mice were placed on normal chow at six months of age and *Nestin-Cre Erbb3<sup>lox/lox</sup>* mice weighed significantly less than their wild-type littermates at the study's end. However, our lab has assessed the brain phenotype in *Nestin-Cre Egf<sup>lox/lox</sup>* mice and found neurodegeneration and growth retardation similar to what is found in *Egfr* null mice (138). Therefore this decreased weight may not be directly due to ERBB3's effects on feeding and energy, but rather on neuronal survival.

## REFERENCES

1. **Fowler KJ, Walker F, Alexander W, Hibbs ML, Nice EC, Bohmer RM, Mann GB, Thumwood C, Maglitto R, Danks JA, et al.** 1995 A mutation in the epidermal growth factor receptor in waved-2 mice has a profound effect on receptor biochemistry that results in impaired lactation. *Proceedings of the National Academy of Sciences of the United States of America* 92:1465-1469
2. **Ellis AG, Doherty MM, Walker F, Weinstock J, Nerrie M, Vitali A, Murphy R, Johns TG, Scott AM, Levitzki A, McLachlan G, Webster LK, Burgess AW, Nice EC** 2006 Preclinical analysis of the analinoquinazoline AG1478, a specific small molecule inhibitor of EGF receptor tyrosine kinase. *Biochemical pharmacology* 71:1422-1434
3. **Johnston JB, Navaratnam S, Pitz MW, Maniate JM, Wiechec E, Baust H, Gingerich J, Skliris GP, Murphy LC, Los M** 2006 Targeting the EGFR pathway for cancer therapy. *Current medicinal chemistry* 13:3483-3492
4. **Chan HW, Smith NJ, Hannan RD, Thomas WG** 2006 Tackling the EGFR in pathological tissue remodelling. *Pulmonary pharmacology & therapeutics* 19:74-78
5. **Gan HK, Walker F, Burgess AW, Rigopoulos A, Scott AM, Johns TG** 2007 The epidermal growth factor receptor (EGFR) tyrosine kinase inhibitor AG1478 increases the formation of inactive untethered EGFR dimers. Implications for combination therapy with monoclonal antibody 806. *The Journal of biological chemistry* 282:2840-2850
6. **Schulze WX, Deng L, Mann M** 2005 Phosphotyrosine interactome of the ErbB-receptor kinase family. *Molecular systems biology* 1:2005 0008
7. **Holbro T, Hynes NE** 2004 ErbB receptors: directing key signaling networks throughout life. *Annu Rev Pharmacol Toxicol* 44:195-217
8. **Seals DF, Courtneidge SA** 2003 The ADAMs family of metalloproteases: multidomain proteins with multiple functions. *Genes & development* 17:7-30
9. **Yarden Y, Sliwkowski MX** 2001 Untangling the ErbB signalling network. *Nat Rev Mol Cell Biol* 2:127-137
10. **Xian CJ, Zhou XF** 1999 Roles of transforming growth factor-alpha and related molecules in the nervous system. *Mol Neurobiol* 20:157-183
11. **Baulida J, Kraus MH, Alimandi M, Di Fiore PP, Carpenter G** 1996 All ErbB receptors other than the epidermal growth factor receptor are endocytosis impaired. *The Journal of biological chemistry* 271:5251-5257

12. **Sanderson MP, Dempsey PJ, Dunbar AJ** 2006 Control of ErbB signaling through metalloprotease mediated ectodomain shedding of EGF-like factors. *Growth Factors* 24:121-136
13. **Higashiyama S, Iwabuki H, Morimoto C, Hieda M, Inoue H, Matsushita N** 2008 Membrane-anchored growth factors, the epidermal growth factor family: beyond receptor ligands. *Cancer Sci* 99:214-220
14. **Statistics NcfH** 2006 Prevalence of Overweight Among Children and Adolescents: United States, 2003-2004. In:
15. **Flegal KM, Carroll MD, Ogden CL, Curtin LR** Prevalence and trends in obesity among US adults, 1999-2008. *JAMA* 303:235-241
16. **Allan MF, Eisen EJ, Pomp D** 2004 The M16 mouse: an outbred animal model of early onset polygenic obesity and diabetes. *Obesity research* 12:1397-1407
17. **Kang M, Oh JW, Lee HK, Chung HS, Lee SM, Kim C, Lee HJ, Yoon DW, Choi H, Kim H, Shin M, Hong M, Bae H** 2004 Anti-obesity effect of PM-F2-OB, an anti-obesity herbal formulation, on rats fed a high-fat diet. *Biological & pharmaceutical bulletin* 27:1251-1256
18. **Lorincz AM, Sukumar S** 2006 Molecular links between obesity and breast cancer. *Endocrine-related cancer* 13:279-292
19. **Farrell GC, Larter CZ** 2006 Nonalcoholic fatty liver disease: from steatosis to cirrhosis. *Hepatology (Baltimore, Md)* 43:S99-S112
20. **Tsai AG, Williamson DF, Glick HA** Direct medical cost of overweight and obesity in the USA: a quantitative systematic review. *Obes Rev*
21. **Das UN** 2001 Is obesity an inflammatory condition? *Nutrition (Burbank, Los Angeles County, Calif)* 17:953-966
22. **Cano P, Cardinali DP, Rios-Lugo MJ, Fernandez-Mateos MP, Reyes Toso CF, Esquifino AI** 2009 Effect of a High-fat Diet on 24-Hour Pattern of Circulating Adipocytokines in Rats. *Obesity (Silver Spring)*
23. **Samad F, Uysal KT, Wiesbrock SM, Pandey M, Hotamisligil GS, Loskutoff DJ** 1999 Tumor necrosis factor alpha is a key component in the obesity-linked elevation of plasminogen activator inhibitor 1. *Proceedings of the National Academy of Sciences of the United States of America* 96:6902-6907
24. **Hotamisligil GS, Arner P, Caro JF, Atkinson RL, Spiegelman BM** 1995 Increased adipose tissue expression of tumor necrosis factor-alpha in human obesity and insulin resistance. *The Journal of clinical investigation* 95:2409-2415

25. **Serino M, Menghini R, Fiorentino L, Amoruso R, Mauriello A, Lauro D, Sbraccia P, Hribal ML, Lauro R, Federici M** 2007 Mice heterozygous for tumor necrosis factor-alpha converting enzyme are protected from obesity-induced insulin resistance and diabetes. *Diabetes* 56:2541-2546
26. **Wu JJ, Roth RJ, Anderson EJ, Hong EG, Lee MK, Choi CS, Neuffer PD, Shulman GI, Kim JK, Bennett AM** 2006 Mice lacking MAP kinase phosphatase-1 have enhanced MAP kinase activity and resistance to diet-induced obesity. *Cell metabolism* 4:61-73
27. **Tilg H, Moschen AR** 2006 Adipocytokines: mediators linking adipose tissue, inflammation and immunity. *Nature reviews* 6:772-783
28. **Valsamakis G, McTernan PG, Chetty R, Al Daghri N, Field A, Hanif W, Barnett AH, Kumar S** 2004 Modest weight loss and reduction in waist circumference after medical treatment are associated with favorable changes in serum adipocytokines. *Metabolism: clinical and experimental* 53:430-434
29. **Silha JV, Krsek M, Skrha JV, Sucharda P, Nyomba BL, Murphy LJ** 2003 Plasma resistin, adiponectin and leptin levels in lean and obese subjects: correlations with insulin resistance. *European journal of endocrinology / European Federation of Endocrine Societies* 149:331-335
30. **King PJ** 2005 The hypothalamus and obesity. *Curr Drug Targets* 6:225-240
31. **Jequier E** 2002 Leptin signaling, adiposity, and energy balance. *Ann N Y Acad Sci* 967:379-388
32. **Schwartz MW, Woods SC, Porte D, Jr., Seeley RJ, Baskin DG** 2000 Central nervous system control of food intake. *Nature* 404:661-671
33. **Ziylan YZ, Baltaci AK, Mogulkoc R** 2009 Leptin transport in the central nervous system. *Cell Biochem Funct* 27:63-70
34. **Hutley L, Prins JB** 2005 Fat as an endocrine organ: relationship to the metabolic syndrome. *Am J Med Sci* 330:280-289
35. **Rosen ED, Spiegelman BM** 2000 Molecular regulation of adipogenesis. *Annual review of cell and developmental biology* 16:145-171
36. **Collins S, Martin TL, Surwit RS, Robidoux J** 2004 Genetic vulnerability to diet-induced obesity in the C57BL/6J mouse: physiological and molecular characteristics. *Physiology & behavior* 81:243-248
37. **Surwit RS, Wang S, Petro AE, Sanchis D, Raimbault S, Ricquier D, Collins S** 1998 Diet-induced changes in uncoupling proteins in obesity-prone and obesity-resistant strains of mice. *Proceedings of the National Academy of Sciences of the United States of America* 95:4061-4065

38. **Kibenge MT, Chan CB** 2002 The effects of high-fat diet on exercise-induced changes in metabolic parameters in Zucker fa/fa rats. *Metabolism: clinical and experimental* 51:708-715
39. **Schwartz MB, Brownell KD** 2007 Actions necessary to prevent childhood obesity: creating the climate for change. *J Law Med Ethics* 35:78-89
40. **Mullerova D, Kopecky J** 2007 White adipose tissue: storage and effector site for environmental pollutants. *Physiological research / Academia Scientiarum Bohemoslovaca* 56:375-381
41. **Li QQ, Loganath A, Chong YS, Tan J, Obbard JP** 2006 Persistent organic pollutants and adverse health effects in humans. *Journal of toxicology and environmental health* 69:1987-2005
42. **Tuma RS** 2007 Environmental chemicals--not just overeating--may cause obesity. *Journal of the National Cancer Institute* 99:835
43. **Newbold RR, Padilla-Banks E, Snyder RJ, Jefferson WN** 2007 Perinatal exposure to environmental estrogens and the development of obesity. *Molecular nutrition & food research* 51:912-917
44. **Enan E, El-Sabeawy F, Moran F, Overstreet J, Lasley B** 1998 Interruption of estradiol signal transduction by 2,3,7,8-tetrachlorodibenzo-p-dioxin (TCDD) through disruption of the protein phosphorylation pathway in adipose tissues from immature and mature female rats. *Biochemical pharmacology* 55:1077-1090
45. **Liu PC, Matsumura F** 2006 TCDD suppresses insulin-responsive glucose transporter (GLUT-4) gene expression through C/EBP nuclear transcription factors in 3T3-L1 adipocytes. *J Biochem Mol Toxicol* 20:79-87
46. **Hanlon PR, Cimafranca MA, Liu X, Cho YC, Jefcoate CR** 2005 Microarray analysis of early adipogenesis in C3H10T1/2 cells: cooperative inhibitory effects of growth factors and 2,3,7,8-tetrachlorodibenzo-p-dioxin. *Toxicology and applied pharmacology* 207:39-58
47. **Mukku VR, Stancel GM** 1985 Regulation of epidermal growth factor receptor by estrogen. *The Journal of biological chemistry* 260:9820-9824
48. **Hausman DB, DiGirolamo M, Bartness TJ, Hausman GJ, Martin RJ** 2001 The biology of white adipocyte proliferation. *Obes Rev* 2:239-254
49. **Tanaka T, Yoshida N, Kishimoto T, Akira S** 1997 Defective adipocyte differentiation in mice lacking the C/EBPbeta and/or C/EBPdelta gene. *The EMBO journal* 16:7432-7443
50. **Klaus S** 2004 Adipose tissue as a regulator of energy balance. *Curr Drug Targets* 5:241-250

51. **Seale P, Lazar MA** 2009 Brown fat in humans: turning up the heat on obesity. *Diabetes* 58:1482-1484
52. **Cinti S** 2009 Transdifferentiation properties of adipocytes in the Adipose Organ. *American journal of physiology*
53. **Cinti S** 2009 Reversible physiological transdifferentiation in the adipose organ. *Proc Nutr Soc* 68:340-349
54. **Rangwala SM, Lazar MA** 2000 Transcriptional control of adipogenesis. *Annu Rev Nutr* 20:535-559
55. **Saito M, Okamatsu-Ogura Y, Matsushita M, Watanabe K, Yoneshiro T, Nio-Kobayashi J, Iwanaga T, Miyagawa M, Kameya T, Nakada K, Kawai Y, Tsujisaki M** 2009 High incidence of metabolically active brown adipose tissue in healthy adult humans: effects of cold exposure and adiposity. *Diabetes* 58:1526-1531
56. **Smas CM, Sul HS** 1995 Control of adipocyte differentiation. *The Biochemical journal* 309 ( Pt 3):697-710
57. **Gregoire FM, Smas CM, Sul HS** 1998 Understanding adipocyte differentiation. *Physiological reviews* 78:783-809
58. **Ntambi JM, Young-Cheul K** 2000 Adipocyte differentiation and gene expression. *The Journal of nutrition* 130:3122S-3126S
59. **Darlington GJ, Ross SE, MacDougald OA** 1998 The role of C/EBP genes in adipocyte differentiation. *The Journal of biological chemistry* 273:30057-30060
60. **Hu E, Kim JB, Sarraf P, Spiegelman BM** 1996 Inhibition of adipogenesis through MAP kinase-mediated phosphorylation of PPARgamma. *Science (New York, NY)* 274:2100-2103
61. **Smyth MJ, Sparks RL, Wharton W** 1993 Preadipocyte cell lines: models of cellular proliferation and differentiation. *J Cell Sci* 106 ( Pt 1):1-9
62. **Font de Mora J, Porras A, Ahn N, Santos E** 1997 Mitogen-activated protein kinase activation is not necessary for, but antagonizes, 3T3-L1 adipocytic differentiation. *Molecular and cellular biology* 17:6068-6075
63. **Camp HS, Tafuri SR** 1997 Regulation of peroxisome proliferator-activated receptor gamma activity by mitogen-activated protein kinase. *The Journal of biological chemistry* 272:10811-10816
64. **Lee JS, Suh JM, Park HG, Bak EJ, Yoo YJ, Cha JH** 2008 Heparin-binding epidermal growth factor-like growth factor inhibits adipocyte differentiation at commitment and early induction stages. *Differentiation* 76:478-487

65. **Lee JS, Kim JM, Hong EK, Kim SO, Yoo YJ, Cha JH** 2009 Effects of heparin-binding epidermal growth factor-like growth factor on cell repopulation and signal transduction in periodontal ligament cells after scratch wounding in vitro. *J Periodontal Res* 44:52-61
66. **Boney CM, Gruppuso PA, Faris RA, Frackelton AR, Jr.** 2000 The critical role of Shc in insulin-like growth factor-I-mediated mitogenesis and differentiation in 3T3-L1 preadipocytes. *Mol Endocrinol* 14:805-813
67. **Pagano E, Coso O, Calvo JC** 2008 Down-modulation of erbB2 activity is necessary but not enough in the differentiation of 3T3-L1 preadipocytes. *Journal of cellular biochemistry* 104:274-285
68. **Adachi H, Kurachi H, Homma H, Adachi K, Imai T, Sakata M, Matsuzawa Y, Miyake A** 1995 Involvement of epidermal growth factor in inducing adiposity of age female mice. *The Journal of endocrinology* 146:381-393
69. **Adachi H, Kurachi H, Homma H, Adachi K, Imai T, Morishige K, Matsuzawa Y, Miyake A** 1994 Epidermal growth factor promotes adipogenesis of 3T3-L1 cell in vitro. *Endocrinology* 135:1824-1830
70. **Kurachi H, Adachi H, Ohtsuka S, Morishige K, Amemiya K, Keno Y, Shimomura I, Tokunaga K, Miyake A, Matsuzawa Y, et al.** 1993 Involvement of epidermal growth factor in inducing obesity in ovariectomized mice. *Am J Physiol* 265:E323-331
71. **Serrero G, Mills D** 1991 Physiological role of epidermal growth factor on adipose tissue development in vivo. *Proceedings of the National Academy of Sciences of the United States of America* 88:3912-3916
72. **Harrington M, Pond-Tor S, Boney CM** 2007 Role of epidermal growth factor and ErbB2 receptors in 3T3-L1 adipogenesis. *Obesity (Silver Spring)* 15:563-571
73. **Bost F, Aouadi M, Caron L, Binetruy B** 2005 The role of MAPKs in adipocyte differentiation and obesity. *Biochimie* 87:51-56
74. **Sugawara K, Schneider MR, Dahlhoff M, Kloepper JE, Paus R** Cutaneous consequences of inhibiting EGF receptor signaling in vivo: Normal hair follicle development, but retarded hair cycle induction and inhibition of adipocyte growth in *Egfr(Wa5)* mice. *J Dermatol Sci*
75. **Pagano E, Calvo JC** 2003 ErbB2 and EGFR are downmodulated during the differentiation of 3T3-L1 preadipocytes. *Journal of cellular biochemistry* 90:561-572
76. **Surwit RS, Feinglos MN, Rodin J, Sutherland A, Petro AE, Opara EC, Kuhn CM, Rebuffe-Scrive M** 1995 Differential effects of fat and sucrose on the

- development of obesity and diabetes in C57BL/6J and A/J mice. *Metabolism: clinical and experimental* 44:645-651
77. **Koza RA, Nikonova L, Hogan J, Rim JS, Mendoza T, Faulk C, Skaf J, Kozak LP** 2006 Changes in gene expression foreshadow diet-induced obesity in genetically identical mice. *PLoS genetics* 2:e81
  78. **Beck B** 2006 Neuropeptide Y in normal eating and in genetic and dietary-induced obesity. *Philos Trans R Soc Lond B Biol Sci* 361:1159-1185
  79. **Friedman JM, Halaas JL** 1998 Leptin and the regulation of body weight in mammals. *Nature* 395:763-770
  80. **Zhang Y, Proenca R, Maffei M, Barone M, Leopold L, Friedman JM** 1994 Positional cloning of the mouse obese gene and its human homologue. *Nature* 372:425-432
  81. **Threadgill DW, Dlugosz AA, Hansen LA, Tennenbaum T, Lichti U, Yee D, LaMantia C, Mourton T, Herrup K, Harris RC, et al.** 1995 Targeted disruption of mouse EGF receptor: effect of genetic background on mutant phenotype. *Science (New York, NY)* 269:230-234
  82. **Sibilia M, Steinbach JP, Stingl L, Aguzzi A, Wagner EF** 1998 A strain-independent postnatal neurodegeneration in mice lacking the EGF receptor. *The EMBO journal* 17:719-731
  83. **Luetkeke NC, Qiu TH, Peiffer RL, Oliver P, Smithies O, Lee DC** 1993 TGF alpha deficiency results in hair follicle and eye abnormalities in targeted and waved-1 mice. *Cell* 73:263-278
  84. **Mann GB, Fowler KJ, Gabriel A, Nice EC, Williams RL, Dunn AR** 1993 Mice with a null mutation of the TGF alpha gene have abnormal skin architecture, wavy hair, and curly whiskers and often develop corneal inflammation. *Cell* 73:249-261
  85. **Fitch KR, McGowan KA, van Raamsdonk CD, Fuchs H, Lee D, Puech A, Herault Y, Threadgill DW, Hrabe de Angelis M, Barsh GS** 2003 Genetics of dark skin in mice. *Genes & development* 17:214-228
  86. **Lee D, Cross SH, Strunk KE, Morgan JE, Bailey CL, Jackson IJ, Threadgill DW** 2004 Wa5 is a novel ENU-induced antimorphic allele of the epidermal growth factor receptor. *Mamm Genome* 15:525-536
  87. **Galli-Taliadoros LA, Sedgwick JD, Wood SA, Korner H** 1995 Gene knock-out technology: a methodological overview for the interested novice. *Journal of immunological methods* 181:1-15

88. **Barlow C, Schroeder M, Lekstrom-Himes J, Kylefjord H, Deng CX, Wynshaw-Boris A, Spiegelman BM, Xanthopoulos KG** 1997 Targeted expression of Cre recombinase to adipose tissue of transgenic mice directs adipose-specific excision of loxP-flanked gene segments. *Nucleic acids research* 25:2543-2545
89. **Weisberg SP, McCann D, Desai M, Rosenbaum M, Leibel RL, Ferrante AW, Jr.** 2003 Obesity is associated with macrophage accumulation in adipose tissue. *The Journal of clinical investigation* 112:1796-1808
90. **Cooke D, Bloom S** 2006 The obesity pipeline: current strategies in the development of anti-obesity drugs. *Nat Rev Drug Discov* 5:919-931
91. **Posey KA, Clegg DJ, Printz RL, Byun J, Morton GJ, Vivekanandan-Giri A, Pennathur S, Baskin DG, Heinecke JW, Woods SC, Schwartz MW, Niswender KD** 2009 Hypothalamic proinflammatory lipid accumulation, inflammation, and insulin resistance in rats fed a high-fat diet. *American journal of physiology* 296:E1003-1012
92. **Morton GJ, Cummings DE, Baskin DG, Barsh GS, Schwartz MW** 2006 Central nervous system control of food intake and body weight. *Nature* 443:289-295
93. **Barsh GS, Schwartz MW** 2002 Genetic approaches to studying energy balance: perception and integration. *Nat Rev Genet* 3:589-600
94. **Kim EK, Kleman AM, Ronnett GV** 2007 Fatty acid synthase gene regulation in primary hypothalamic neurons. *Neurosci Lett* 423:200-204
95. **Robidoux J, Martin TL, Collins S** 2004 Beta-adrenergic receptors and regulation of energy expenditure: a family affair. *Annu Rev Pharmacol Toxicol* 44:297-323
96. **Greenberg AS, Shen WJ, Muliro K, Patel S, Souza SC, Roth RA, Kraemer FB** 2001 Stimulation of lipolysis and hormone-sensitive lipase via the extracellular signal-regulated kinase pathway. *The Journal of biological chemistry* 276:45456-45461
97. **Schreyer SA, Cummings DE, McKnight GS, LeBoeuf RC** 2001 Mutation of the RIIbeta subunit of protein kinase A prevents diet-induced insulin resistance and dyslipidemia in mice. *Diabetes* 50:2555-2562
98. **Newhall KJ, Cummings DE, Nolan MA, McKnight GS** 2005 Deletion of the RIIbeta-subunit of protein kinase A decreases body weight and increases energy expenditure in the obese, leptin-deficient ob/ob mouse. *Mol Endocrinol* 19:982-991

99. **Collins S, Cao W, Robidoux J** 2004 Learning new tricks from old dogs: beta-adrenergic receptors teach new lessons on firing up adipose tissue metabolism. *Mol Endocrinol* 18:2123-2131
100. **Robidoux J, Kumar N, Daniel KW, Moukdar F, Cyr M, Medvedev AV, Collins S** 2006 Maximal beta3-adrenergic regulation of lipolysis involves Src and epidermal growth factor receptor-dependent ERK1/2 activation. *The Journal of biological chemistry* 281:37794-37802
101. **Soeder KJ, Snedden SK, Cao W, Della Rocca GJ, Daniel KW, Luttrell LM, Collins S** 1999 The beta3-adrenergic receptor activates mitogen-activated protein kinase in adipocytes through a Gi-dependent mechanism. *The Journal of biological chemistry* 274:12017-12022
102. **Plata-Salaman CR** 1991 Epidermal growth factor and the nervous system. *Peptides* 12:653-663
103. **Wong RW, Guillaud L** 2004 The role of epidermal growth factor and its receptors in mammalian CNS. *Cytokine & growth factor reviews* 15:147-156
104. **Leung WY, Thomas GN, Chan JC, Tomlinson B** 2003 Weight management and current options in pharmacotherapy: orlistat and sibutramine. *Clinical therapeutics* 25:58-80
105. **Vendrell J, Broch M, Vilarrasa N, Molina A, Gomez JM, Gutierrez C, Simon I, Soler J, Richart C** 2004 Resistin, adiponectin, ghrelin, leptin, and proinflammatory cytokines: relationships in obesity. *Obesity research* 12:962-971
106. **Milan G, Granzotto M, Scarda A, Calcagno A, Pagano C, Federspil G, Vettor R** 2002 Resistin and adiponectin expression in visceral fat of obese rats: effect of weight loss. *Obesity research* 10:1095-1103
107. **Corsetti JP, Sterry JA, Sparks JD, Sparks CE, Weintraub M** 1991 Effect of weight loss on serum lipoprotein(a) concentrations in an obese population. *Clinical chemistry* 37:1191-1195
108. **Finer N, James WP, Kopelman PG, Lean ME, Williams G** 2000 One-year treatment of obesity: a randomized, double-blind, placebo-controlled, multicentre study of orlistat, a gastrointestinal lipase inhibitor. *Int J Obes Relat Metab Disord* 24:306-313
109. **Slordal L, Spigset O** 2006 Heart failure induced by non-cardiac drugs. *Drug Saf* 29:567-586
110. **Bray GA, Tartaglia LA** 2000 Medicinal strategies in the treatment of obesity. *Nature* 404:672-677

111. **Crandall DL, Quinet EM, El Ayachi S, Hreha AL, Leik CE, Savio DA, Juhan-Vague I, Alessi MC** 2006 Modulation of adipose tissue development by pharmacological inhibition of PAI-1. *Arteriosclerosis, thrombosis, and vascular biology* 26:2209-2215
112. **Venugopal J, Hanashiro K, Nagamine Y** 2007 Regulation of PAI-1 gene expression during adipogenesis. *Journal of cellular biochemistry* 101:369-380
113. **Wang SJ, Birtles S, de Schoolmeester J, Swales J, Moody G, Hislop D, O'Dowd J, Smith DM, Turnbull AV, Arch JR** 2006 Inhibition of 11beta-hydroxysteroid dehydrogenase type 1 reduces food intake and weight gain but maintains energy expenditure in diet-induced obese mice. *Diabetologia* 49:1333-1337
114. **Araki K, Masaki T, Katsuragi I, Tanaka K, Kakuma T, Yoshimatsu H** 2006 Telmisartan prevents obesity and increases the expression of uncoupling protein 1 in diet-induced obese mice. *Hypertension* 48:51-57
115. **Harari PM** 2004 Epidermal growth factor receptor inhibition strategies in oncology. *Endocrine-related cancer* 11:689-708
116. **Rowinsky EK** 2004 The erbB family: targets for therapeutic development against cancer and therapeutic strategies using monoclonal antibodies and tyrosine kinase inhibitors. *Annual review of medicine* 55:433-457
117. **Feng FY, Lopez CA, Normolle DP, Varambally S, Li X, Chun PY, Davis MA, Lawrence TS, Nyati MK** 2007 Effect of epidermal growth factor receptor inhibitor class in the treatment of head and neck cancer with concurrent radiochemotherapy in vivo. *Clin Cancer Res* 13:2512-2518
118. **Jimeno A, Hidalgo M** 2006 Pharmacogenomics of epidermal growth factor receptor (EGFR) tyrosine kinase inhibitors. *Biochimica et biophysica acta* 1766:217-229
119. **Levitzki A, Gazit A** 1995 Tyrosine kinase inhibition: an approach to drug development. *Science (New York, NY)* 267:1782-1788
120. **Barrick CJ, Yu M, Chao HH, Threadgill DW** 2008 Chronic pharmacologic inhibition of EGFR leads to cardiac dysfunction in C57BL/6J mice. *Toxicol Appl Pharmacol* 228:315-325
121. **Prada PO, Ropelle ER, Mourao RH, de Souza CT, Pauli JR, Cintra DE, Schenka A, Rocco SA, Rittner R, Franchini KG, Vassalo J, Velloso LA, Carnevalheira JB, Saad MJ** 2009 An EGFR Tyrosine-Kinase Inhibitor (PD153035) Improves Glucose Tolerance and Insulin Action in High-Fat Diet-Fed Mice. *Diabetes*

122. **Suc I, Meilhac O, Lajoie-Mazenc I, Vandaele J, Jurgens G, Salvayre R, Negre-Salvayre A** 1998 Activation of EGF receptor by oxidized LDL. *FASEB J* 12:665-671
123. **Gouni-Berthold I, Sachinidis A** 2004 Possible non-classic intracellular and molecular mechanisms of LDL cholesterol action contributing to the development and progression of atherosclerosis. *Curr Vasc Pharmacol* 2:363-370
124. **Wellen KE, Hotamisligil GS** 2003 Obesity-induced inflammatory changes in adipose tissue. *The Journal of clinical investigation* 112:1785-1788
125. **Navab M, Gharavi N, Watson AD** 2008 Inflammation and metabolic disorders. *Current opinion in clinical nutrition and metabolic care* 11:459-464
126. **Cuif JP, Denis A, Frerotte B, Rekkab D** 2000 Distribution of minor elements during secretion of the microstructural sequence in the shells of some mollusks. *Comptes rendus des séances de l'Académie des sciences Série II, Mécanique, physique, chimie, sciences de l'univers, sciences de la terre* 91:121-122
127. **Livak KJ, Schmittgen TD** 2001 Analysis of relative gene expression data using real-time quantitative PCR and the 2<sup>(-Delta Delta C(T))</sup> Method. *Methods* 25:402-408
128. **Luetke NC, Phillips HK, Qiu TH, Copeland NG, Earp HS, Jenkins NA, Lee DC** 1994 The mouse waved-2 phenotype results from a point mutation in the EGF receptor tyrosine kinase. *Genes & development* 8:399-413
129. **Argyropoulos G, Harper ME** 2002 Uncoupling proteins and thermoregulation. *J Appl Physiol* 92:2187-2198
130. **Simoncic M, Horvat S, Stevenson PL, Bungler L, Holmes MC, Kenyon CJ, Speakman JR, Morton NM** 2008 Divergent physical activity and novel alternative responses to high fat feeding in polygenic fat and lean mice. *Behav Genet* 38:292-300
131. **Coyle CA, Strand SC, Good DJ** 2008 Reduced activity without hyperphagia contributes to obesity in Tubby mutant mice. *Physiology & behavior* 95:168-175
132. **Malisch JL, Breuner CW, Gomes FR, Chappell MA, Garland T, Jr.** 2008 Circadian pattern of total and free corticosterone concentrations, corticosteroid-binding globulin, and physical activity in mice selectively bred for high voluntary wheel-running behavior. *Gen Comp Endocrinol* 156:210-217
133. **Digby JE, Montague CT, Sewter CP, Sanders L, Wilkison WO, O'Rahilly S, Prins JB** 1998 Thiazolidinedione exposure increases the expression of uncoupling protein 1 in cultured human preadipocytes. *Diabetes* 47:138-141

134. **Vernochet C, Peres SB, Davis KE, McDonald ME, Qiang L, Wang H, Scherer PE, Farmer SR** 2009 C/EBPalpha and the corepressors CtBP1 and CtBP2 regulate repression of select visceral white adipose genes during induction of the brown phenotype in white adipocytes by peroxisome proliferator-activated receptor gamma agonists. *Molecular and cellular biology* 29:4714-4728
135. **Das UN** 2009 Obesity: Genes, brain, gut, and environment. Nutrition (Burbank, Los Angeles County, Calif
136. **Lee K, Villena JA, Moon YS, Kim KH, Lee S, Kang C, Sul HS** 2003 Inhibition of adipogenesis and development of glucose intolerance by soluble preadipocyte factor-1 (Pref-1). *The Journal of clinical investigation* 111:453-461
137. **Lee TC, Threadgill DW** 2009 Generation and validation of mice carrying a conditional allele of the epidermal growth factor receptor. *Genesis* 47:85-92
138. **Lee T** 2008 Functional analysis of EGFR using a conditional allele. In: Genetics. Chapel Hill: University of North Carolina; 117
139. **Yu M** 2008 The Importance of ERBB Receptor Tyrosine Kinase Signaling in Colorectal Cancer— Implications for EGFR-Targeted Therapies. In: Genetics. Chapel Hill: University of North Carolina; 146
140. **Kloting N, Koch L, Wunderlich T, Kern M, Ruschke K, Krone W, Bruning JC, Bluher M** 2008 Autocrine IGF-1 action in adipocytes controls systemic IGF-1 concentrations and growth. *Diabetes* 57:2074-2082
141. **Schrauwen P, Hesselink M** 2002 UCP2 and UCP3 in muscle controlling body metabolism. *J Exp Biol* 205:2275-2285
142. **Schrauwen P, Hesselink MK, Blaak EE, Borghouts LB, Schaart G, Saris WH, Keizer HA** 2001 Uncoupling protein 3 content is decreased in skeletal muscle of patients with type 2 diabetes. *Diabetes* 50:2870-2873
143. **Gong DW, He Y, Reitman ML** 1999 Genomic organization and regulation by dietary fat of the uncoupling protein 3 and 2 genes. *Biochem Biophys Res Commun* 256:27-32
144. **Sharif A, Duhem-Tonnelle V, Allet C, Baroncini M, Loyens A, Kerr-Conte J, Collier F, Blond S, Ojeda SR, Junier MP, Prevot V** 2009 Differential erbB signaling in astrocytes from the cerebral cortex and the hypothalamus of the human brain. *Glia* 57:362-379
145. **Lin S, Storlien LH, Huang XF** 2000 Leptin receptor, NPY, POMC mRNA expression in the diet-induced obese mouse brain. *Brain research* 875:89-95
146. **Lafontan M** 2008 Advances in adipose tissue metabolism. *Int J Obes (Lond)* 32 Suppl 7:S39-51

147. **Jaworski K, Ahmadian M, Duncan RE, Sarkadi-Nagy E, Varady KA, Hellerstein MK, Lee HY, Samuel VT, Shulman GI, Kim KH, de Val S, Kang C, Sul HS** 2009 AdPLA ablation increases lipolysis and prevents obesity induced by high-fat feeding or leptin deficiency. *Nat Med* 15:159-168
148. **Ito M, Ishihara A, Gomori A, Matsushita H, Metzger JM, Marsh DJ, Haga Y, Iwaasa H, Tokita S, Takenaga N, Sato N, MacNeil DJ, Moriya M, Kanatani A** Mechanism of the anti-obesity effects induced by a novel melanin-concentrating hormone 1-receptor antagonist in mice. *Br J Pharmacol* 159:374-383
149. **Wajchenberg BL** 2000 Subcutaneous and visceral adipose tissue: their relation to the metabolic syndrome. *Endocr Rev* 21:697-738
150. **Ahmadian M, Duncan RE, Sul HS** 2009 The skinny on fat: lipolysis and fatty acid utilization in adipocytes. *Trends Endocrinol Metab* 20:424-428
151. **Tu Y, Thupari JN, Kim EK, Pinn ML, Moran TH, Ronnett GV, Kuhajda FP** 2005 C75 alters central and peripheral gene expression to reduce food intake and increase energy expenditure. *Endocrinology* 146:486-493
152. **Corica F, Allegra A, Corsonello A, Buemi M, Calapai G, Ruello A, Nicita Mauro V, Ceruso D** 1999 Relationship between plasma leptin levels and the tumor necrosis factor-alpha system in obese subjects. *Int J Obes Relat Metab Disord* 23:355-360
153. **Langin D, Arner P** 2006 Importance of TNFalpha and neutral lipases in human adipose tissue lipolysis. *Trends Endocrinol Metab* 17:314-320
154. **Yakar S, Liu JL, Stannard B, Butler A, Accili D, Sauer B, LeRoith D** 1999 Normal growth and development in the absence of hepatic insulin-like growth factor I. *Proceedings of the National Academy of Sciences of the United States of America* 96:7324-7329
155. **Roudabush FL, Pierce KL, Maudsley S, Khan KD, Luttrell LM** 2000 Transactivation of the EGF receptor mediates IGF-1-stimulated shc phosphorylation and ERK1/2 activation in COS-7 cells. *The Journal of biological chemistry* 275:22583-22589
156. **Boney CM, Sekimoto H, Gruppuso PA, Frackelton AR, Jr.** 2001 Src family tyrosine kinases participate in insulin-like growth factor I mitogenic signaling in 3T3-L1 cells. *Cell Growth Differ* 12:379-386
157. **Brindley DN, Kok BP, Kienesberger PC, Lehner R, Dyck JR** Shedding light on the enigma of myocardial lipotoxicity: The involvement of known and putative regulators of fatty acid storage and mobilization. *American journal of physiology*

158. **Arteaga CL** 2001 The epidermal growth factor receptor: from mutant oncogene in nonhuman cancers to therapeutic target in human neoplasia. *J Clin Oncol* 19:32S-40S